The Off-Design Modelling of a Combined-Cycle Power Plant

Prepared by:

Rushavya Naidu

NDXRUS001

Department of Mechanical Engineering

University of Cape Town

Supervisor:

A/Prof. Wim Fuls

February 2020

Submitted to the Department of Mechanical Engineering at the University of Cape Town in partial fulfilment of the academic requirements for a Masters of Science degree in Mechanical Engineering

Key Words: combined-cycle; HRSG; Brayton cycle; Rankine cycle; Off-design

Abstract

The shift towards renewable energy has steered the focus of power plant operation towards flexibility and fast response which are more attainable through the use of combined-cycle power plants. These aspects are required to account for the fluctuation of the supply as well as the demand of power that is associated with renewable energy.

Combined-cycle power plants consist of a gas turbine as the topping cycle, forming the core of the plant, and a Rankine cycle with a steam turbine as the bottoming cycle. A component called the Heat Recovery Steam Generator (HRSG) forms a connection point between the two cycles. It uses the heat released from the gas turbine to produce high pressure and temperature steam to be sent to the steam turbine.

The objective of this project is to develop a model of a combined-cycle power plant in Flownex which can be solved in off-design conditions in order to compare it to plant data. The verification of this model will show that Flownex can be used to effectively and efficiently model a combined-cycle power plant.

The process of development of the final Flownex model was achieved using various additional software. Initially, an analytical model was developed in Mathcad (software used for engineering calculations). This software provides a tool for understanding knowns, unknowns and what is being calculated in the system. Manual calculations of the Heat Recovery Steam Generator (HRSG) were done using heat balance equations. A temperature profile of the gas and water/steam in the HRSG was developed so that the duties of each component (economiser, evaporator, superheater) could be calculated. The overall conductance (UA) of each component was calculated in the design mode for the system to be evaluated in off-design mode. The development of an analytical model provided detailed understanding of the process of mathematical modelling used in commercial tools.

Thereafter, a model was built in Virtual Plant, a thermodynamic modelling software for assessing plant performance. Virtual Plant uses plant design information and first engineering principles to predict plant performance. Finally, the Flownex model was designed. Flownex uses endpoint values (initial pressure and temperature and outgoing mass flow) and the UA of each component to calculate the characteristics of the flow at each intermediate point.

For the single-, double-, and triple-pressure combined-cycle power plant systems, the analytical, Virtual Plant and Flownex models were compared. The results of all the models agreed closely with one another. The triple-pressure design and off-design Virtual Plant and Flownex models were also compared to plant data and it was concluded that Flownex was successful in modelling the design and off-design conditions of a combined-cycle power plant.

Declaration

I, Rushavya Naidu, know the meaning of plagiarism and declare that all the work in the document, save for that which is properly acknowledged, is my own. This thesis/dissertation has been submitted to the Turnitin module (or equivalent similarity and originality checking software) and I confirm that my supervisor has seen my report and any concerns revealed by such have been resolved with my supervisor.

Name Signed by candidate 26/02/2020

Date

Acknowledgements

"The end of education is character" – Sri Sathya Sai Baba

First and foremost, I'd like to extend my utmost gratitude to my Divine Master for guiding me through this journey and allowing me to achieve what I have through His love and abundance.

I'd like to thank my parents and brother for their endless support. For helping me believe in myself throughout my academic career and being there for me whenever I needed them.

I'd like to thank my supervisor, A/Prof. Wim Fuls, for his assistance, patience and sacrifice towards this thesis. Thank you for sharing your knowledge with me.

I'm grateful to the ATProM group for providing a wonderful working environment in which assistance was always readily available as well as for providing funding for this project.

I'd also like to thank THRIP at M-Tech Industrial for providing a portion of the funding for this project.

Table of Contents

List of Figures

List of Tables

List of Nomenclature

General symbols

A	Area (m^2)
C	Fluid heat capacity rate (W/K)
c_p	Specific heat capacity (J/kg.K)
D	Hydraulic diameter (m)
F	Gas property factor
g	Gravitational acceleration (m/s^2)
h	Enthalpy (kJ/kg)
ΔH	Fluid head (m)
k_g	Thermal conductivity of gas (W/m.K)
M	Molecular weight (g/mol)
$\dot{m}$	Mass flow rate (kg/s)
Nu	Nusselt number (-)
P	Pressure (Pa)
Pr	Prandtl number (-)
q	Heat transfer per unit mass (kJ/kg)
r_p	Pressure ratio (-)
Q	Rate of heat transfer (W)
R	Ratio of fluid heat capacity rates (-)
Re	Reynolds number (-)
T	Temperature (°C)
ΔT_m	Log mean temperature difference (K)
U	Overall heat transfer coefficient ($W/m^2.K$)
UA	Overall conductance (W/K)
V	Volumetric flow rate (m^3/s)
w	Net work (W)
y	Volume fraction of a gas constituent (%)
Subscripts	
actual	Actual value
Brayton	Brayton Cycle

CC	Combined-Cycle
cold	Cold fluid
design	Design case
ec	Economiser
ev	Evaporator
g	Gas phase
g1, g2, g3…	Gas properties at points of the HRSG
hot	Hot fluid
in; i	In/Entering
max	Maximum
min	Minimum
net	Net/Total
off	Off-design case
out; o	Out/Exiting
Rankine	Rankine Cycle
s	Water/steam phase
sh	Superheater
so	Steam exiting superheater
v	Saturated steam
w1	Water entering economiser
w2	Water exiting economiser

Greek symbols

η	Efficiency (-)
ρ	Density (kg/m^3)
ε	Effectiveness (-)
Δ	Change
μ	Dynamic viscosity (Pa.s)
π	Pi

Acronyms and Abbreviations

AP	Approach point
ECON	Economiser
EVAP	Evaporator
HP	High pressure
HRSG	Heat Recovery Steam Generator
HT	High temperature
IP	Intermediate pressure
IT	Intermediate temperature
LP	Low pressure
LT	Low temperature
NTU	Number of transfer units
PP	Pinch point
RH	Reheater
SH	Superheater

1. Introduction

1.1 Background

Energy is a crucial component of human society. It is a necessity for growing food, providing warmth and comfort as well as many other basic needs in various sectors of life such as agriculture, industry and transportation [1]. Energy is primarily derived from fossil fuels, solar radiation, wind, tidal waves and geothermal. The conversion, distribution and utilisation of energy fall within the field of engineering. The worldwide energy demand is rapidly increasing due to the exponential growth of the population, continuous rise in living standards and the focus on creating energy intensive industries in numerous newly emerging countries, in order to improve their economies so that poverty and deprivation may be overcome.

Fossil fuels such as coal, oil and gas are currently responsible for supplying more than 95% of the energy required worldwide [1]. Fossil fuels are, however, a finite resource. Therefore, the reserves on the planet are diminishing sharply. This resource also has a negative impact on the environment. Once combusted, fossil fuels release toxic gases – polluting the atmosphere and paying forth to global warming. Thus, the future use of fossil fuels is unethical with regards to energy conservation as well as the environment and its fortification.

Renewable energy presents itself as a solution to the downfalls of fossil fuels, however, these resources are only able to account for less than 10% of the world's total energy demand [1]. Unfortunately, this statistic is not expected to change significantly in the near future. As a result of this, and in order to ensure the conservation of fossil fuels, the increase of efficiency in present power generation systems is critical.

Combined-cycle power plants have the highest efficiency in the world in comparison to other power plants that operate on power grids. They have efficiencies of up to 62.22% [2]. These plants consist of a gas turbine as the topping cycle, forming the core of the plant, and a steam turbine as the bottoming cycle. A component called the Heat Recovery Steam Generator (HRSG) forms a connection point between the two cycles. It uses the heat released from the gas turbine to produce high-pressure steam to be sent to the steam turbine. The process involves a Brayton cycle (gas turbine) to produce electricity and steam for the Rankine cycle (steam turbine) in order to generate additional power. The basic layout of a combined cycle power plant is shown in Figure 1.

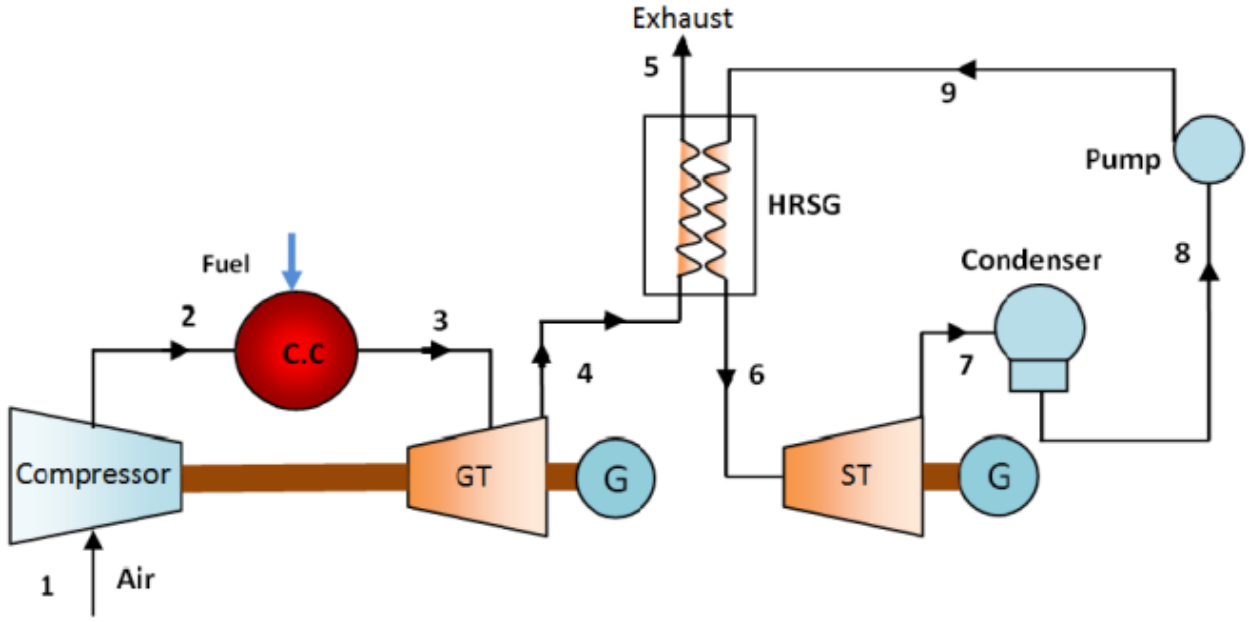

Figure 1: Basic Combined-Cycle Power Plant[3]

1.2 Primary Objective

The objective of this project was to develop an off-design model of a combined-cycle power plant in Flownex in order to compare it to plant data so that it may be verified. This software provides a simulation tool for systems within which a fluid is the driving force. The verification of this model will show that Flownex can be used to effectively and efficiently model a combined-cycle power plant.

The focus of the project was to show that it is possible to do equivalent studies, based on combined-cycle power plants, in Flownex, that have been done previously. The success of this project will open opportunities for the optimization of combined-cycle power plants using Flownex. The methods developed and lessons learned in this study will enable future modelling of such plants in Flownex.

1.3 Scope of Study

This project analyses the thermodynamic properties of the steam side of a combined-cycle power plant. The process of the development of the final Flownex model was understood and documented using various additional software. Initially, Mathcad was used as a learning platform to develop the analytical model. Thereafter, a model was designed using Virtual Plant, a thermodynamic modelling software for assessing plant performance. Finally, the design and off-design models were developed in Flownex, a thermohydraulic network solver.

The analytical model examined the HRSG in detail and included calculations for the steam turbine. In terms of the gas cycle, only properties of the exhaust gas (such as temperature, mass flow, composition and specific heat) were considered.

A model was then created in Virtual Plant in order to predict and assess the performance of the plant. This model also omitted the details of the gas cycle and only included the exhaust gas characteristics. It analysed detailed steam characteristics through the HRSG, steam turbine, condenser and pumps.

The Flownex model did not include the full steam cycle of the combined-cycle power plant. This model only focussed on components of the HRSG, steam turbines and pumps. The remaining components (condenser and feedwater pump) were not included as they would add unnecessary complications by trying to create a closed cycle in Flownex. The modelling of these components was also not vital to this project.

The gas cycle was not considered in any of the models due to the fact that generic gas plant models can be used in order to provide the exhaust gas required. The gas cycle was, therefore, not included in the scope of this project.

A model for single-, double- and triple-pressure systems was done using each software for design and off-design cases. However, only the triple-pressure models were compared to real plant data. This was because plant data for the single- and double-pressure models was not available. These models were compared to textbook results in order to validate them.

2. Literature Review

2.1 The Gas Cycle

Gas turbines generally involve an open cycle where ambient air enters the compressor within which the temperature and pressure are raised [4]. The air then flows to the combustion chamber which burns the injected fuel at a constant pressure resulting in a high temperature gas. The gas flows to a turbine where it expands to the atmospheric pressure and the enthalpy of the gas is used to produce mechanical energy which is then generated into electrical energy. The exhaust gases from the turbine are released into the atmosphere resulting in the process being an open cycle. The schematic of this cycle is shown in Figure 2.

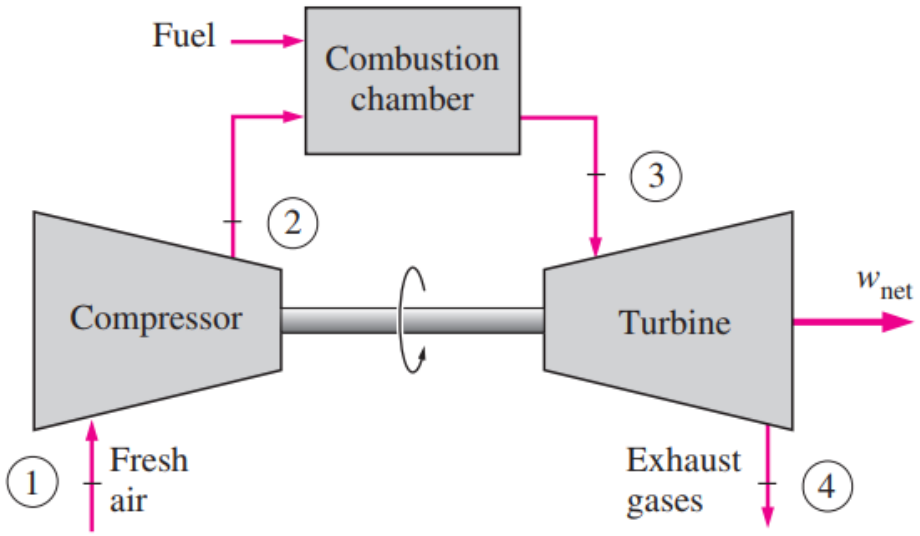

Figure 2: Schematic of a Gas Cycle [4]

If the open cycle gas-turbine cycle were to be modelled as a closed cycle instead, this would form the Brayton cycle. The compression and expansion processes are unchanged but the combustion process becomes an isobaric (constant pressure) heat addition and the exhaust process becomes an isobaric heat rejection to the ambient air [4]. Referring to Figure 3, the following processes occur: isentropic compression from **1**-**2**; the addition of heat at constant pressure in the heat exchanger from **2**-**3**; isentropic expansion from **3**-**4**; and heat rejection at constant pressure from **4**-**1**. A temperature-entropy, T-s, diagram of the Brayton cycle is shown in Figure 4. The thermal efficiency of the Brayton cycle can be calculated as shown in equation (2.1).

$$\eta_{Brayton} = 1 - \frac{1}{r_p^{\frac{k-1}{k}}} \tag{2.1}$$

Where,

$$r_p = \frac{P_2}{P_1} = \frac{P_3}{P_4} \tag{2.2}$$

r_p – pressure ratio

k – specific heat ratio

P – pressure of gas at the respective point in the cycle [Pa]

Therefore, the thermal efficiency of a Brayton cycle depends on the pressure ratio of the gas turbine and the specific heat ratio of the working fluid.

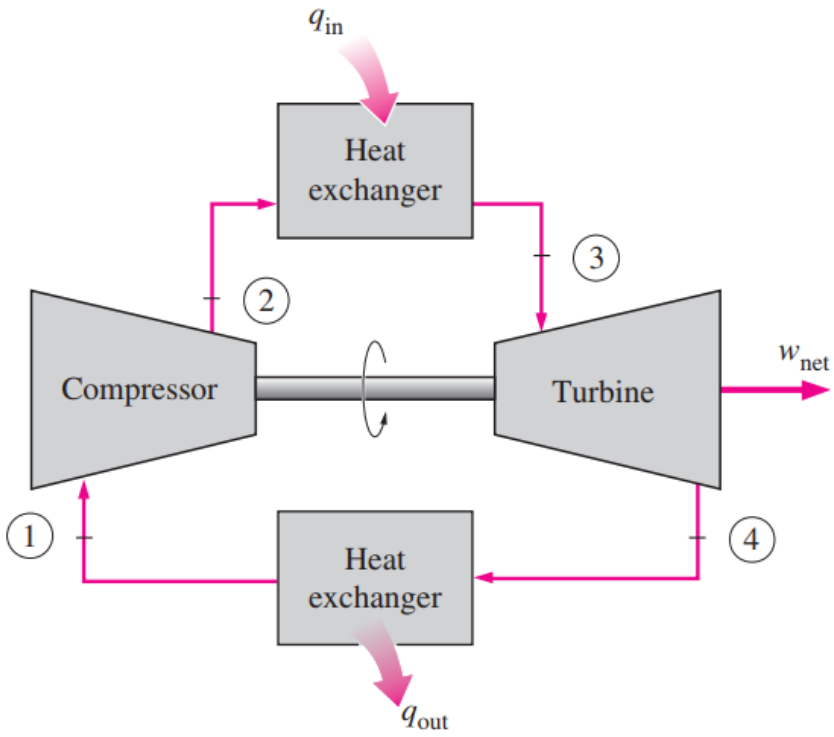

Figure 3: Schematic of a Brayton Cycle [4]

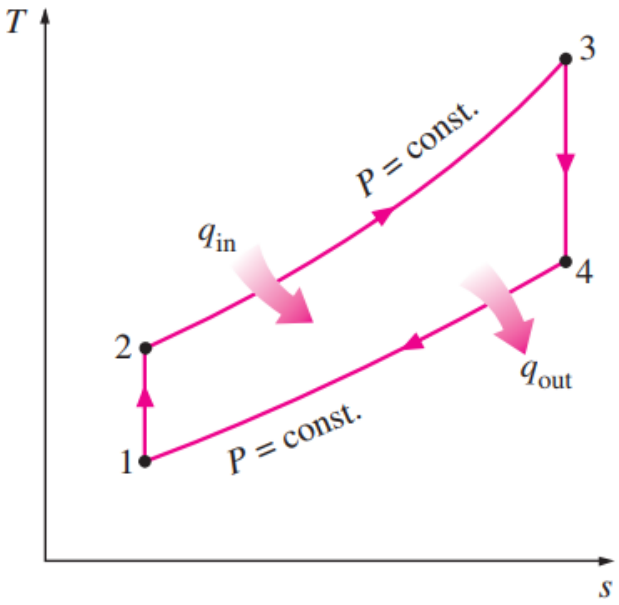

Figure 4: T-s diagram for a Brayton Cycle [4]

2.2 Steam Cycle

In a steam power plant, fossil fuels are used to convert the energy released by them into mechanical work [5]. The working fluid in a steam cycle is water, the phase of which varies between liquid and vapour. The energy given off by the burning of fossil fuels is transferred to water in the boiler in order for steam to be produced at a high pressure and temperature. The pressure of the steam is then decreased in the turbine by means of expansion which allows for the creation of shaft work. Steam then exits the turbine to be condensed back to water. The condenser makes use of the circulation of cooling water which transfers heat away from the steam. The condensate is then pumped back into the boiler creating a continuous cycle. Because of its cyclic nature, the internal energy of the fluid will remain constant throughout the cycle. Therefore, the net energy absorbed as heat by a unit mass of the fluid should equal the net energy transferred as work from the fluid.

If the processes in the steam cycle were to be ideal, i.e. no extraneous effects such as heat loss, the cycle would then be called a Rankine cycle.

The Rankine cycle is the most commonly used thermodynamic process for the generation of electricity and does not comprise of any internal irreversibilities [6]. Referring to Figure 5, the following processes occur: isentropic compression of water in the pump from **1**-**2**; the addition of heat at constant pressure in the boiler from **2**-**3**; isentropic expansion of steam in the turbine from **3**-**4**; and heat rejection at constant pressure in the condenser from **4**-**1** [4]. This can be represented

by means of a T-s, diagram shown in Figure 6. The area under a process curve on a T-s diagram symbolises the heat transfer for that process (being that the process is internally reversible). Therefore, the area below the curve **2**-**3** symbolises the heat transferred to the water in the boiler and the area below the curve **4**-**1** symbolises the heat transferred away from the water in the condenser. The difference between these areas is shown by the area enclosed by the cycle, which represents the net work produced by the cycle. The thermal efficiency of the Rankine cycle can be calculated using equation (2.3).

$$\eta_{Rankine} = \frac{w_{net}}{q_{in}} = 1 - \frac{q_{out}}{q_{in}} \tag{2.3}$$

w_{net} – net work produced by the cycle [W]

$q_{in,out}$ – heat transferred to and from the working fluid [W]

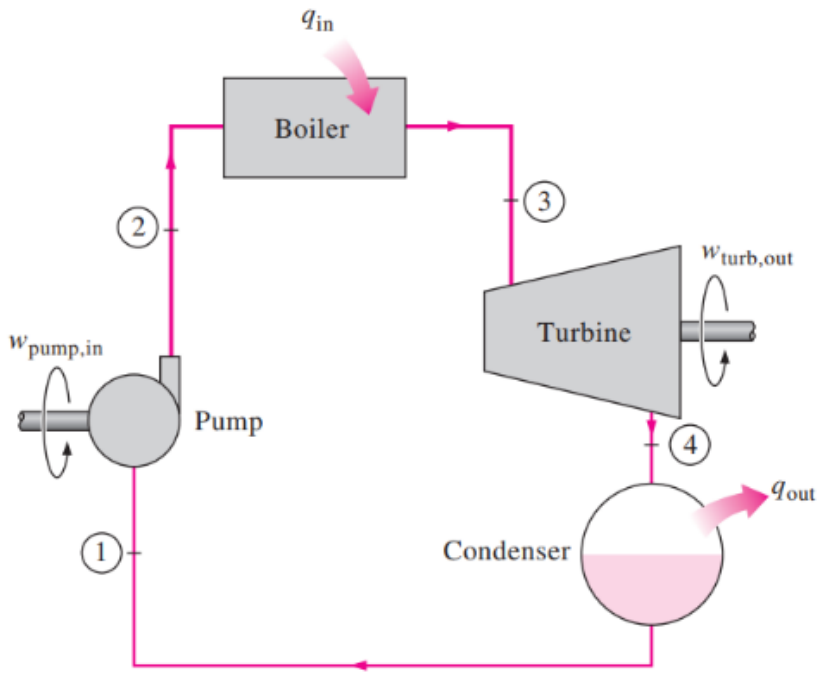

Figure 5: Schematic of a Rankine cycle [4]

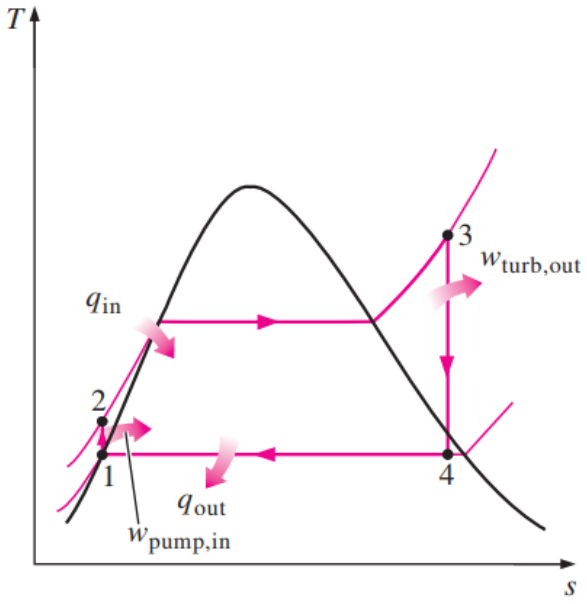

Figure 6: T-s diagram for a Rankine cycle [4]

2.3 The Brayton-Rankine Cycle

A combined-cycle power plant makes use of a 'Brayton-Rankine cycle' [7]. The hot gas exiting the gas turbine is used to produce superheated steam for a steam turbine. The exchange of energy is done in an HRSG instead of a boiler and may be supplementary fired too. The schematic of a combined-cycle power plant is shown in Figure 7.

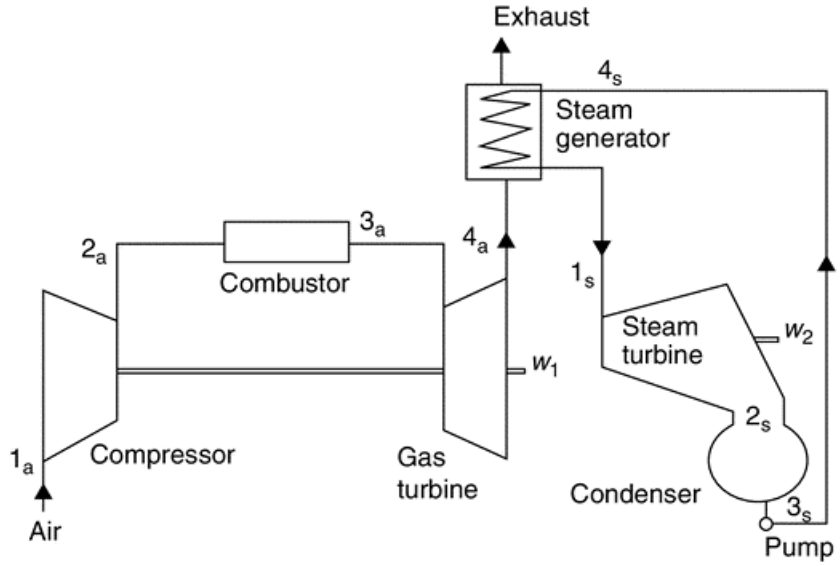

Figure 7: Schematic of a combined-cycle power plant [7]

Approximately 40% of the energy in the system is converted to power through the gas turbine. The rest of the energy, about 60%, is sent to the HRSG and is utilised by powering a steam turbine which converts around 20% of this energy to power. The energy distribution of the system is shown in Figure 8.

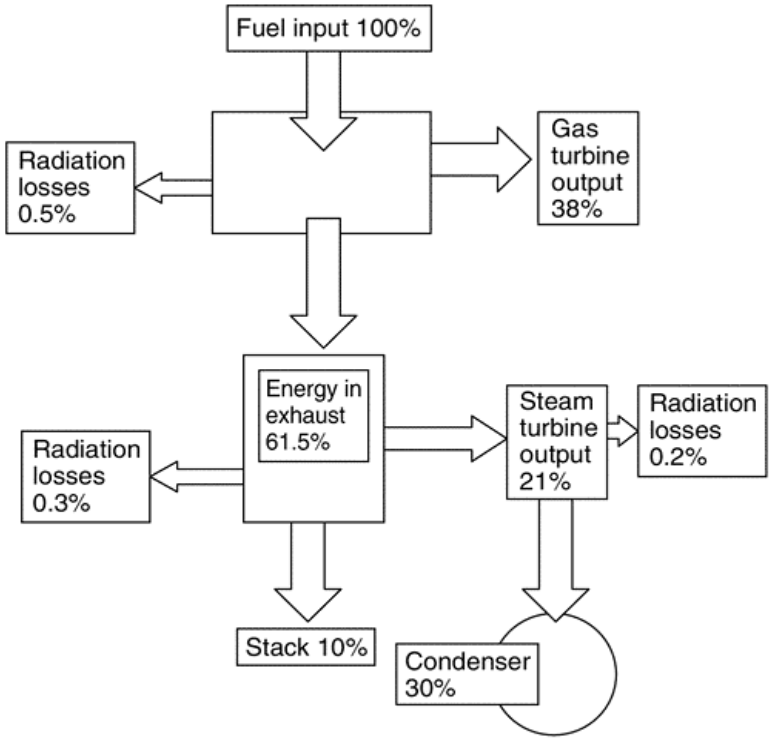

Figure 8: Energy distribution in a combined-cycle power plant [7]

The efficiency of a combined-cycle power plant, with no supplementary firing in the HRSG, is shown in equation (2.4)[8].

$$\eta_{CC} = \eta_{Brayton} + \eta_{Rankine}(1-\eta_{Brayton}) \tag{2.4}$$

2.4 Heat Recovery Steam Generator

The Heat Recovery Steam Generator (HRSG) acts as a heat exchanger which uses exhaust gases from the gas turbine to generate steam. When designing an HRSG, the evaluation of steam generation and steam temperature profiles are important starting points [9]. For the HRSG, unlike typical heat exchangers, the desired steam flow rate and exit gas temperature cannot be assumed in order to determine the amount of fuel required in the gas cycle. Due to the low inlet gas temperature and large gas to steam ratio in an HRSG, making assumptions for the steam flow rate and exit gas temperature may lead to temperature cross situations. As a result of the low inlet gas temperature, the generation of steam by an HRSG is lower than a conventional steam generator (using the same gas flow). Figure 9 shows the schematic of an HRSG.

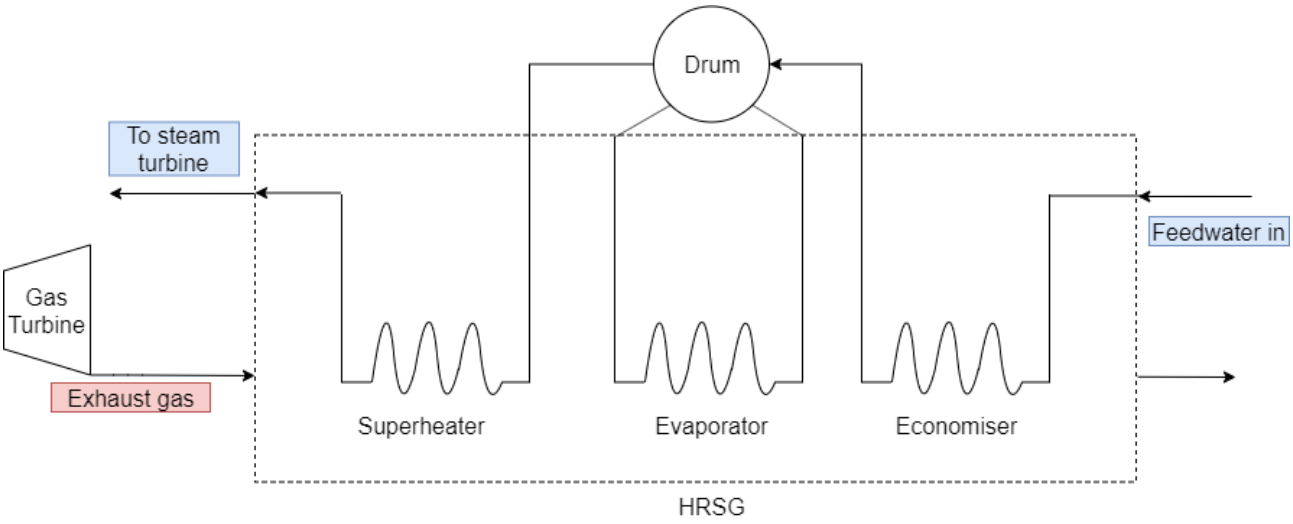

Figure 9: Schematic of an HRSG

A basic single pressure HRSG is composed of an economiser, evaporator and superheater. The components work together to convert thermal energy from the exhaust gas into steam. Feedwater is heated in the economiser after which it enters the drum at slightly subcooled conditions. The water then circulates in the evaporator, re-entering the drum as a water/steam mixture [5]. The water and steam separate in the drum and the saturated steam travels to the superheater where it experiences the maximum heat exchange temperature (inlet temperature of the exhaust gas from the gas turbine) and is superheated to the desired temperature. The T-s diagram for these components is shown in Figure 10.

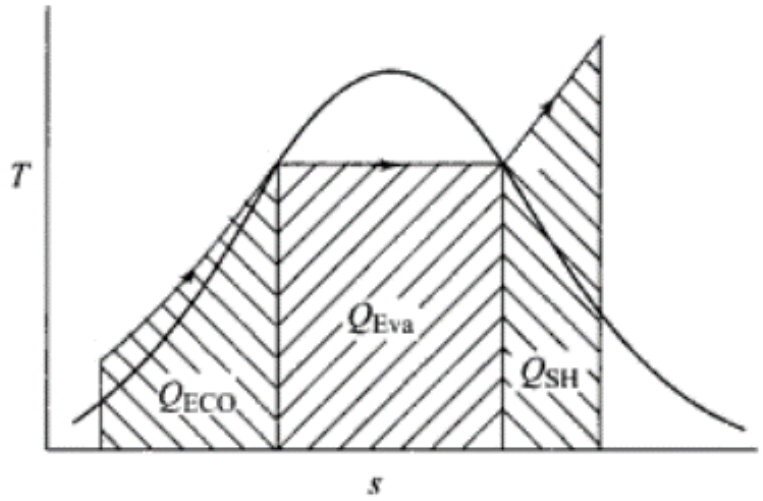

Figure 10: T-s diagram for an HRSG [5]

The steam production and gas and steam temperature profiles are dependent on the assumed pinch point and approach point values [9]. HRSG's can be thermally designed without having to physically size them [10]. A temperature profile is shown in Figure 11 with the red line representing the flow of gas and the blue line representing the flow of water and steam. The pinch point is the minimum temperature difference between the two fluids i.e. the difference between the temperature of the gas exiting the evaporator and the saturation temperature of steam. A pinch point is required in order to prevent a temperature cross situation – which is when the temperature of water exceeds the temperature of gas. This would cause heat to be transferred from water back to gas. The approach point is the difference between the saturation temperature of steam and the temperature of the water that exits the economiser. This value is used to prevent steaming in the economiser which occurs at off-design conditions. This means that steam starts to form in a component which is intended only for the liquid phase. Having steam in this component would lead to flow and operational problems. Therefore, water should always be kept at a subcooled liquid state in the component. The pinch and approach points will determine the size of the superheater, evaporator and economiser. The conditions (flow rate, temperature, etc.) of the gas entering the HRSG also has an impact on the amount of steam produced [10]. The exhaust gas of the gas turbine can be used to develop the temperature profile, which establishes the foundation of the HRSG sizing. The pinch point and approach point values for the design case can then be selected which leads to the final sizing of the HRSG. However, different gas conditions will result in the variation of the pinch point and approach point which can be evaluated in a simulation of the HRSG. A simulation will allow for the optimisation of temperature profiles as well as the HRSG design.

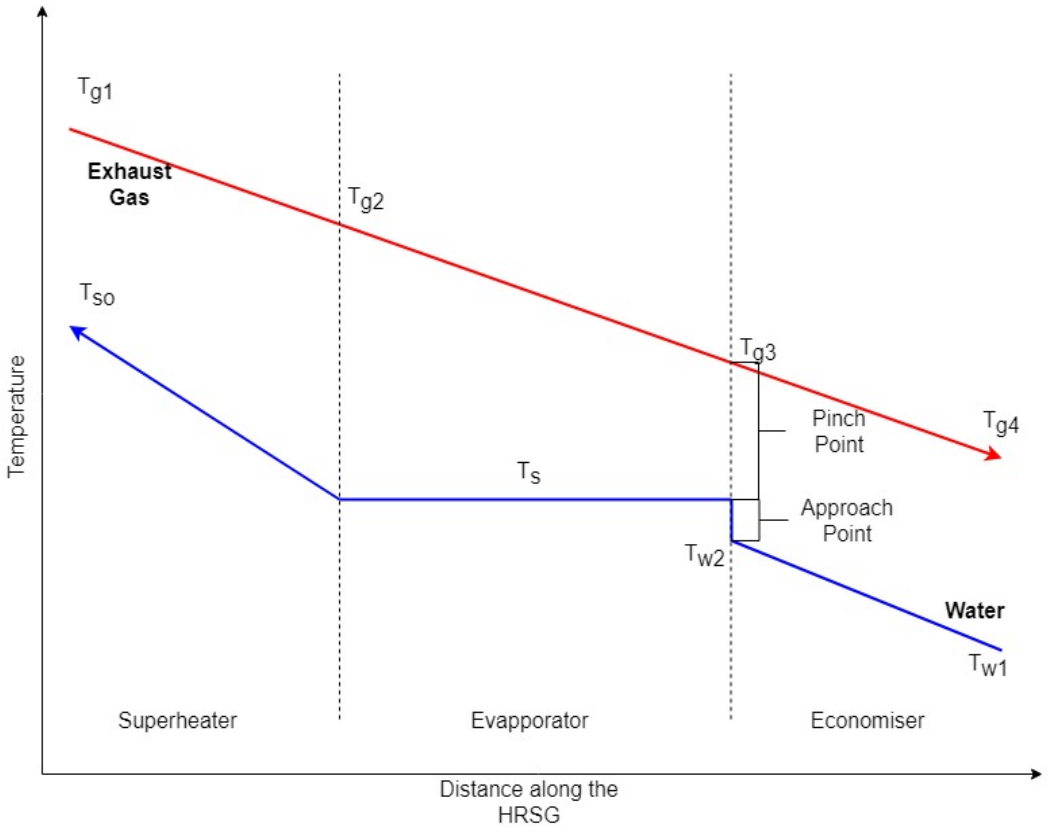

Figure 11: Temperature profile for an HRSG

Ganapathy provided suggestions for the ranges of pinch and approach points that should be used based on the inlet gas temperature [10]. These can be seen in Table 1.

Table 1: Suggested Pinch and Approach Points

Evaporator Type:	**Plain Tubes**	**Finned Tubes**	**Both**
Inlet Gas Temp. (°C)	Pinch Point (°C)	Pinch Point (°C)	Approach Point (°C)
650-900	60-85	20-35	20-40
375-650	40-60	5-20	5-20

At high inlet gas temperatures, a low pinch point is not practical as it would lead to a temperature cross situation at off-design conditions [10]. In contrast, to optimise steam generation, lower pinch and approach points should be used. The choice of approach point depends on whether the HRSG is going to be operating at low loads as well as whether steam formation in the economiser is expected. If there are multiple pressure levels and the generation of steam in the second pressure level is a higher priority, a large pinch point can be chosen for the low-pressure level and a smaller one for the second pressure level.

2.5 Pressure Levels and Arrangement of an HRSG

The primary use of multiple pressure levels in a combined-cycle power plant is to attain maximum efficiency [11]. In a single-pressure combined-cycle power plant, the exhaust gases in the stack usually have temperatures of between 110°C-140°C, whereas a triple-pressure plant would have stack temperatures of between 80°C-100°C. The result of the use of three pressure levels as compared to one is an increase of efficiency of around 3%.

The components that make up a combined-cycle power plant (e.g. compressors, pumps, turbines and valves) are usually standard machinery in various sizes [12]. However, the HRSG is one of the few components that are custom made depending on details of the specific plant. Therefore, it is practically the only component of the combined-cycle power plant where all factors of the steam cycle performance have been considered and can be optimised. Any change in the design of the HRSG affects all performance factors of the steam cycle directly. As a result, it is vital to optimise its design parameters and the layout of its heat exchangers.

Mohagheghi and Shayegan found that the most critical factors affecting all decision variables and the net power output are the *type* of HRSG used (single-, double-, or triple-pressure, with or without reheat) and the *layout* of its heat exchangers [12]. It was shown that the use of multiple pressure levels and the optimisation of heat exchanger layout led to an increase in power output in comparison to a single pressure HRSG. Using a triple-pressure HRSG with reheat and an optimised layout of heat exchangers provided the highest power output which showed a 22.5% increase of power compared to that of a single pressure cycle.

2.6 Circulation Systems in an HRSG

HRSG's can be sorted into three categories according to their circulation systems, these being natural circulation, forced circulation and once-through [10]. Natural circulation systems are composed of vertical tubes and horizontal gas flow, while forced circulation systems have horizontal tubes with vertical gas flow. Once-through systems can be designed either way. These systems can be seen in Figure 12. Natural circulation is enabled by the density difference between the down-coming colder, denser water and the rising hotter, less dense steam mixture in the evaporator.

A once-through HRSG does not have distinct regions separating the economiser, evaporator and superheater [10]. The only point of control for a once-through system is the feedwater control valve. The mass flow of water/steam varies in this system depending on the gas inlet temperature and the steam exit temperature. This process does not make use of a drum and instead uses a smaller scale water chamber. Hence, these have a faster response to load fluctuations.

The difference between natural and forced circulation HRSG's poses various factors such as the fact that natural circulation systems do not entail a pump for circulation in the evaporator tubes [10]. The presence of pumps in the forced circulation system leads to operational as well as maintenance costs. These pumps also pose the risk of the HRSG shutting down in the case of their failure. The distribution of water and steam in the pipes of the natural circulation system is more beneficial as the pipe walls are wetted evenly, considering water moves *downward* and steam rises *upward*. Whereas in the case of forced circulation there is a temperature difference between the upper and lower parts of the horizontal tubes, which may lead to thermal fatigue [10]. The vertical tubes in a natural circulation system allow for higher heat flux than horizontal tubes in a forced circulation system.

Natural circulation HRSG's make use of more floor space than that of forced circulation ones, especially if multiple modules are used [10]. Although the floor space taken up by forced circulation systems is smaller, their height is greater causing the need for ladders, platforms and more steel support structures.

This study will focus on HRSG's making use of a drum. Whether the flow is circulated naturally or forced does not affect the thermodynamic modelling approach.

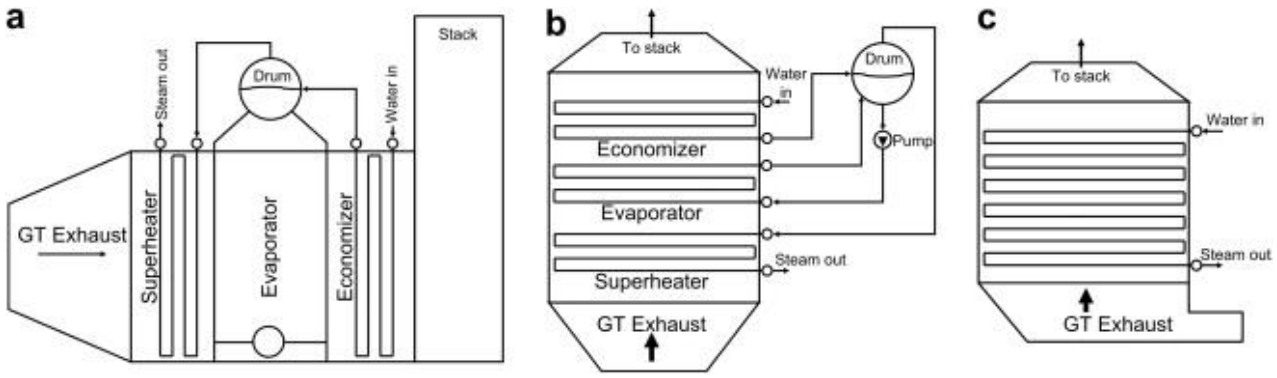

Figure 12: a.) Natural circulation HRSG b.) Forced circulation HRSG c.) Once-through HRSG [33]

2.7 Calculations for Temperature Profile

Using the temperature profile in Figure 11, the known values for the system are shown in Table 2 [9].

Table 2: Known values for temperature profile

Description	**Variable**
Gas flow rate	$\dot{m}_g$
Gas temperature at the inlet of the HRSG	T_{g1}
Feedwater temperature	T_{w1}
Temperature of the steam exiting the superheater	T_{so}
Pressure of the steam	P_s
Saturation temperature in the evaporator can be determined using steam properties for the chosen pressure	T_s

The gas temperature exiting the evaporator and the water temperature exiting the economiser can be found using the drum temperature and pinch and approach points as shown in equation (2.5) and (2.6).

$$T_{g3} = T_s + Pinch\ Point \tag{2.5}$$

$$T_{w2} = T_s - Approach\ Point \tag{2.6}$$

Using the energy balance across the superheater and evaporator, the energy absorbed by these components is shown in equation (2.7).

$$Q_{sh,ev} = \dot{m}_g c_{pg} (T_{g1} - T_{g3}) = \dot{m}_s \left(h_{so} - h_{w2} \right) \tag{2.7}$$

$Q_{sh,ev}$ – duty of the superheater and evaporator combined [W]

$\dot{m}_{g,s}$ – mass flow rate of gas or steam [kg/s]

c_{pg} – specific heat of gas [J/kg.K]

T_g – temperature of gas [°C]

$h_{so,\ w2}$ – enthalpy of the fluid exiting the superheater or economiser [J/kg]

T_{g1} and T_{g3} are known, therefore the duty of the superheater and evaporator combined, $Q_{sh,ev}$, and the steam mass flow rate, $\dot{m}_s$, can be calculated.

The energy absorbed by the superheater can be calculated as shown in equation (2.8).

$$Q_{sh} = \dot{m}_s (h_{so} - h_v) = \dot{m}_g c_{pg} (T_{g1} - T_{g2}) \tag{2.8}$$

Q_{sh} – duty of the superheater [W]

$h_{so,v}$ – enthalpy of superheated or saturated steam [J/kg]

The temperature of the gas exiting the superheater, T_{g2}, can therefore be calculated.

The energy balance of the economiser provides equation (2.9).

$$Q_{ec} = \dot{m}_s(h_{w2} - h_{w1}) = \dot{m}_g c_{pg}(T_{g3} - T_{g4}) \tag{2.9}$$

Q_{ec} – duty of the economiser [W]

The temperature of the gas exiting the economiser, T_{g4}, can therefore be calculated.

The calculated variables will allow for the gas and steam temperature profiles as well as the steam generation to be determined once a pinch point and approach point is selected.

2.8 Heat Exchanger Modelling

Once the temperature profile and duty of the HRSG in design mode is obtained, the way in which it performs in the off-design mode may be determined. Thus, the HRSG can be thermally designed and its performance analysed without having to evaluate its geometry. From the design mode, the LMTD method is utilised in order to obtain the performance of the HRSG or its components. This is done by first calculating a value for the overall conductance, *UA*, of each component as shown in equation (2.10).

$$UA = \frac{Q}{\Delta T_m} \tag{2.10}$$

U – overall heat transfer coefficient of the component [W/m^2.K]

A – surface area of the component [m^2]

Q – duty of the component [W]

ΔT_m – log mean temperature difference between the two fluids [K]

The equation for log mean temperature difference is shown in equation (2.11).

$$\Delta T_m = \frac{\Delta T_1 - \Delta T_2}{\ln\left(\frac{\Delta T_1}{\Delta T_2}\right)} \tag{2.11}$$

Where ΔT_1 is the temperature difference between the two fluids at the inlet of the heat exchanger and ΔT_2 is the temperature difference between the two fluids at the outlet.

The overall heat transfer coefficient, *U*, need not be calculated since the overall conductance, *UA*, can be used as a singular term. In the off-design mode, the *UA* is corrected for each component

according to the change in gas flow and temperature [10]. The corrected *UA* is then used in the effectiveness-NTU method in order to evaluate the off-design performance.

Effectiveness is the ratio of the actual heat transfer to the maximum possible heat transfer of a heat exchanger. It is defined as shown in equation (2.12) [13].

$$\varepsilon = \frac{Q_{actual}}{Q_{max}} \tag{2.12}$$

ε – effectiveness of the heat exchanger

$Q_{actual,max}$ – actual or maximum heat that can be transferred by the heat exchanger [W]

Q_{actual} can be calculated as shown in equation (2.13).

$$Q_{actual} = C_{hot}(Th_i - Th_o) = C_{cold}(Tc_o - Tc_i) \tag{2.13}$$

Where,

$$C = \dot{m} \cdot c_p \tag{2.14}$$

$C_{hot,cold}$ – fluid heat capacity rate of the hot or cold fluid [W/K]

$Th_{i,o}$ – temperature of hot fluid flowing in or out of the component [°C]

$Tc_{i,o}$ – temperature of cold fluid flowing in or out of the component [°C]

Q_{max} is the maximum possible heat transfer that could be achieved by the heat exchanger. This is the heat transferred if one of the fluids has a temperature change equal to the temperature difference between the incoming hot and cold fluids. It is therefore defined using the minimum (limiting) fluid heat capacity rate and the maximum temperature difference between the two fluids as shown in equation (2.15) [13].

$$Q_{\max} = C_{\min}(Th_i - Tc_i) \tag{2.15}$$

While the actual heat transfer factors in the effectiveness of the component shown in (2.16).

$$Q_{actual} = \varepsilon \cdot C_{\min}(Th_i - Tc_i) \tag{2.16}$$

The effectiveness depends on the geometry of the heat exchanger, what the flow pattern is (parallel flow, counter flow, cross flow, etc.) and the number of transfer units [14]. The equation for the effectiveness of a counter flow heat exchanger is shown in equation (2.17).

$$\varepsilon = \frac{1 - e^{-NTU(1-R)}}{1 - R \cdot e^{-NTU(1-R)}} \tag{2.17}$$

Where,

$$NTU = \frac{UA}{C_{\min}} \tag{2.18}$$

And,

$$R = \frac{C_{\min}}{C_{\max}} \tag{2.19}$$

Due to water vaporising in the evaporator, $C_{\max}$ becomes immense and R approaches zero which leads to the effectiveness equation shown in (2.20).

$$\varepsilon = 1 - e^{-NTU} \tag{2.20}$$

The specific heat capacities of gas can be calculated using the gas composition, specific heats of the gas constituents at each component's average temperature and the molar masses of the gas constituents [10]. The formula is shown in equation (2.21).

$$c_{pg} = \frac{\sum y \cdot c_{p,constituent} \cdot M}{\sum y \cdot M} \tag{2.21}$$

y – volume fraction of the constituent [%]

$c_{p,constituent}$ – specific heat of the constituent at the average gas temperature [J/kg.K]

M – molecular weight of the constituent [g/mol]

The specific heat capacity of steam/water in each component can be calculated using the change in enthalpy and temperature as shown in equation (2.22).

$$c_{ps} = \frac{h_{s.out} - h_{s.in}}{T_{s.out} - T_{s.in}} \tag{2.22}$$

Using these equations, the effectiveness of each component in the off-design mode can be calculated.

2.9 Off-Design UA

The UA value under off-design conditions has been calculated differently by various researchers. Ganapathy used the relationship in equation (2.23) [10].

$$UA_{off} = UA_{design} \cdot \left(\frac{\dot{m}_{g,off}}{\dot{m}_{g,design}} \right)^{0.65} \cdot \left(\frac{\dot{m}_{s,off}}{\dot{m}_{s,design}} \right)^{0.15} \cdot \left(\frac{F_{g,off}}{F_{g,design}} \right) \tag{2.23}$$

F_g is a gas property factor as shown in equation (2.24).

$$F_g = \frac{{c_{pg}}^{0.33} {k_g}^{0.67}}{{\mu_g}^{0.32}} \tag{2.24}$$

k_g – thermal conductivity of the gas [W/m.K]

μ_g – dynamic viscosity of the gas [Pa.s]

Equation (2.25) shows that used by Kehlhofer [15].

$$UA_{off} = UA_{design} \cdot \left(\frac{\dot{m}_{g,off}}{\dot{m}_{g,design}} \right)^m \cdot \left(\frac{k_{g,off}}{k_{g,design}} \right) \cdot \left(\frac{\mu_{g,design}}{\mu_{g,off}} \right)^m \tag{2.25}$$

Where *m* is a constant that depends on the geometry of the heat exchanger, usually assumed between 0.57 and 0.65 [16].

Haglind [17] expressed the ratio of overall conductance of either the gas or steam side as shown in equation (2.26).

$$UA_{off} = UA_{design} \cdot \left(\frac{\dot{m}_{off}}{\dot{m}_{design}} \right)^m \cdot \left(\frac{k_{off}}{k_{design}} \right) \cdot \left(\frac{\mu_{design}}{\mu_{off}} \right)^m \cdot \left(\frac{\mathrm{Pr}_{off}}{\mathrm{Pr}_{design}} \right)^n \tag{2.26}$$

Pr – Prandtl number of gas or steam

Physical properties of the fluids may often be assumed to remain constant. Hence, the off-design overall conductance of the gas side can be expressed as shown in equation (2.27) [17].

$$UA_{off} = UA_{design} \cdot \left(\frac{\dot{m}_{g,off}}{\dot{m}_{g,design}} \right)^m \tag{2.27}$$

The Virtual Plant software tool employs equation (2.28) to calculate off-design UA.

$$UA_{off} = UA_{design} \cdot \left(\frac{\dot{m}_{g,off}}{\dot{m}_{g,design}} \right)^m \cdot \left(\frac{k_{g,off}}{k_{g,design}} \right)^{\frac{2}{3}} \cdot \left(\frac{\mu_{g,off}}{\mu_{g,design}} \right)^{\frac{2}{3}} \cdot \left(\frac{c_{pg,off}}{c_{pg,design}} \right)^{\frac{1}{3}} \tag{2.28}$$

One can also derive a similar equation for the off-design UA from first principles as follows: The equation for the overall heat transfer coefficient of the heat exchanger can be calculated using equation (2.29).

$$\frac{1}{U} = \frac{1}{h_g} + \frac{L}{k} + \frac{1}{h_s} \tag{2.29}$$

U – overall heat transfer coefficient [W/m^2.K]

$h_{g,s}$ – convective heat transfer coefficient of the gas or steam [W/m^2.K]

L – thickness of the tube [m]

k – thermal conductivity of the pipe[W/m.K]

Assuming the thickness of the pipe is negligible allows for the thermal resistance of the pipe to be ignored. The heat transfer on the steam side (h_s) is typically much larger than that of the gas side (h_g). Thus, the overall heat transfer coefficient can be approximated as shown in equation (2.30).

$$U \approx h_g = \frac{Nu \cdot k_g}{D} \tag{2.30}$$

Nu – Nusselt number of gas

D – hydraulic diameter of the tube [m]

The Nusselt number for the cross flow of gases over plain tube banks is shown in equation (2.31) [10].

$$Nu = 0.33 \cdot \mathrm{Re}^{m} \cdot \mathrm{Pr}^{0.33} \tag{2.31}$$

Re – Reynolds number of gas

The equations for Reynolds and Prandtl numbers are shown in equation (2.32) and (2.33).

$$\mathrm{Re} = \frac{\rho_g \cdot v_g \cdot D}{\mu_g} \tag{2.32}$$

ρ_g – density of gas [kg/m^3]

v_g – velocity of gas [m/s]

$$\mathrm{Pr} = \frac{c_{pg} \cdot \mu_g}{k_g} \tag{2.33}$$

Substituting equation (2.32) and (2.33) into equation (2.31) results in equation (2.34).

$$\begin{aligned} Nu &= 0.33 \cdot \left(\frac{\rho_g \cdot v_g \cdot D}{\mu_g} \right)^{m} \cdot \left(\frac{c_{pg} \cdot \mu_g}{k_g} \right)^{0.33} \\ &= 0.33 \left(\rho_g \cdot v_g \cdot D \right)^{m} \cdot \left(\frac{c_{pg}}{k_g} \right)^{0.33} \cdot \left(\frac{1}{\mu_g} \right)^{m-0.33} \end{aligned} \tag{2.34}$$

Equation (2.34) can then be substituted into equation (2.30) to produce equation (2.35).

$$U = 0.33 \left(\rho_g \cdot v_g \right)^{m} \cdot \left(\frac{1}{D} \right)^{1-m} \cdot {c_{pg}}^{0.33} \cdot {k_g}^{0.67} \cdot \left(\frac{1}{\mu_g} \right)^{m-0.33} \tag{2.35}$$

The velocity of gas can be calculated as shown in equation (2.36).

$$\begin{aligned} v_g &= \frac{\dot{m}_g}{\rho_g \cdot A_x} \\ &= \frac{\dot{m}_g}{\rho_g \cdot \frac{\pi \cdot D^2}{4}} \end{aligned} \tag{2.36}$$

A_x – cross-sectional area of pipe [m^2]

Substituting equation (2.36) into equation (2.35) leads to equation (2.37).

$$U = 0.33\left(\frac{\dot{m}_g \cdot 4}{\pi}\right)^m \cdot \left(\frac{1}{D}\right)^{1+m} \cdot {c_{pg}}^{0.33} \cdot {k_g}^{0.67} \cdot \left(\frac{1}{\mu_g}\right)^{m-0.33} \tag{2.37}$$

The ratio of UA in the off-design case to that of the design case can therefore be expressed as shown in equation (2.38).

$$\begin{aligned} \frac{UA_{off}}{UA_{design}} &= \frac{0.33\left(\frac{\dot{m}_{g,off} \cdot 4}{\pi}\right)^m \cdot \left(\frac{1}{D}\right)^{1+m} \cdot {c_{pg,off}}^{0.33} \cdot {k_{g,off}}^{0.67} \cdot \left(\frac{1}{\mu_{g,off}}\right)^{m-0.33}}{0.33\left(\frac{\dot{m}_{g,design} \cdot 4}{\pi}\right)^m \cdot \left(\frac{1}{D}\right)^{1+m} \cdot {c_{pg,design}}^{0.33} \cdot {k_{g,design}}^{0.67} \cdot \left(\frac{1}{\mu_{g,design}}\right)^{m-0.33}} \\ &= \left(\frac{\dot{m}_{g,off}}{\dot{m}_{g,design}}\right)^m \cdot \left(\frac{c_{pg,off}}{c_{pg,design}}\right)^{0.33} \cdot \left(\frac{k_{g,off}}{k_{g,design}}\right)^{0.67} \cdot \left(\frac{\mu_{g,design}}{\mu_{g,off}}\right)^{m-0.33} \end{aligned} \tag{2.38}$$

If physical properties of gas are assumed to remain constant at lower loads, the UA at off-design conditions can be calculated using equation (2.39), which is the same as equation (2.27).

$$UA_{off} = UA_{design}\left(\frac{\dot{m}_{g,off}}{\dot{m}_{g,design}}\right)^m \tag{2.39}$$

This assumption, however, slightly decreases the accuracy of the calculation since the physical properties of gas would change at various temperatures.

The NTU in the off-design mode can then be calculated using the off-design UA. The effectiveness for each component can therefore be evaluated. This allows for the duty of each component to be found in the off-design mode.

2.10 Off-Design Behaviour

For the design case, components in the steam cycle are designed to meet specific criteria. However, for the off-design case, the performance of the plant is reliant on the behaviour of the fixed components as a result of deviations in the operating environment [8].

It is vital to have a detailed understanding of the steady state and dynamic operating performance of the plant [8]. However, theoretical modelling of the dynamic performance is costly and problematic. Hence, knowledge gained from existing plants as well as estimates must be used in conjunction with steady state plant calculations in order to predict dynamic performance.

There is a substantial difference between the calculation of the steady state design and off-design conditions of the steam part of a combined-cycle power plant and that of a conventional steam plant [8]. The difference is mainly based on the boiler and the design mode of the plant. In an HRSG, heat transfer is largely attributed to convection, unlike a conventional boiler where radiation is responsible for most of the heat transferred.

The most economical method of steam turbine operation in a combined-cycle power plant is through the use of sliding pressure [8]. Steam characteristics depend on the exhaust gas flow and temperature and on the swallowing capacity of the steam turbine. This is opposed to a conventional steam plant which often runs at a fixed pressure (where live-steam pressure and temperature remain constant) – this allows for calculations to be straight forward due to steam temperature and pressure being known in advance as well as for the boiler and steam turbine to be assessed separately. In a combined-cycle power plant, however, the design of the HRSG and the steam turbine have to be done in conjunction with each other.

2.11 Gas Turbine Low Load Control

Control of the electrical output of a combined-cycle power plant (with no supplementary firing) is solely managed by the gas turbine [8]. The power generation of the steam turbine then follows the trend of the gas turbine since it utilises the amount of steam that the HRSG produces.

Variable inlet guide vane (VIGV) control and gas turbine inlet temperature (TIT) control are used to govern the power output of the gas turbine [8]. The control of the TIT is done using the fuel flow into the combustor and the VIGV setting. Recent gas turbines are designed with up to three rows of VIGV's allowing for high gas turbine exit temperatures from full load to as low as around 40% load. At loads below 40%, the TIT is lowered further in order to prevent the decrease of gas flow, since a further reduction of gas flow is not desirable. Therefore, from 0% to around 40% load, the VIGV's are closed resulting in the exhaust gas mass flow remaining constant while exhaust gas temperature

increases until it reaches design temperature [18]. After this point (approximately 40% load), the VIGV's start to open causing the exhaust gas flow to increase while the exhaust gas temperature remains constant. The graph shown in Figure 13 shows an example of the trend resulting from VIGV control.

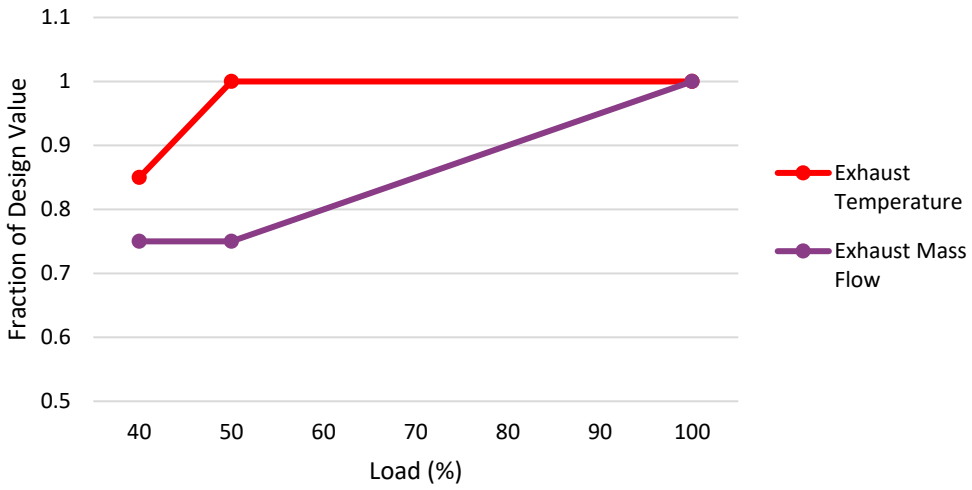

Figure 13: Graph of exhaust gas parameters at different loads

When a change in load of the gas turbine occurs, the steam turbine responds automatically after a small delay [8]. The gas cycle is responsible for around two thirds of the total power output of the plant. Thus, a control variable for the steam turbine power output, which causes complications and lower efficiencies, is not necessary. Modern gas turbines also have a fast response to changes in frequency, and usually balance the effect of the delay in steam turbine response.

2.12 Turbine Flow Control

Generally, power plants reach their maximum efficiency at design conditions, therefore, at lower load conditions their efficiency drops [19]. Certain power plants may have higher thermal efficiencies at off design conditions while others see substantial drops in efficiency with relatively minor load drops. Combined-cycle power plants use a concept called sliding pressure in order to increase the thermal efficiency at off-design conditions.

The control of the steam turbine output is essential when it comes to the efficiency of power generation at lower loads [19]. The reduction of the power output involves the control of steam flow which can be attained through throttle control or nozzle control. Throttle control decreases the amount of steam flowing through the turbine by means of a throttle valve, after which, steam is fully admitted to the first turbine stage. Nozzle control uses multiple control valves that may be

partially closed in order to control the flow. Steam is partially admitted to the collection of nozzles in the control stage.

Sliding pressure may also be used by the steam generator in order to control steam flow to the turbine. In sliding pressure conditions, throttle devices remain fully open allowing the boiler pressure to 'slide' in order to preserve a balance between the volumetric flow of the steam turbine and the heat exchanger [19].

2.13 Turbine Pressure

2.13.1 Mass Flow Coefficient

Turbines have a specific flow path area which governs the maximum steam flow rate that the turbine can accommodate at a given steam condition. This is called the swallowing capacity of the turbine. Equation (2.40) shows the relationship between steam flow rate through the turbine and steam parameters used by M. P Polsky [19].

$$\dot{m}_s \sqrt{\frac{T_i}{P_i^2 - P_o^2}} = constant \tag{2.40}$$

$\dot{m}_s$ – steam mass flow rate [kg/s]

T_i – temperature of steam entering the turbine [°C]

$P_{i,o}$ – pressure of steam entering or exiting the turbine [Pa]

For condensing steam turbines, the pressure of steam exiting the turbine is negligible compared to that entering. Thus, the equation can be simplified as shown in equation (2.41).

$$\dot{m}_s \sqrt{\frac{T_i}{P_i^2}} = constant \tag{2.41}$$

The ideal gas law (shown in equation (2.42)) is then used to replace temperature in equation (2.41)

.

$$T = \frac{P \cdot v}{R} \tag{2.42}$$

T – temperature of gas [°C]

P – pressure of gas [Pa]

v – specific volume of gas [m^3/kg]

R – ideal gas constant [J/K.mol]

Therefore, equation (2.43) is formed, which is called the flow coefficient.

$$\dot{m}_s \sqrt{\frac{v}{P}} = constant \tag{2.43}$$

Equations (2.41) and (2.43) show that the steam flow that a steam turbine can accommodate is dependent on the inlet steam parameters. The flow coefficient can be rewritten as shown in equation (2.44). This shows that at specific inlet steam conditions, there is a fixed volumetric flow rate that a steam turbine can swallow.

$$\dot{m}_s \sqrt{\frac{v}{P}} = \frac{\dot{m}_s \cdot v}{\sqrt{P \cdot v}} = \frac{V}{\sqrt{P \cdot v}} = constant \tag{2.44}$$

V – volumetric flow rate [m^3/s]

Using equations (2.41) and (2.43), it can also be shown that the steam pressure at the first stage of the turbine is dependent on steam mass flow and temperature or specific volume. This is shown in equation (2.45).

$$P_i = \frac{\dot{m}_s \sqrt{T_i}}{constant} = \frac{v \cdot \dot{m}_s{}^2}{constant} \tag{2.45}$$

If the steam temperature entering the turbine remains constant, the steam mass flow is then directly proportional to steam pressure.

The amount of steam generated by the HRSG depends on exhaust gas flow, exhaust gas temperature and steam pressure [19]. The lower the pressure of the steam, the lower the exit gas temperature from the evaporator and the more energy from the gas that the steam is able to absorb – leading to more steam being produced at the same gas conditions. The control valves being fully open means that the steam generated by the HRSG is controlled by the steam turbine swallowing capacity. A decrease in load results in the temperature or mass flow of the exhaust gas being decreased, which would lead to decreased steam being generated by the HRSG. However, if the throttle valves are positioned fully open, the pressure of steam decreases and the amount of steam generated increases. When the volumetric flow rate generated by the HRSG corresponds with the turbine swallowing capacity, the steam pressure and rate of steam generation stabilise. This defines the operating point for the specified load. The mass flow rate of water in the evaporator, however, is dependent on the desired heat uptake by the evaporator as well as the drum pressure.

2.13.2 Stodola Ellipse Law

Stodola found that if the mass flow of a fluid through a turbine were to be plotted against its exit pressure, the graph would form an elliptical shape [20][21]. This is related to the fact that a graph of the pressure ratio across a turbine versus the corrected mass flow would be asymptotic. The

pressure ratio used to form the asymptotic graph is evaluated as $\frac{P_{inlet}}{P_{outlet}}$. However, when the inverse pressure ratio is used $\left(\frac{P_{outlet}}{P_{inlet}}\right)$, the graph would represent an elliptical shape. Hence, the steam mass flow during off-design modes may be calculated using that of the design condition. This forms the basis of the ellipse law shown in equation (2.46) in temperature form.

$$\dot{m}_{off} = \dot{m}_{design} \cdot \frac{P_{i,off}}{P_{i,design}} \cdot \sqrt{\frac{T_{i,design}}{T_{i,off}}} \cdot \sqrt{\frac{1-\left(\frac{P_{o,off}}{P_{i,off}}\right)^2}{1-\left(\frac{P_{o,design}}{P_{i,design}}\right)^2}} \tag{2.46}$$

$\dot{m}_{design,off}$ – steam mass flow rate in design or off-design conditions [kg/s]

T_i – temperature of steam entering the turbine [°C]

$P_{i,o}$ – pressure of steam entering or exiting the turbine [Pa]

The Stodola ellipse law produces more accurate results as compared to the constant flow coefficient model, specifically for non-condensing turbines. However, not all software tools utilise this method since it adds complications to the solving algorithms.

2.14 Attemperation

The temperature of steam generated by the HRSG will sometimes be higher than desired due to the variation of steam flow rate [22]. The steam cycle usually requires for the generated steam to remain at a specific temperature. Thus, a temperature control device needs to be utilised. Power plants should be designed so that the desired steam temperature is attained at design conditions. The temperature of the steam will therefore only need to be decreased when operating at off-design conditions.

A way in which the temperature of steam may be brought down is to spray fine droplets of relatively cool water into the steam [22]. The combination of the hot steam and cold droplets results in the droplets evaporating and the mixture having a lower temperature with an increased volume of steam. This process is done by an attemperator. The use of attemperation causes a change in mass flow after the attemperator. Attemperation usually occurs at the exit of a superheater in order to control the output steam temperature, using coolant from the feedwater. There are various types of attemperators, some of which are mentioned below.

- Mechanically Atomised Attemperator

A mechanically atomised attemperator is one in which high-pressure cooling water is mechanically atomised into small droplets at a nozzle. This allows for the area of contact between the steam and water to be maximised [22].

- Variable-Area Attemperator

By using a variable-area attemperator, the limitations presented by a fixed nozzle may be overcome due to the fact that the profile changes with the quantity of spray water [22]. A sliding plug is used and moved by an actuator which changes the number of nozzles through which the water is sprayed.

- Variable-Annulus Desuperheater

A variable-annulus desuperheater offers accurate control of steam temperature over the widest possible dynamic range [22]. As the coolant enters the stream, its velocity is instantaneously increased, and pressure decreased so that it vaporises and develops into a micron-thin layer that is then peeled off the head and driven downstream.

2.15 Previous Work

There are numerous models of combined-cycle power plants that have been developed previously. Ali and Abdalla developed a model in order to assess the performance of combined-cycle power plants at full and part loads [23]. The model equations were solved using Matlab and were used to examine the effect of load changes and heat losses in the combustion chamber on the performance of the plant. The results were compared to that of actual plant data and it was found that deviations were between 3-5%. An exergy analysis was also performed on the model which showed that the maximum exergy destruction occurred in the combustion chamber for full and part loads. It was found that as the heat loss in the combustion chamber increases, fuel mass flow rate and the net work of the gas turbine increases while the thermal efficiency decreases.

Tică et al. developed a combined-cycle power plant for optimisation [18]. The model was developed using Dymola/Modelica, with the use of ThermoPower which is a library for modelling thermal power plants, and the components were validated by experimental data. The paper presented a method to turn a physical combined-cycle power plant model, designed for simulation, into one that optimised the start-up procedure of the plant.

Rauch et al. developed a model in Matlab which determined the maximum thermal efficiency of a combined-cycle power plant limited by gas temperature entering and exiting the gas turbine, condenser temperature and the dryness fraction at the outlet of the steam turbine [24]. The impact of adiabatic flame temperature, pinch point and the dryness fraction on the thermal efficiency of the plant was also investigated. The adiabatic flame temperature was found to have the largest

impact on the thermal efficiency of the plant with the increase in temperature causing an increase in efficiency.

Mohanty et al. investigated the effect of a change in operating parameters, such as the maximum temperature and pressure of the Rankine cycle; turbine inlet temperature; and pressure ratio of the Brayton cycle, on the net work and thermal efficiency of a combined-cycle power plant [25]. A model was developed in Matlab in order to achieve a higher net work and thermal efficiency of the plant.

Ebaid and Al-Hamdan considered the effect on combined-cycle performance of different configurations of the gas turbine engine operating as part of the plant [1]. Visual Basic was used to develop the model. It was shown that the maximum efficiency of the plant occurred when the gas cycle was not at its maximum efficiency or specific work output. It was also shown that supplementary heating or gas turbine reheating decrease the efficiency of the combined-cycle power plant. Finally, even though gas turbine intercooling enhances the performance of the gas cycle, it has a minimal effect on the performance of the plant as a whole.

Srinivas et al. used computer simulation software to assess the performance of a combined-cycle power plant at part loads [26]. The study presented the optimum process parameters of steam exiting the HRSG at part loads. It also presented the optimum combination of thermal efficiency, power output and decision variables. It was found that at lower loads, the plant requires a lower high-pressure value in order to produce suitable dry steam exiting the turbine.

Ganapathy developed a program for HRSG simulation in order to produce the thermal design and off-design performance of unfired, fired, simple or complex, multimodule, multi-pressure gas turbine HRSGs without having to physically size them [10]. This uses the known gas flow, temperature, gas analysis and steam parameters to produce temperature profiles for gas and steam as well as the duty of each component of the HRSG in design mode. The off-design performance of the HRSG can then be analysed. Textbooks by Ganapathy presented various examples of HRSG simulation.

Alobaid et al. presented a comparative study of different dynamic process simulation codes for combined-cycle power plants at design and off-design conditions [27]. A combined-cycle power plant utilising a sub-critical triple-pressure HRSG was developed using Aspen Plus Dynamics and Apros. These models were validated against plant data at 100%, 80% and 60% load. The models showed close agreement to plant data with a maximum error of around 5% for pressure and less than 1% for temperature and mass flow rate. The models were also compared to dynamic plant data during a transient operation. The models were able to predict plant data qualitatively but achieved a maximum error of 10% for quantitative predictions. The results concluded that the Aspen and

Apros models accurately predict plant data at various steady-state loads, however, the prediction of plant behaviour at low loads is less accurate.

2.16 Software

The software tools used in this study were Mathcad, Virtual Plant and Flownex [28]–[30]. Initially, Mathcad was used as a learning platform. This is a software tool used for engineering calculations and provides a tool for understanding knowns, unknowns and what is being calculated in the system.

Virtual Plant is a thermodynamic modelling software tool used for assessing plant performance. This uses plant design information and first engineering principles to predict the performance of a power plant cycle. Virtual Plant models operate as a connected system of plant components with the conservation of energy and mass. It uses design inputs such as temperature, enthalpy and mass flow (i.e. what the plant is required to do) in order to calculate the duties of each component as well as actual temperatures, enthalpies and mass flow in the system. Virtual Plant provides an HRSG component which was beneficial to this study. The fundamentals of Virtual Plant are similar to those used in the Mathcad models, therefore, the process of mathematical modelling used by Virtual Plant was well understood.

Flownex is a thermohydraulic network solver based on the numerical solutions of the governing equations of fluid dynamics and heat transfer. In order to obtain the mass flow, pressure and temperature distributions in a network, it solves partial differential equations for the conservation of mass, momentum and energy. It allows for the modelling of integrated systems in order to efficiently size components, perform flow balances and test control methodologies. For the models developed in this study, each component of the HRSG was modelled using heat exchangers or heat transfer components available on the Flownex library. Flownex uses endpoint values (initial pressure and temperature and outgoing mass flow) and the overall conductance of each component to calculate the characteristics of the flow at each intermediate point (such as temperature, enthalpy, mass flow, quality etc.). The model requires an input of what the plant will look like and calculates what it will do.

3. Single Pressure Model

3.1 Methodology

First, a single pressure system was analysed and modelled in the design mode. The steam generation, gas and steam temperature profiles and duties of the economiser, evaporator and superheater were calculated without calculating the tube sizes or lengths, fin geometry, surface area or tube spacing etc. The models only focussed on the steam cycle and the use of the exhaust gas.

The analysis of the HRSG was done using heat balance equations. Figure 14 provides a schematic showing the representation of each variable name. The variables in blue represent water/steam and those in red represent gas. The design values used for this model were obtained from a textbook written by V. Ganapathy [31]. The architecture and inputs used for the model were therefore based on that of the textbook.

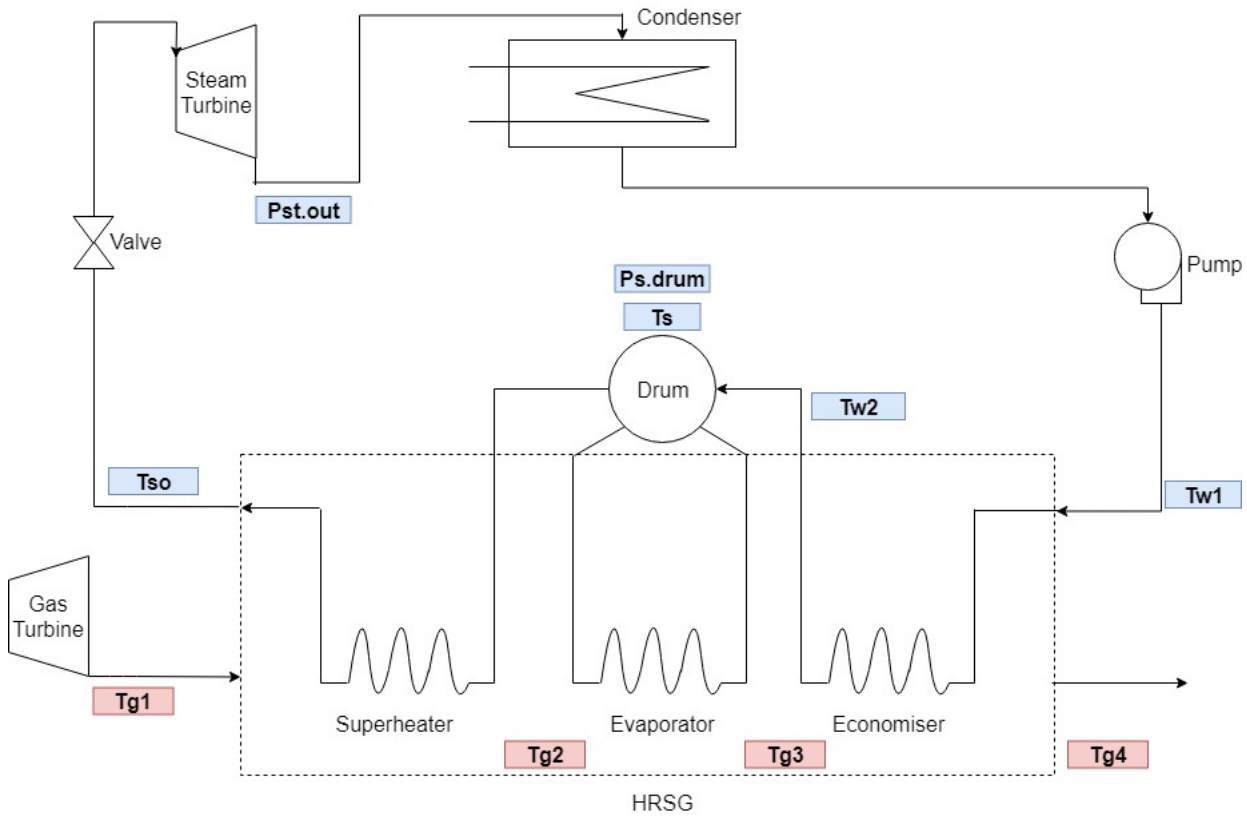

Figure 14: Schematic of a single-pressure combined-cycle power plant

3.1.1 Analytical Model - Design Case

A temperature profile of both the gas and water/steam in the HRSG was developed so that the duties of each component could be calculated and the foundation of the HRSG could be established.

The known values for the system were the exhaust gas mass flow and temperature, desired pressure of the water/steam in the HRSG, temperature of the feedwater into the HRSG and the desired temperature of steam to be generated. These values are shown in Figure 15.

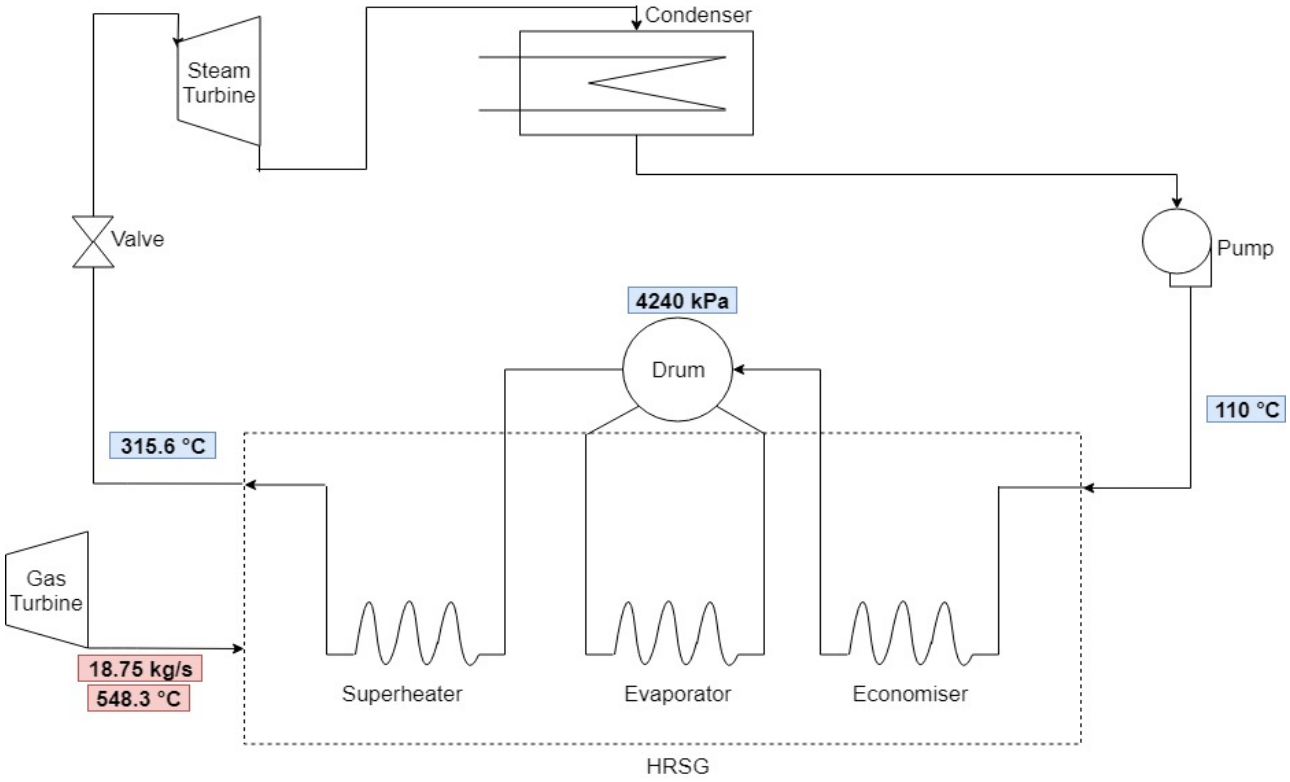

Figure 15: Schematic of the single-pressure model showing known variables

Assumptions for the pinch and approach points (8.3°C each) were made in order to form the basis of the HRSG design. The saturation temperature of water/steam in the drum was found using steam tables and the known pressure. The gas temperature exiting the evaporator, T_{g3}, and the water temperature exiting the economiser, T_{w2}, were found using the drum temperature and pinch and approach points.

The block diagram in Figure 16 shows the sequence of how the remaining values were calculated.

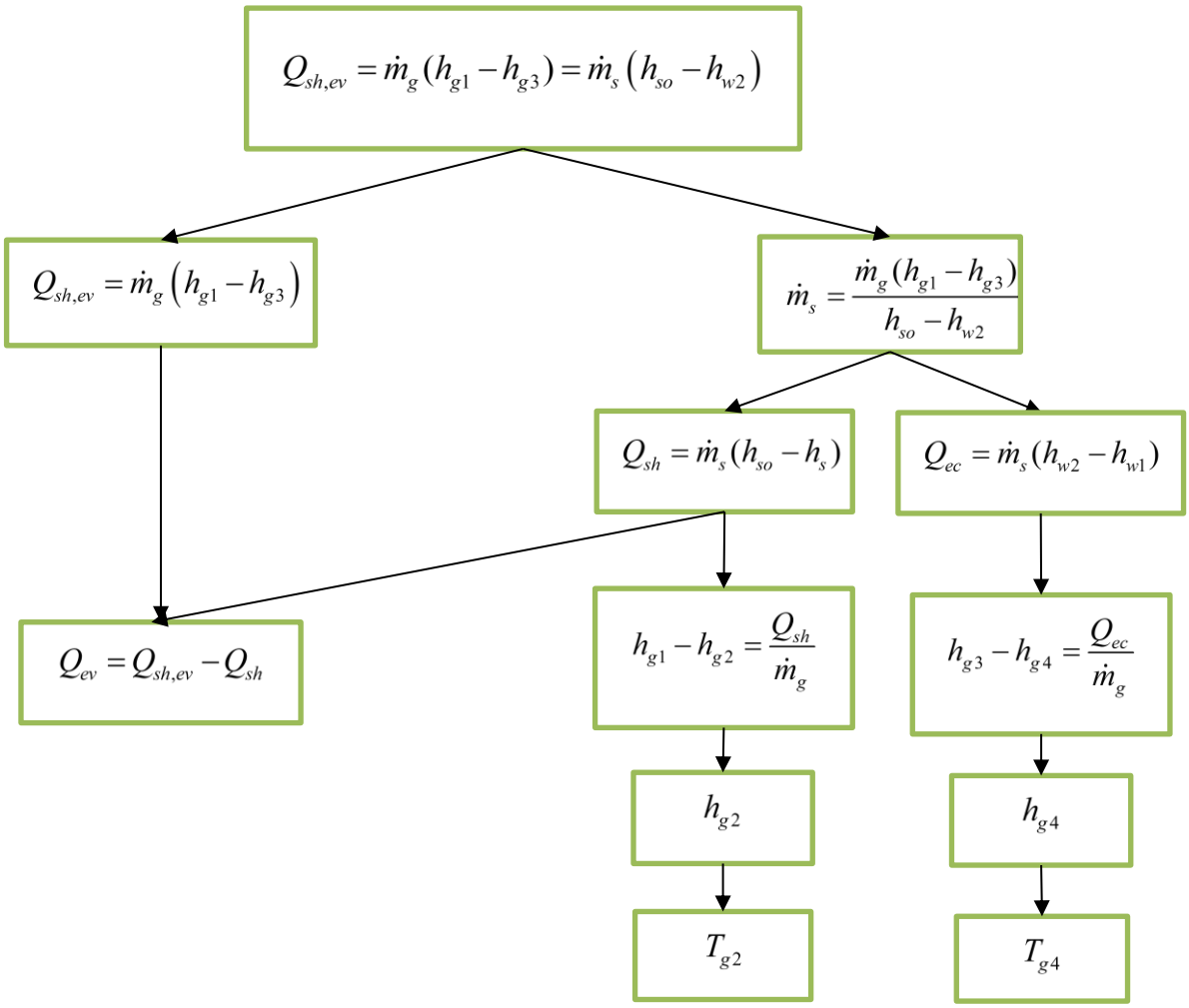

Figure 16: Block diagram showing the sequence of variables being calculated

An energy balance was done across the superheater and evaporator using the gas mass flow and change in enthalpy as shown in equation (3.1).

$$Q_{sh,ev} = \dot{m}_g\left(h_{g1} - h_{g3}\right) \tag{3.1}$$

The enthalpy of gas was used instead of specific heat (as shown in equation (2.7)), the relationship between these two characteristics is shown in equation (3.2).

$$\Delta h_g = c_{pg} \cdot (\Delta T_g) \tag{3.2}$$

As a simplification, a formula for the enthalpy of air was used to calculate the enthalpy of gas at certain temperatures. This formula for pure air is shown in equation (3.3) [32].

$$h_g(T) = 0.9816 \cdot T + 1.245 \times 10^{-4} \cdot T^2 - 1.308 \times 10^{-8} \cdot T^3 - 2.154 \times 10^{-12} \cdot T^4 \tag{3.3}$$

The duty of the superheater and evaporator as well as the change in enthalpy of steam was then used to calculate the mass flow of steam/water as shown in equation (3.4). The enthalpy of steam and water was found using steam tables.

$$\dot{m}_s = \frac{Q_{sh,ev}}{h_{so} - h_{w2}} \tag{3.4}$$

The duty of the superheater was then calculated using the steam mass flow rate as shown in equation (3.5).

$$Q_{sh} = \dot{m}_s (h_{so} - h_v) \tag{3.5}$$

The duty of the superheater was used to calculate the change in enthalpy of gas in the superheater as shown in equation (3.6).

$$h_{g1} - h_{g2} = \frac{Q_{sh}}{\dot{m}_g} \tag{3.6}$$

This was used to calculate the enthalpy of gas exiting the superheater, h_{g2}, using the known enthalpy of gas entering the superheater, h_{g1}. The enthalpy of gas exiting the superheater was then used to find the gas temperature exiting the superheater, using equation (3.3).

The duties of the evaporator and economiser were then calculated as shown in equation (3.7) and (3.8).

$$Q_{ev} = Q_{sh,ev} - Q_{sh} \tag{3.7}$$

$$Q_{ec} = \dot{m}_s (h_{w2} - h_{w1}) \tag{3.8}$$

The duty of the economiser was used to calculate the change in enthalpy of gas in the economiser, as shown in equation (3.9). This allowed for the gas temperature exiting the economiser, T_{g4}, to be calculated using equation (3.3).

$$h_{g3} - h_{g4} = \frac{Q_{ec}}{\dot{m}_g} \tag{3.9}$$

The overall conductance (UA) of each component was calculated using equation (3.10) in order for the system to be evaluated in the off-design model.

$$UA = \frac{Q}{\Delta T_{lm}} \tag{3.10}$$

Finally, the pressure drop over the steam turbine was calculated. The saturated pressure of water in the condenser was found using steam tables and the known temperature of water entering the HRSG. Using the feedwater to find the condenser pressure was for simplicity reasons and led to a

high condenser temperature and pressure. This was done to avoid a temperature change in the feedwater pump. This did not decrease the accuracy of the model as it was just for example sake. A schematic of the system showing calculated variables is shown in Figure 17.

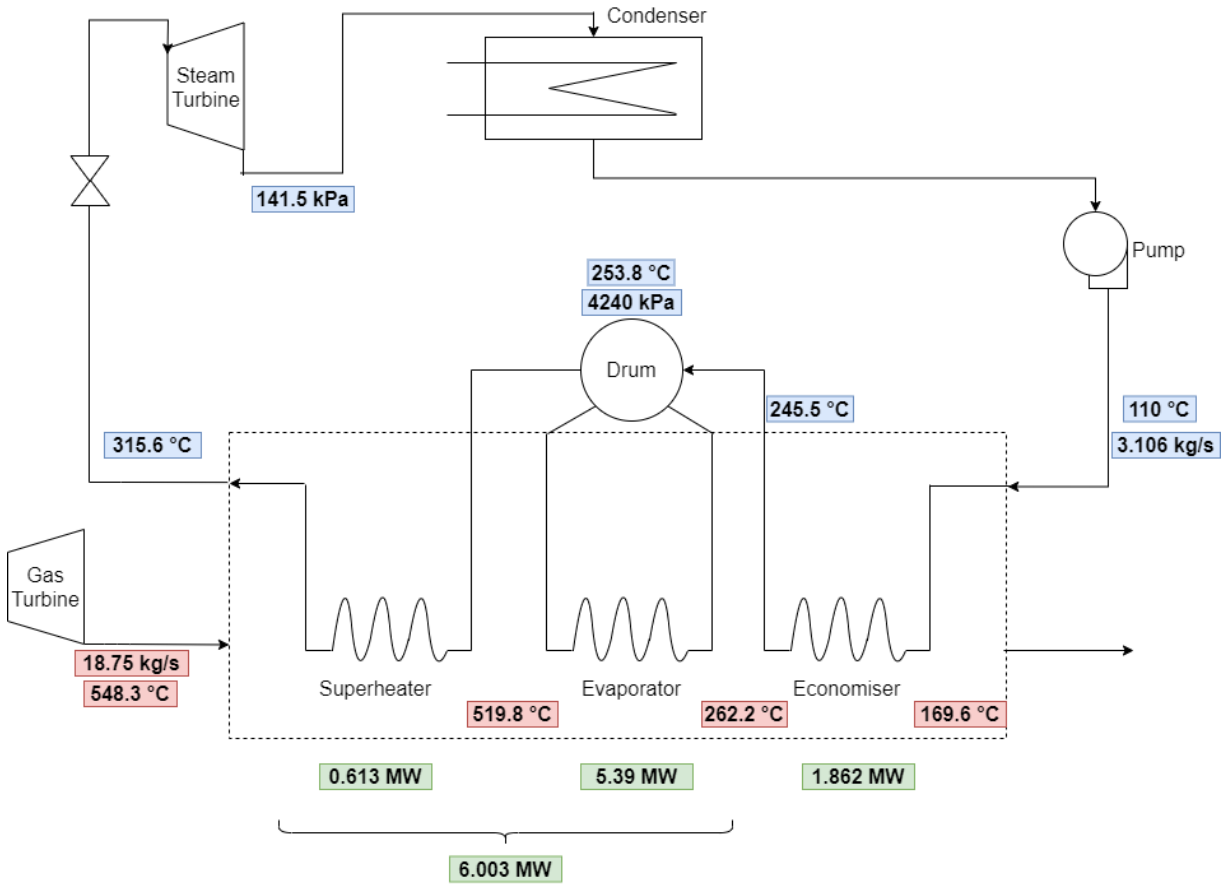

Figure 17: Single pressure schematic showing known variables

3.1.2 Analytical Model - Off-Design Case

The exhaust gas mass flow and temperature in the off-design mode followed the trend shown in Figure 13. The other known variable in the system was the temperature of the feedwater into the HRSG. The main differences between the design and off-design case are that the pinch and approach points as well as steam pressure are unknown in the off-design case. This requires a substantially different calculation sequence, which involves making an assumption for the drum pressure and iterating until a convergence is achieved.

The effectiveness of each component was used to calculate the duty of the component. First, the off-design overall conductance (UA) of each component was calculated using equation (2.39) with the assumption of *m* as 0.65. In doing so, it was assumed that the gas properties remained constant

in design and off-design cases. This would be a valid assumption since the change in the gas properties would be minimal.

In order to calculate effectiveness, the fluid heat capacity rate for both gas and water/steam in each component was required. This was done by first calculating the respective specific heat capacities at each component's average temperature and multiplying those by mass flow rates. Since no temperatures were known in the off-design case yet, the specific heat capacities were calculated using design characteristics.

An assumption was made for the steam mass flow rate in order for the fluid heat capacity rate of steam to be calculated. This value was then iterated until it equated to the calculated steam mass flow rate, as illustrated in Figure 18. In order to calculate the actual mass flow rate of steam, an assumption for the temperature of water entering the evaporator, T_{w2}, was made. This value was then iterated until it equated to the calculated value. The actual value for the temperature of water entering the evaporator was calculated using an energy balance across the economiser to calculate the enthalpy of water entering the evaporator and using steam tables to find the temperature.

The effectiveness of each component was calculated using the number of transfer units (NTU) and the fluid heat capacity rates of gas and water/steam for that component. First, the minimum and maximum fluid heat capacity rates between gas and water/steam were identified. Thereafter, the NTU and effectiveness were calculated. The effectiveness formula used for the superheater and economiser was that of a counter flow heat exchanger and for the evaporator was that considering a phase change. These were then used to calculate the duties of each component using equation (2.16). Figure 19 shows the sequence in which duties and gas temperatures were calculated.

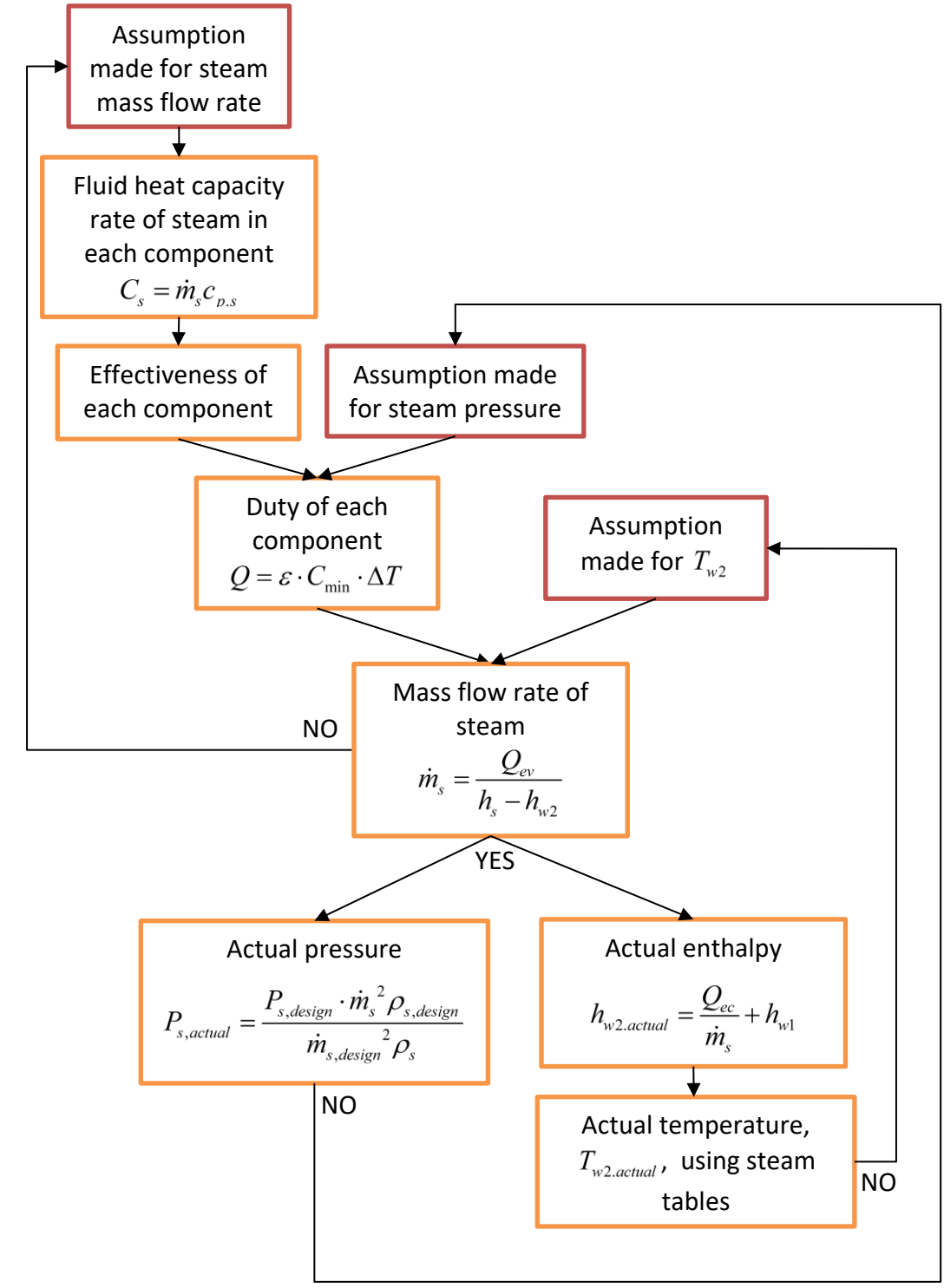

Figure 18: Iterative processes in the off-design model

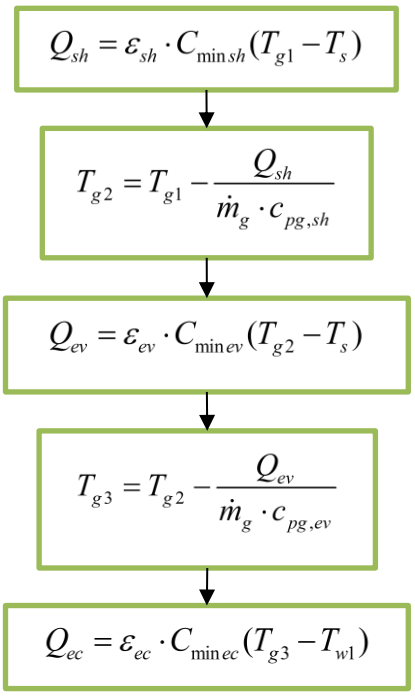

Figure 19: Block diagram showing the sequence of duties and gas temperatures being calculated

A relation between the mass flow rate of steam in the design and off-design cases was used to calculate the pressure entering the steam turbine in the off-design case. It is derived from the flow coefficient shown in equation (2.43). This is consistent with the equation used by Virtual Plant to calculate off-design pressure. The relation is shown in equation (3.11).

$$\dot{m}_{s,off} = \dot{m}_{s,design} \frac{\sqrt{P_{in,off}\rho_{in,off}}}{\sqrt{P_{in,design}\rho_{in,design}}} \tag{3.11}$$

Ideally, all valves should be open and the steam pressure in the HRSG should be equal to the turbine inlet pressure. This was used to make the iterative adjustment to the steam pressure in order to find the operational pressure at the chosen low load condition.

3.1.3 Virtual Plant Model

The inputs as well as the results obtained from the design base analytical model are needed to construct the Virtual Plant model. First, the components were connected as shown in Figure 20.

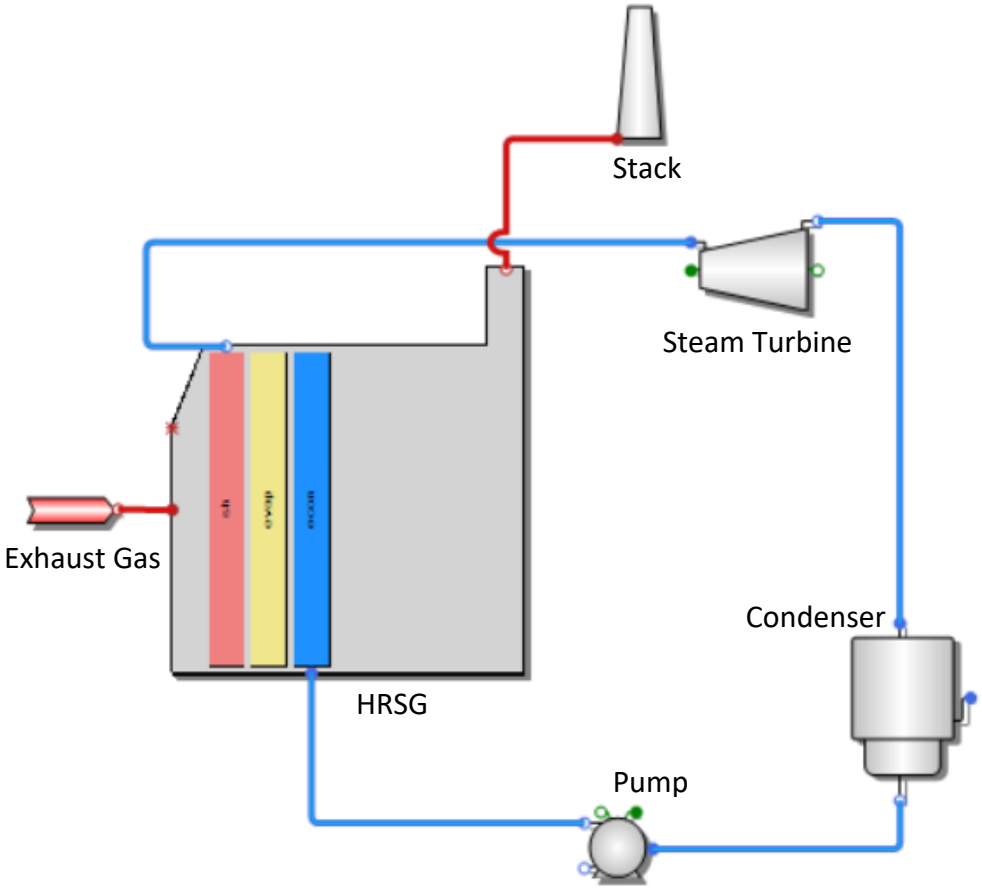

Figure 20: Single Pressure Virtual Plant model

Thereafter, the inputs to each component were defined. The gas source for the exhaust gas was defined as shown in Figure 21. This allows for the mass flow rate, pressure, temperature and composition of the inlet gas to be input. The composition of gas used was similar to that of air in order to be consistent with the enthalpy calculation done in the analytical model.

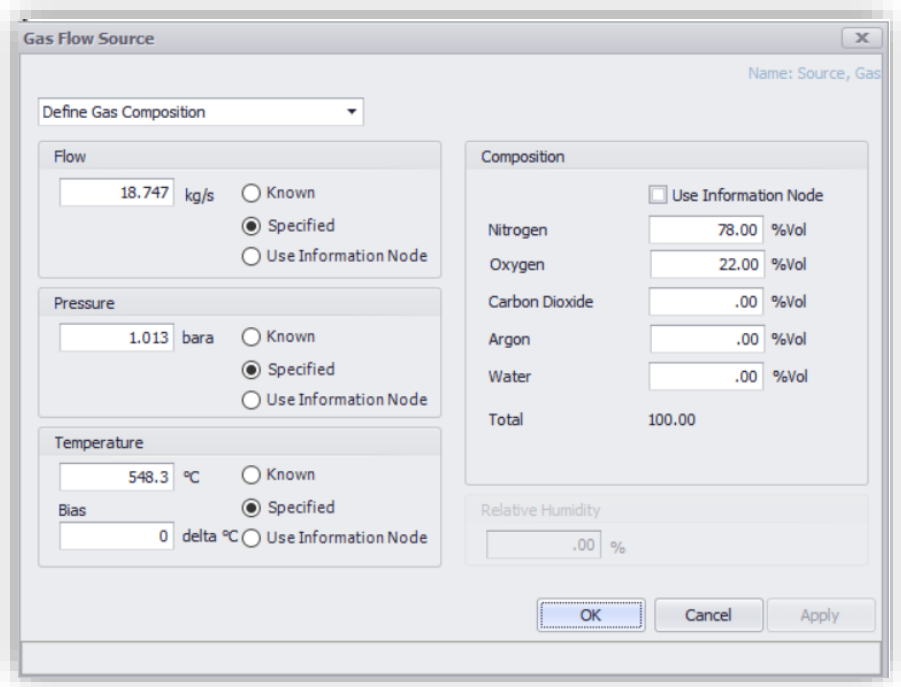

Figure 21: Exhaust gas inputs in single pressure Virtual Plant Model

The data for the HRSG was input as shown in Figure 22. The Virtual Plant model cannot be built without the analytical model as a basis, since it provides process conditions around each component which is required by Virtual Plant. The 'Gas Path Arrangement' tab requires the components to be listed in order of gas flow from hot to cold – which is first the superheater, followed by the evaporator and then economiser. A percentage of the total gas flow across the component was specified as 100% for each. The flow arrangement was chosen as counter flow for the superheater and economiser as the general flow of steam/water through them opposes the general flow of gas. This allows for the heat transfer effectiveness calculations to be the same as those in the analytical model. No changes were made to the 'Steam Side Arrangement' which provides the option to use desuperheater sprays, mixers, splitters and bypasses. 'HT Design Data' allows for most of the design process data to be defined. Gas inlet conditions and the pressure, enthalpy and mass flow rate of water/steam entering and exiting each component was entered. The 'UA Adjustment Multiplier' is used to multiply the off-design UA value when the performance of the component is below expectations as a result of fouling, or above expectations due to radiation. The 'UA Mass Flow Scaling Exponent' is used to calculate the off-design UA value. It is the exponent of the ratio of design gas flow to off-design gas flow (shown as *m* in equation (2.28)). The 'Design Fuel and Flue Gas' was used to define the composition of gas which was consistent with the composition in Figure 21.

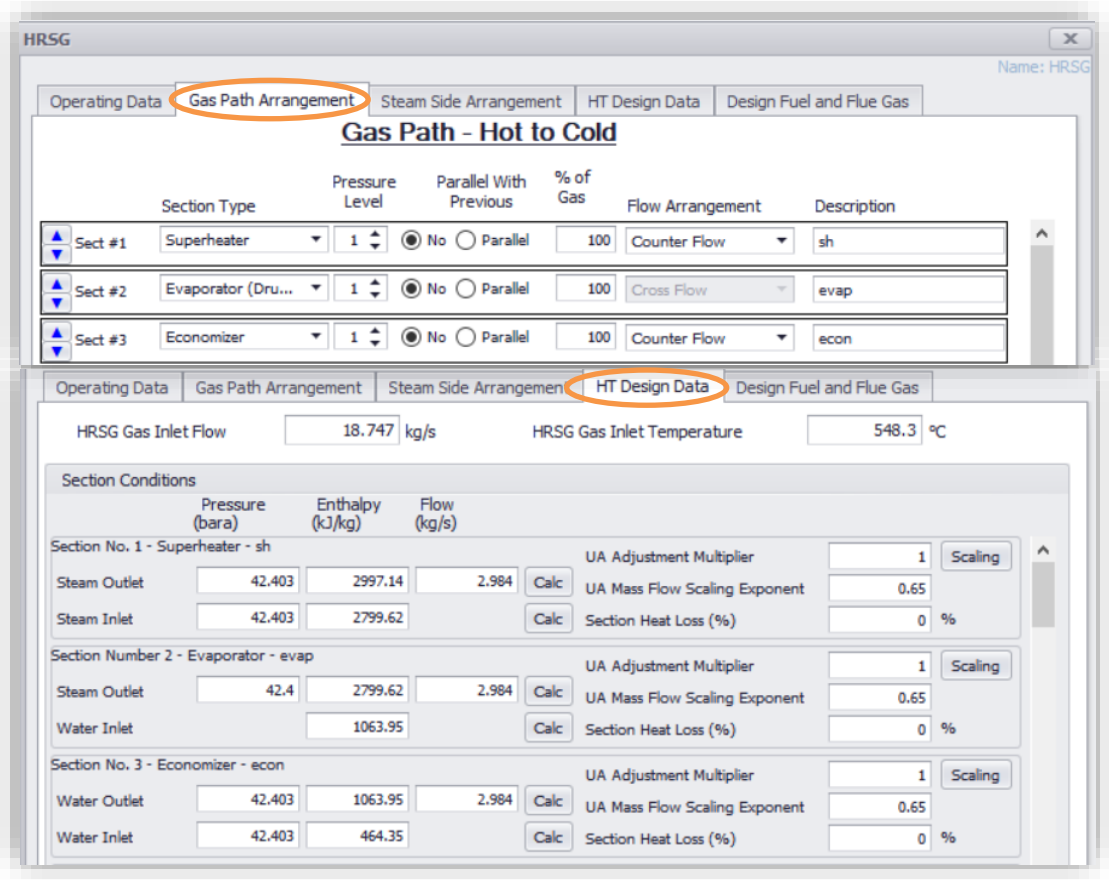

Figure 22: HRSG inputs in single pressure Virtual Plant model

Once all the data was entered on Virtual Plant and all the nodes connected, the process of running the model commenced. Virtual Plant first calculates the design UA for each component. The fluid heat capacity rate, C, of the component is then calculated for each fluid, which allows for the minimum fluid heat capacity rate, C_{min}, to be identified. The design base duty, Q, is calculated using the design data (pressure, flow and enthalpy) that was entered. Virtual Plant uses the bisection method to iteratively solve for the NTU of the component. This method solves the effectiveness equation (equation (2.17) or (2.20)) and heat transfer equation (equation (2.16)) with two unknowns (effectiveness and NTU). The UA of the component is then calculated once the NTU is found (using equation (2.18)). After calculating the design UA, the off-design UA is calculated using equation (2.28).

All values required to calculate the off-design UA are known and derived from the current iteration. After calculating the current UA, the NTU and effectiveness are calculated. Thereafter the off-design duty of the component is calculated.

This method is repeated for each component in the HRSG. Virtual Plant runs these iterations until a convergence of the outlet flows and enthalpies is achieved. If a convergence is not reached, the

failure is reported. This would mean that the system cannot be successfully calculated using the data entered.

The inputs to the steam turbine are shown in Figure 23. Design inputs included the inlet pressure, enthalpy and mass flow as well as the exhaust pressure. Constant efficiency and efficiency adjustment ratio were chosen, instead of Virtual Plant calculating the efficiency and an adjustment from efficiency curves (change in efficiency vs. throttle flow ratio). The inlet pressure calculation is the source of the relation in equation (3.11), which is derived from the flow coefficient. Virtual Plant calculates the inlet pressure, outlet mass flow and outlet enthalpy depending on the upstream flow data. The outlet pressure is obtained from the condenser. Virtual Plant uses the input design data to perform calculations for off-design modes using the flow coefficient model, similar to what was used in the analytical model.

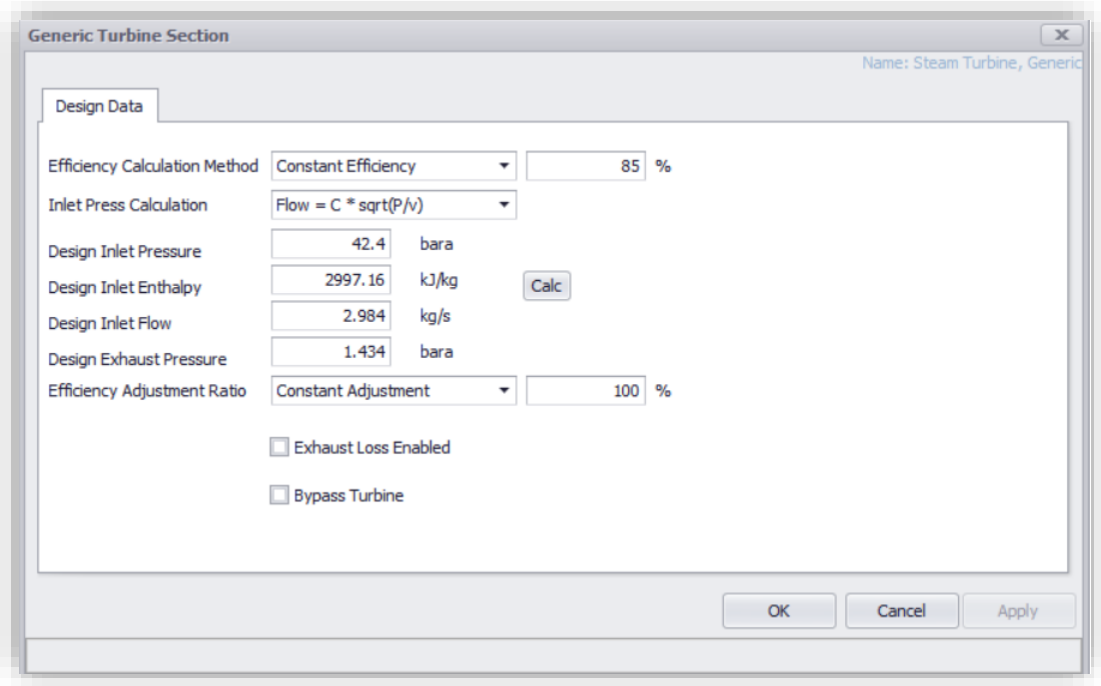

Figure 23: Steam turbine inputs in single pressure Virtual Plant model

Finally, the condenser and pump inputs are shown in Figure 24 and Figure 25. The condenser determines the expected turbine backpressure. Since constant backpressure was chosen, only the pressure and subcooling values needed to be input, which remain constant during the calculations. The subcooling temperature of the condenser was set so that the feedwater temperature equated to the required value. A subcooling temperature of -17.1°C had to be used due to a known error in Virtual Plant which makes a conversion error between 0°C and 0°F. Virtual Plant used steam flow and drain inlet flow to calculate the hotwell flow. The efficiencies, inlet and outlet pressure and outlet flow rate were specified for the pump, though these are only used as initial estimates.

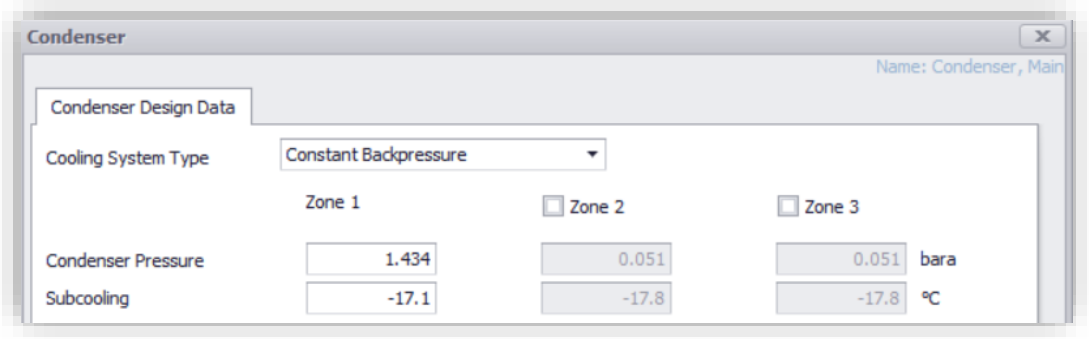

Figure 24: Condenser inputs in single pressure Virtual Plant model

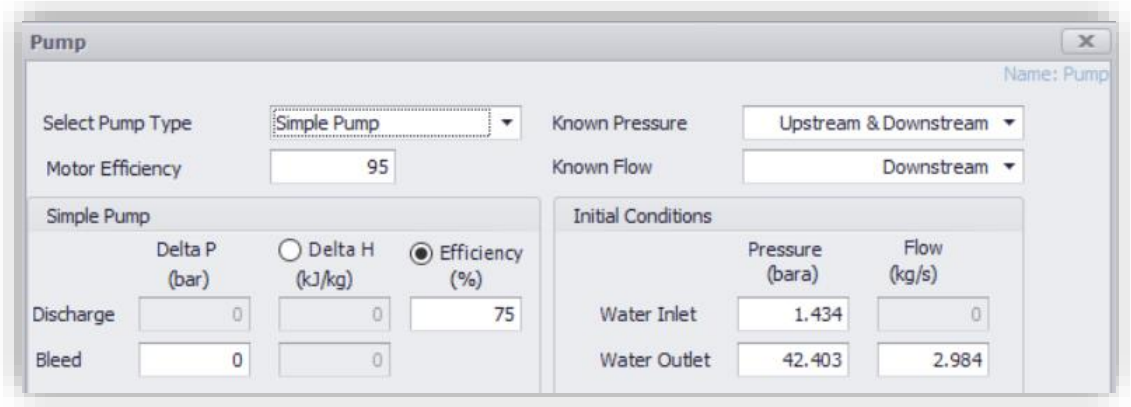

Figure 25: Pump inputs in single pressure Virtual Plant model

3.1.4 Flownex Model

The single pressure model developed in Flownex is shown in Figure 26. Unlike the Virtual Plant model, the condenser and feedwater pump are omitted from this model because creating a closed cycle in Flownex would lead to additional complications due to the difficulty of managing a two-phase tank in the model. However, this would not fundamentally affect the outcome of the HRSG results. The upper path shows the flow of gas and the lower one shows that of water/steam. Boundary conditions were used to set the temperature and pressure at the beginning of each stream. For gas, the boundary condition at the beginning of the stream was also used to set the 'Mass Source Fraction' which defines the gas composition and the one at the end of the stream set the mass flow rate. For steam, the boundary condition at the end of the stream was set as outlet pressure of the turbine. This was done to create a fixed condenser pressure.

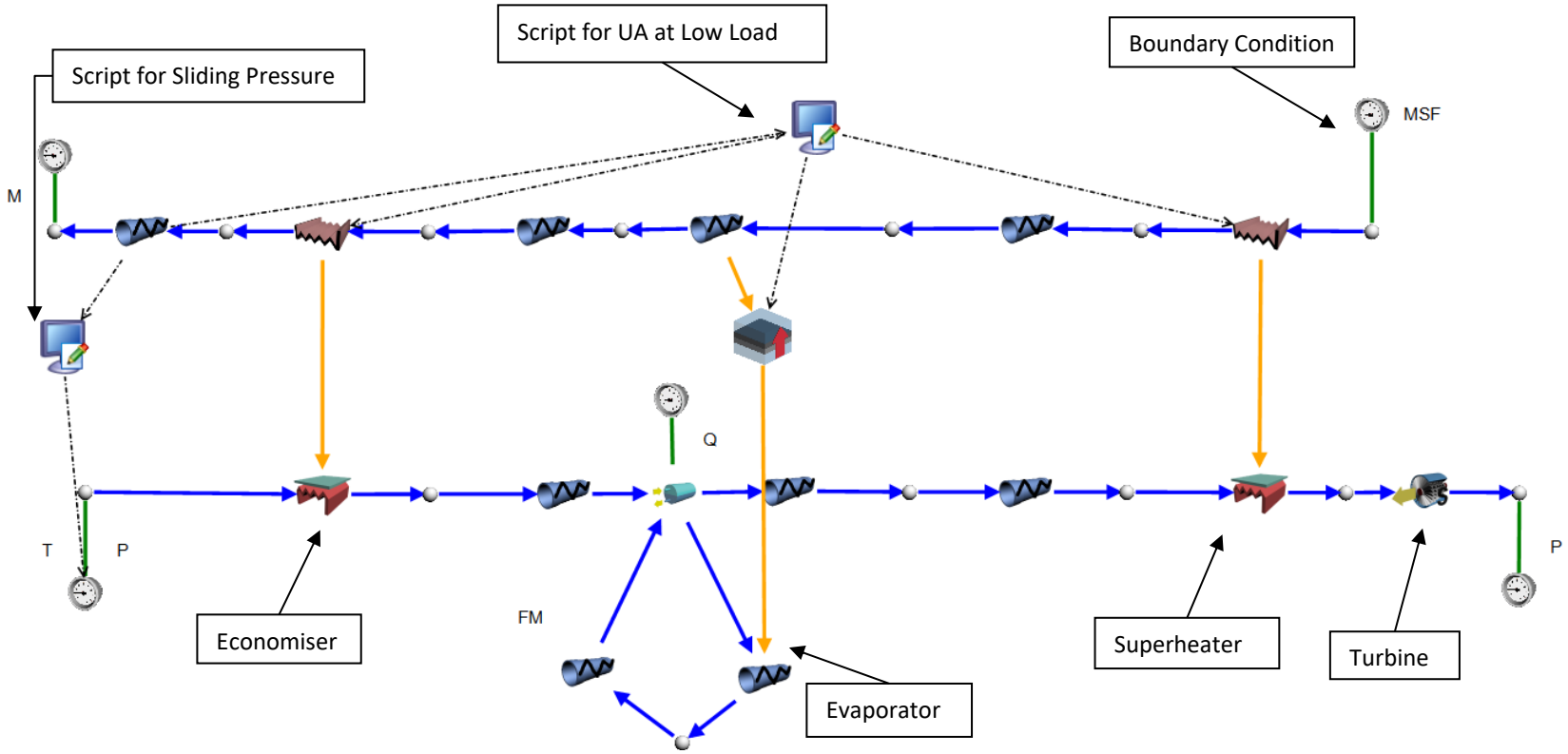

Figure 26: Single pressure Flownex model

Flow Resistance elements were used to connect all components together. These were used due to their allowance of limited geometrical information. The flow admittance to the element is inversely proportional to pressure drop across them. Therefore, these were set to a high flow admittance in order for the pressure drop across them to be negligible as it was not being modelled.

The economiser and superheater were modelled using Primary and Secondary Heat Exchanger components which allow for the overall conductance (UA) as an input. There were other Flownex components that could have been used for the economiser and superheater such as the Finned-Tube Heat Exchangers and the Shell & Tube Heat Exchangers. However, these require physical design information. Thus, the Flownex model for a combined-cycle power plant can only be developed once the analytical solution or detailed design information is available. Coefficients for pressure drop were also required as an input. These were minimised to allow for pressure drop to be negligible. Flownex uses the effectiveness-NTU method to calculate heat transfer in these elements. An example of the inputs to a Primary Heat Exchanger (gas side) is shown in Figure 27.

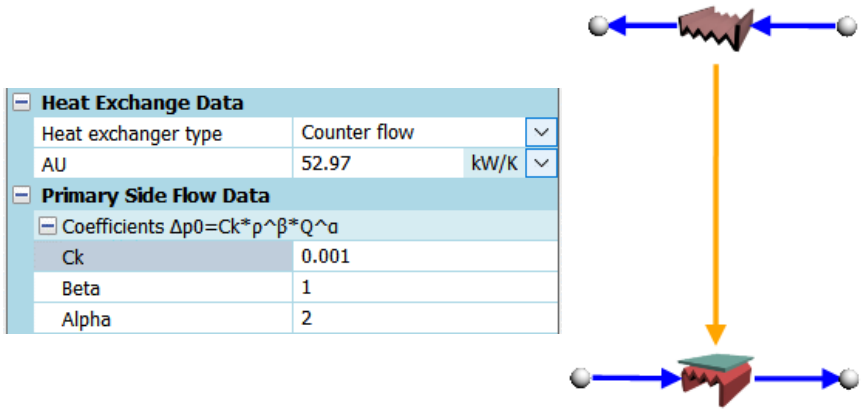

Figure 27: Inputs to a Primary Heat Exchanger

The evaporator could not be modelled using a Heat Exchanger component due to the phase change that takes place in an evaporator. It had to be manually modelled as Flow Resistances connected in a loop to a drum, where a Composite Heat Transfer Element transfers heat from the gas to one of the Flow Resistance elements in the loop. The Flow Resistance elements in the loop were discretised into multiple increments. This means that the element is subdivided into sections of equal volume that are treated as separate elements, where the pressure loss coefficient and heat transfer are equally distributed among them. This was done to accommodate the change in water properties in the evaporator. The Composite Heat Transfer Element was used to model convection to and from the pipe wall and, therefore, required the convective heat transfer coefficient for either side of the pipe wall and an area of the surface as inputs. This could be calculated from the overall conductance

as shown in equation (3.12). An area of $1m^2$ was input and it was assumed that the inner and outer convective heat transfer coefficients were equal.

$$\frac{1}{UA} = \frac{1}{h_i \cdot A_i} + \frac{1}{h_o \cdot A_o} \tag{3.12}$$

Therefore,

$$\frac{1}{UA} = \frac{1}{h} + \frac{1}{h} = \frac{2}{h}$$
$$h = 2 \cdot UA \tag{3.13}$$

UA – overall conductance [W/K]

$h_{i,o}$ – inside or outside convective heat transfer coefficient [W/m^{2}K]

$A_{i,o}$ – inner or outer pipe area [m^2]

A boundary condition was used for the drum setting the quality to 0.2. This ensures that there is always at least some water in the drum. The connection of the outgoing Flow Resistance to the superheater was set to a fraction of 1 so the steam flowing to the superheater exits the drum from the top. The connection of the outgoing Flow Resistance in the loop was set to a fraction of 0 so that water from the bottom of the drum enters the evaporator. Figure 28 depicts the location of the drum fractions.

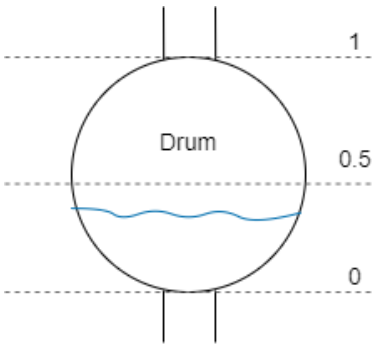

Figure 28: Drum fractions

The mass flow in one of the Flow Resistance elements was fixed to around three times the normal steam mass flow in order to ensure sufficient circulation in the evaporator. The exact value for the mass flow was not crucial, as water would keep circulating until enough heat transfer occurs to produce steam. As long as it was high enough to prevent steam from being produced too early on in the evaporator. The drum was modelled using a two-phase tank which allows for phase separation of a two-phase fluid. A parallel flow configuration was chosen for the Composite Heat Transfer Element since the general direction of flow in the evaporator is the same as (parallel to) the flow of gas. This is also consistent with the Virtual Plant model. The inputs to the Composite Heat Transfer Element are shown in Figure 29.

Conduction		
Area upstream surface	1	m²
Area multiplication factor	1	
Layers	Click here to edit...	...
Area discretization scheme	Standard (average areas)	
Configuration		
Flow configuration	Parallel	
Heat transfer grading factor	1	
Convection Radiation And Wall Flux		
Upstream		
Configuration		
Heat transfer option	Convection	
Convection		
Convection area option	Use area as specified in conduction	
Convection coefficient option	Constant h	
h	139220	W/m².K
Downstream		
Configuration		
Heat transfer option	Convection	
Convection		
Convection area option	Use area as specified in conduction	
Convection coefficient option	Constant h	
h	139220	W/m².K

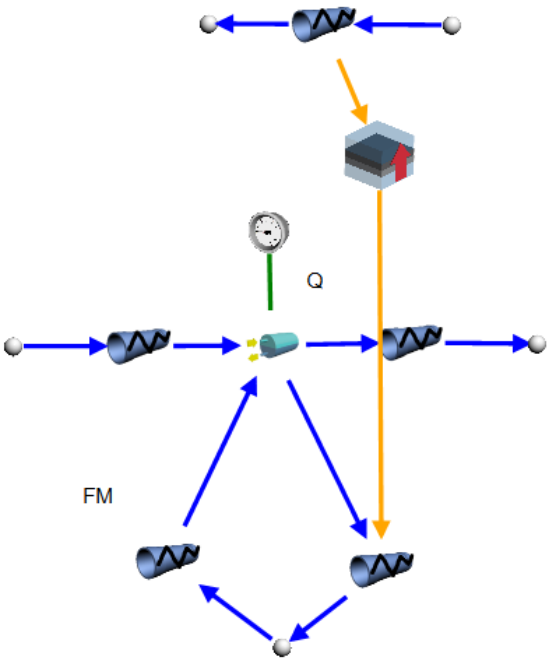

Figure 29: Inputs to a Composite Heat Transfer Element

A Simple Turbine was used to model the turbine. The empirical loss coefficient option was chosen which meant that the off-design pressure calculations were closer to the Stodola Ellipse Law rather than that used in the analytical model and by Virtual Plant. The difference in these calculations, however, were expected to cause only a minor difference in the inlet pressure value. The pressure drop across a component using the empirical loss coefficient is calculated using equation (3.14).

$$\Delta P = C_k \rho^{\beta} V^{\alpha} + \rho g \Delta z \tag{3.14}$$

C_k, β and α – pressure drop constants

V – volume flow rate [m^3/s]

The turbine required the pressure differential, volume flow rate and density at design conditions as inputs. The isentropic efficiency and speed were chosen as shown in Figure 30.

Simple Turbine Inputs		
Loss option	Empirical loss coefficient	
Empirical Loss Coefficient Inputs		
Loss coefficient option	Specify design values	
Design pressure differential	4.097	MPa
Design volume flow rate	0.171	m³/s
Design density	17.411	kg/m³
Operational Inputs		
Isentropic efficiency	0.85	0-1
Speed	5000	rpm

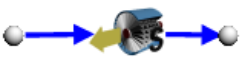

Figure 30: Inputs to the Simple Turbine

In order to find the operational pressure at each low load, the water/steam pressure was manually adjusted until the energy source of the drum became zero. The energy source represents the result of an energy balance at the drum. The reason an energy source occurs is due to over constraining the system as a result of the quality boundary condition at the drum in addition to the boundary conditions at the beginning and end of each flow. If all constraints cannot be met, an external heat source or sink must be utilised. Therefore, in order to ensure that the quality boundary condition was met without external factors, the water/steam pressure was adjusted to eliminate the energy source. Due to this manual operation and the two-phase nature of the model, the use of a condenser and feedwater pump (creating a closed cycle) would have increased the instability of the model when designing for off-load conditions.

There were other methods of finding the operational pressure at each low load such as the 'Designer' function in Flownex. It allows for the specification of an operating condition (e.g. zero energy source) while automatically calculating component sizes and capacities. This, however, was highly unstable especially in the double and triple pressure models due to the two-phase nature of the problem. Another method would be to run the model in transient mode and use a controller to find the operational pressure, however, that was beyond the scope of this project.

Two scripts were added to account for off-design modelling. The first script dealt with the off-design UA, a portion of which is shown in Figure 31. It used the gas mass flow through the Flow Resistance as an input for off-design gas mass flow (shaded in grey on the left), to calculate the off-design UA for each component (using equation (2.39)). These results (unshaded on the left) were then used to control the UA in the economiser and superheater and the convective heat transfer coefficient in the evaporator. Variables are transferred to and from the script and components using Data Transfer Links. These allow for the mass flow to be transferred from the specified Flow Resistance to the script, and for the UA to be transferred from the script to each heat transfer component. They also allow for a multiplication factor for the data being transferred which was set as *2* for the evaporator (in order to calculate the heat transfer coefficient from the UA). The off-design UA equation used in Flownex is consistent with the analytical model, however, different to that used by Virtual Plant. This is a simplification by assuming that gas properties remain constant at lower loads – a fair assumption as it wouldn't drastically change the results between the two models.

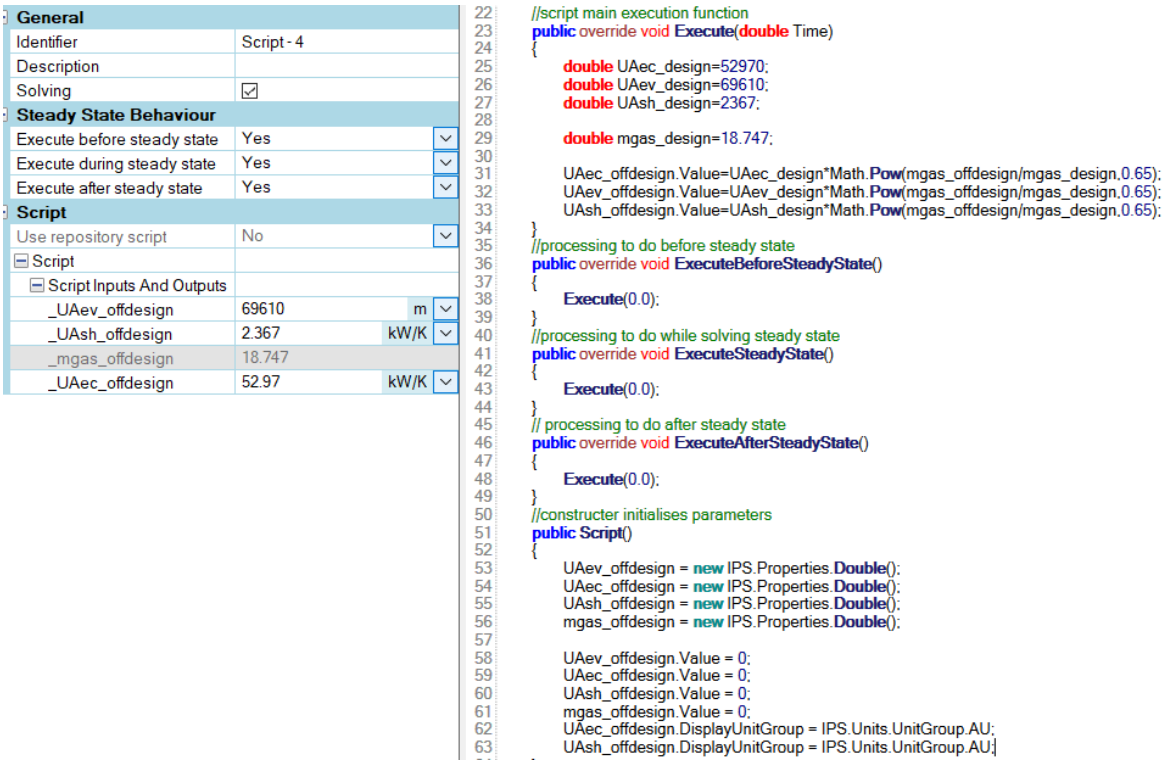

General			
Identifier	Script - 4		
Description			
Solving	☑		
Steady State Behaviour			
Execute before steady state	Yes		
Execute during steady state	Yes		
Execute after steady state	Yes		
Script			
Use repository script	No		
Script			
Script Inputs And Outputs			
_UAev_offdesign	69610	m	
_UAsh_offdesign	2.367	kW/K	
_mgas_offdesign	18.747		
_UAec_offdesign	52.97	kW/K	

```
//script main execution function
public override void Execute(double Time)
{
    double UAec_design=52970;
    double UAev_design=69610;
    double UAsh_design=2367;

    double mgas_design=18.747;

    UAec_offdesign.Value=UAec_design*Math.Pow(mgas_offdesign/mgas_design,0.65);
    UAev_offdesign.Value=UAev_design*Math.Pow(mgas_offdesign/mgas_design,0.65);
    UAsh_offdesign.Value=UAsh_design*Math.Pow(mgas_offdesign/mgas_design,0.65);
}
//processing to do before steady state
public override void ExecuteBeforeSteadyState()
{
    Execute(0.0);
}
//processing to do while solving steady state
public override void ExecuteSteadyState()
{
    Execute(0.0);
}
// processing to do after steady state
public override void ExecuteAfterSteadyState()
{
    Execute(0.0);
}
//constructer initialises parameters
public Script()
{
    UAev_offdesign = new IPS.Properties.Double();
    UAec_offdesign = new IPS.Properties.Double();
    UAsh_offdesign = new IPS.Properties.Double();
    mgas_offdesign = new IPS.Properties.Double();

    UAev_offdesign.Value = 0;
    UAec_offdesign.Value = 0;
    UAsh_offdesign.Value = 0;
    mgas_offdesign.Value = 0;
    UAec_offdesign.DisplayUnitGroup = IPS.Units.UnitGroup.AU;
    UAsh_offdesign.DisplayUnitGroup = IPS.Units.UnitGroup.AU;
```

Figure 31: Script for off-design UA

The second script controlled the sliding pressure on the steam side. This control mechanism was not required to be modelled in Virtual Plant as sliding pressure is automatically accounted for by Virtual Plant. The Flownex script extracted the mass flow rate of gas through the Flow Resistance to control the pressure input at the Boundary Condition for water/steam. In order to achieve this, the model was run at various loads to find the operational pressure at each low load by manually adjusting the pressure until the energy source of the drum was zero. The load was not decreased below 50% to ensure that only exhaust gas mass flow changes and not temperature. The operational pressures were then plotted against the gas mass flow at each load. The trend was linear so the equation for the trendline was used in the script to obtain water/steam pressure from gas mass flow.

3.2 Results

3.2.1 Design Model

The analytical results corresponded exactly with all data in the textbook from which it was obtained [31]. Therefore, the Virtual Plant and Flownex results were also compared to textbook data. The off-design results could not be compared to textbook data as it was not available.

Figure 32 shows results obtained from Virtual Plant for the HRSG. The results contain a design and actual temperature profile of gas through the HRSG; characteristics (mass flow, temperature and enthalpy) of water/steam at the inlet and outlet of each component; the heat input to the HRSG; and characteristics (mass flow, pressure, enthalpy and temperature) of water/steam and gas at the inlet and outlet of the HRSG. The design and actual gas temperatures represent those at design load and off-design load. If the values are the same, it means that the model is running at design base conditions.

Gas Temperature Profile:

Section	Design, °C	Actual, °C
sh	548.3	548.3
evap	519.9	519.9
econ	262.4	262.4
Exit	170.1	170.1

Steam/Water Conditions:

Pressure Level #1:	Inlet	Outlet	
sh	2.984	2.984	kg/s
	253.8	315.6	°C
	2799.62	2997.15	kJ/kg
evap	2.984	2.984	kg/s
	245.5	253.8	°C
	1063.94	2799.62	kJ/kg
econ	2.984	2.984	kg/s
	110	245.5	°C
	464.3	1063.94	kJ/kg

HEAT INPUT: 7.558 MW
Has Run: True

Node Name	Flow kg/s	Press bara	Enth kJ/kg	Temp °C
Duct Burner Controlled Flow	0	0	0	-17.8
Press Level #1 Inlet Node	2.984	42.399	464.3	110
Press Level #1 Outlet Node	2.984	42.399	2997.15	315.6

Node Name	Flow kg/s	Press bara	Enth kJ/kg	Temp °C
GT Compressor Inlet Information	0	0	0	25
Gas into HRSG	18.747	1.013	550.6	548.3
Gas out to Stack	18.747	1.013	147.44	170.1

Figure 32: Results from single pressure Virtual Plant model

The Virtual Plant model also produces results for the steam turbine, condenser, pump, gas source and stack.

The Flownex model produced detailed results such as pressure, temperature, mass flow, quality and numerous fluid variables at each component and node. In order to compare the results of the design case model between each software (Mathcad, Virtual Plant and Flownex), the temperature profiles for water/steam and gas in the HRSG were extracted as this provided the output of the system. The graph in Figure 33 shows the comparison. The 'econ out' and 'evap in' values are the same as well as the 'evap out' and 'sh in' since they represent the points at the end and beginning of the components. These were, however, plotted separately since Virtual Plant calculates these values from either end. Therefore, the horizontal line represents the consistency in the model.

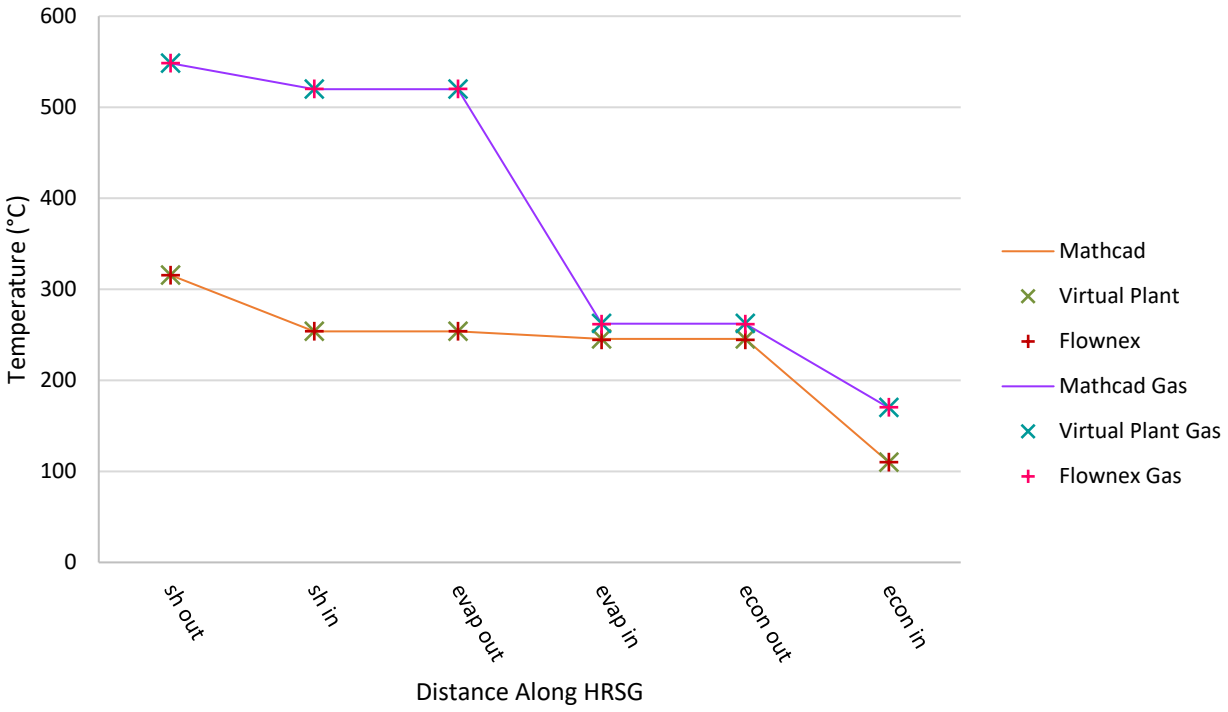

Figure 33: Graph showing comparison of single pressure models

The graph depicts a strong agreement between the models. The other results, such as mass flow rate, pressure and heat uptake, were also consistent throughout all three models. This shows that the analytical and Flownex model produce results as would be expected from a single pressure combined-cycle power plant.

3.2.2 Off-Design Model

The graph of the water/steam and gas temperature profiles for the analytical, Virtual Plant and Flownex single pressure models at 80% load is shown in Figure 34.

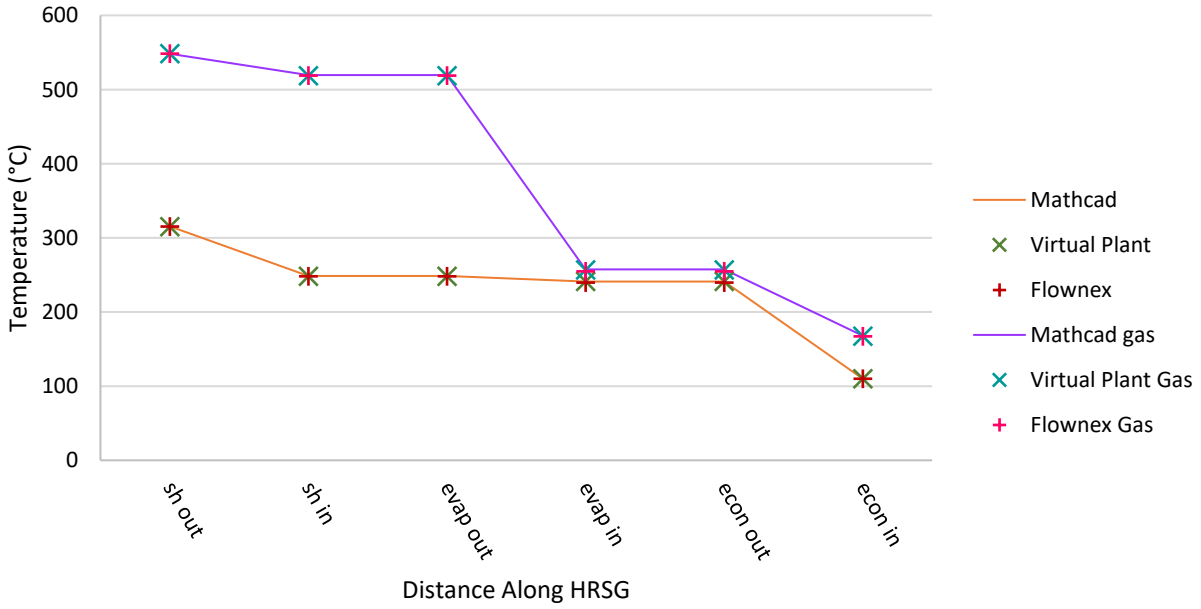

Figure 34: Graph showing comparison of single pressure models at 80% load

The off-design results for all models agreed closely with each other. Results obtained at 60% load are shown in Figure 35.

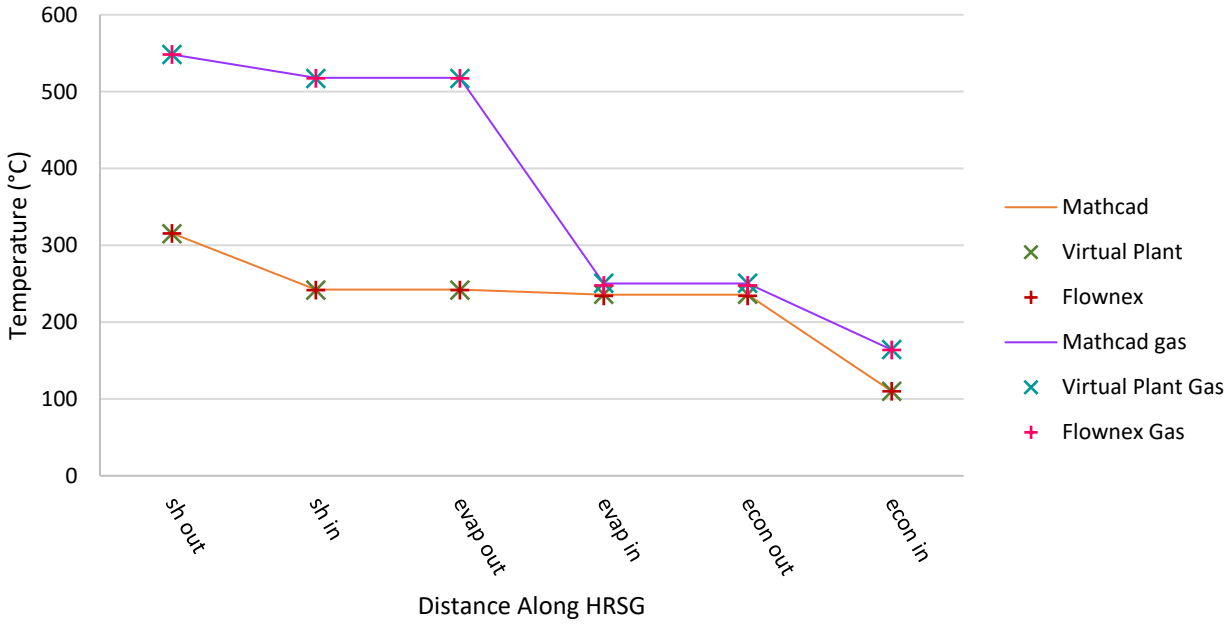

Figure 35: Graph showing comparison of single pressure models at 60% load

Once again, the results agreed closely with each other, which shows that there was consistency in the off-design models. This showed that Flownex was successful for off-design modelling.

4. Double Pressure Model

4.1 Methodology

A double pressure model meant adding another drum. The model is therefore made up of a low-pressure system and a high-pressure system. In this model, the low-pressure system is composed of an economiser and evaporator only and the high-pressure system is composed of an economiser, evaporator and superheater. Water from the low-pressure drum is sent through a pump to the high-pressure economiser. Steam exiting the high-pressure steam turbine and the LP drum mix before entering the low-pressure steam turbine. A schematic of the double pressure model, showing all variable names, is shown in Figure 36. The architecture and values used for this model were obtained from a textbook written by V. Ganapathy [31]. The reason there was no low-pressure superheater in the system was in order to be consistent with the textbook.

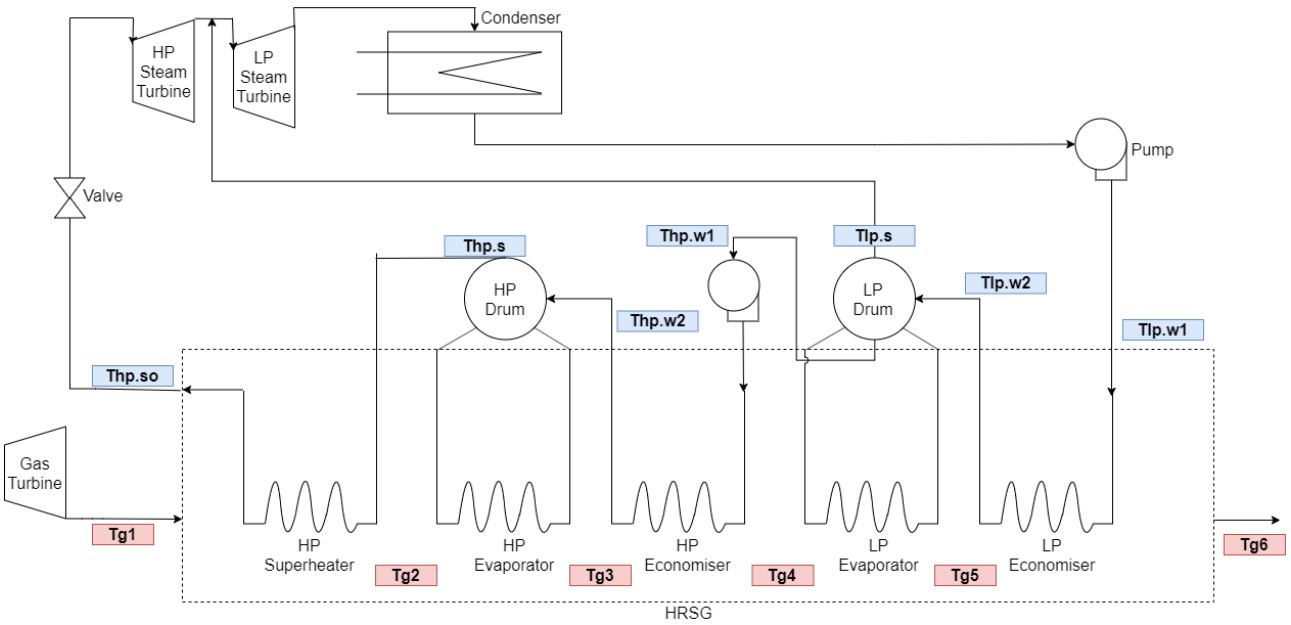

Figure 36: Schematic of a double pressure combined-cycle power plant

4.1.1 Analytical Model

The approach to modelling the double pressure system was similar to that of the single pressure system. However, due to the increased complexity, the mass flow rate of each pressure level had to be known. Figure 37 shows the known variables of the system.

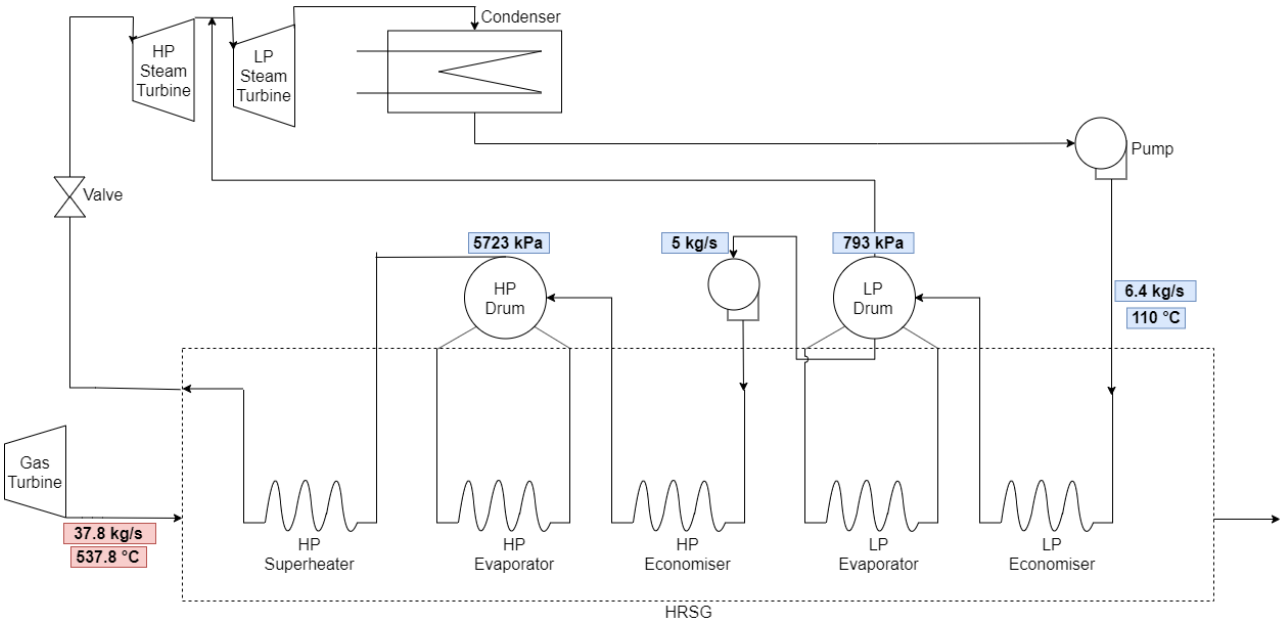

Figure 37: Schematic for a double pressure system showing known variables

Once again, assumptions were made for the pinch points (27.8°C for high-pressure and 5.6°C for low-pressure) and approach points (8.3°C for high-pressure and 5.6°C for low-pressure). The saturation temperatures of water/steam in each drum were found using steam tables and the known pressures. The gas temperature exiting each evaporator, T_{g3} and T_{g5}, and the water temperature exiting each economiser, $T_{LP.w2}$ and $T_{HP.w2}$, were found using the drum temperature and pinch and approach points.

The process of calculations in the double pressure model is shown in Figure 38.

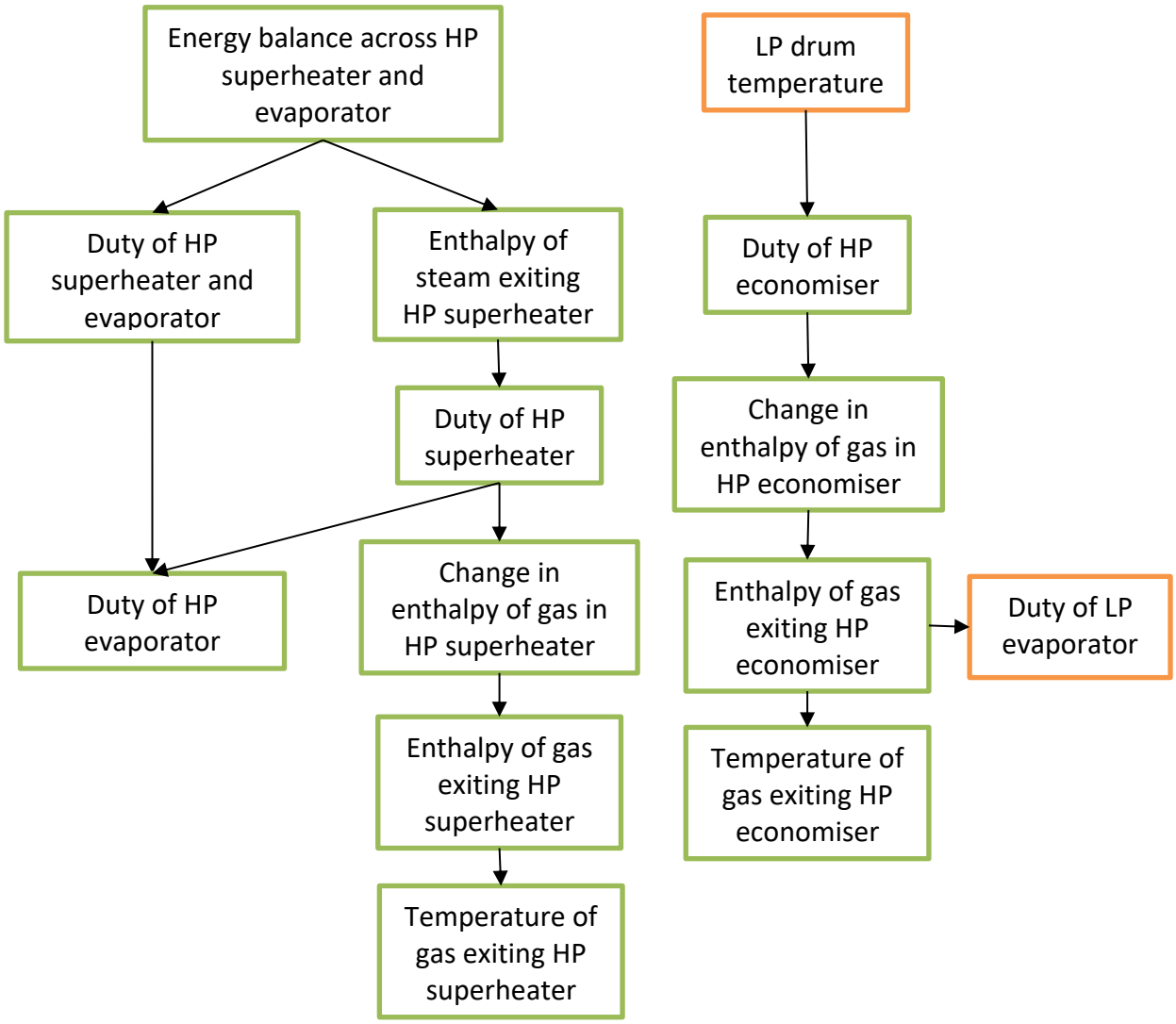

Figure 38: Block diagram showing the sequence of double pressure variables being calculated

An energy balance was done across the high-pressure superheater and evaporator using the gas mass flow and change in enthalpy. The equation used to calculate the enthalpy of gas was the same as that of the single pressure model (shown in equation (3.3)).

The duty of the high-pressure superheater and evaporator combined, steam mass flow rate and the enthalpy of water entering the evaporator were then used to find the temperature of the steam exiting the superheater.

The duty of the high-pressure superheater could then be found using the steam mass flow rate and change in enthalpy. This was used to calculate the enthalpy of gas exiting the superheater using that of gas entering the superheater. The enthalpy of gas exiting the superheater was then used to find the gas temperature exiting the superheater, using the enthalpy equation in equation (3.3).

The duties of the high-pressure evaporator and economiser were then calculated. The duty of the high-pressure economiser allowed for the gas temperature exiting the economiser to be calculated using equation (3.3). The water temperature entering the high-pressure economiser was equated to the low-pressure drum temperature.

The duty of the low-pressure economiser was calculated using the low-pressure steam mass flow and change in enthalpy. This was then used to calculate the gas temperature exiting the HRSG. The duty of the low-pressure evaporator was then calculated using gas mass flow rate and change in enthalpy.

In order to calculate the enthalpy of steam entering the low-pressure turbine, the mixture of the exhaust of the high-pressure turbine and steam from the low-pressure drum had to be considered. First, the entropy of steam entering the high-pressure turbine was found using steam tables. This was then used to find the isentropic enthalpy of steam exiting the high-pressure turbine, also using steam tables. The actual enthalpy could then be found using equation (4.1).

$$h_{ex.actual} = (h_{ex.s} - h_{in}) \cdot \eta_s + h_{in} \tag{4.1}$$

$h_{in,ex}$ – enthalpy entering or exiting the turbine [kJ/kg]

η_s – isentropic efficiency of the turbine

The enthalpy of the mixture was then found using equation (4.2).

$$h_{mix} = \frac{\dot{m}_{s,hp} \cdot h_{ex.actual} + \left(\dot{m}_{s,lp} - \dot{m}_{s,hp}\right) \cdot h_{lp.v}}{\dot{m}_{s,lp}} \tag{4.2}$$

$h_{mix,\ lp.v}$ – enthalpy of the mixture and the flow exiting the LP drum [kJ/kg]

$\dot{m}_{s,\ hp,\ lp}$ – steam mass flow rate of high- and low-pressure flows [kg/s]

The overall conductance (UA) of each component was calculated in order for the system to be evaluated in the off-design mode. The saturation pressure of water in the condenser was found using steam tables and the known temperature of water entering the HRSG.

An analytical off-design model was not done for the double pressure system as there would be too many unknowns.

4.1.2 Virtual Plant

The variables obtained from the analytical model were used in the Virtual Plant model shown in Figure 39.

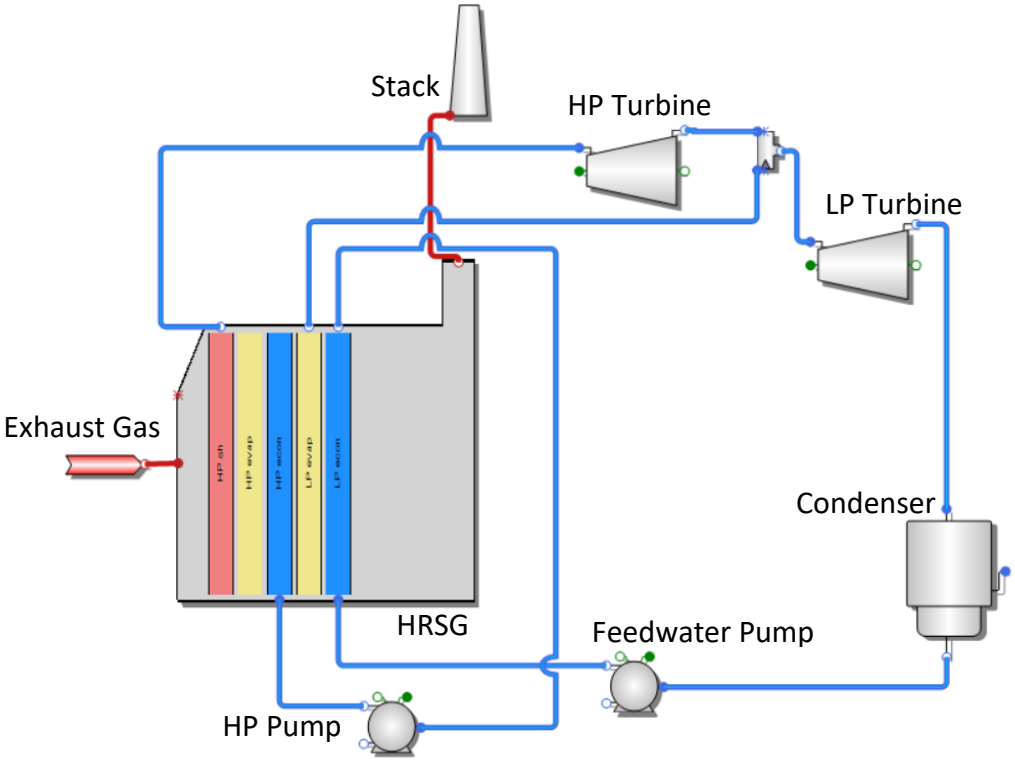

Figure 39: Double pressure Virtual Plant model

The gas composition used for the exhaust gas was, again, similar to that of air. As part of the inputs to the HRSG, the 'Gas Path Arrangement' was set according to the schematic in Figure 37. In the 'Steam Side Arrangement', a split to the cycle was added after the low-pressure economiser to accommodate the water being transferred to the high-pressure system as shown in Figure 40.

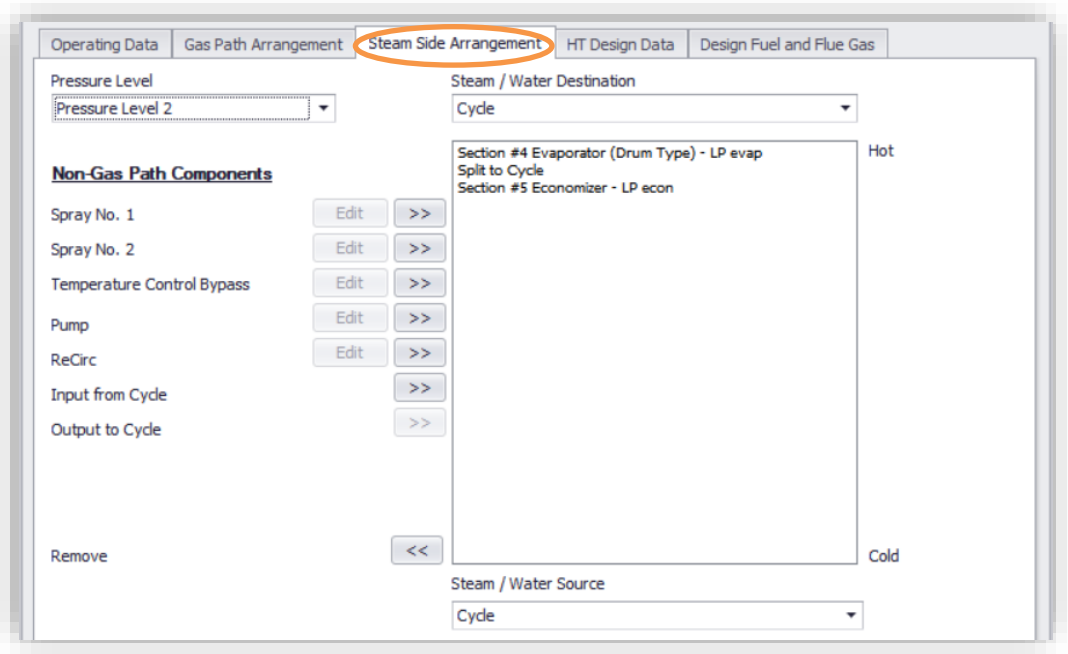

Figure 40: HRSG inputs in double pressure Virtual Plant model

The gas mass flow and temperature and water/steam pressures, enthalpies and mass flows were entered in 'HT Design Data' as shown in Figure 41.

Figure 41: HRSG inputs in double pressure Virtual Plant model

The inputs to the high- and low-pressure turbines were set accordingly. The enthalpy of the gas entering the low-pressure turbine equated to the mixture of the exiting steam from the high-pressure turbine and steam from the low-pressure drum. Constant efficiency and adjustment ratio were chosen. The efficiencies used for both pumps in the system were consistent with that of the single pressure model.

For the off-design model, only the gas mass flow in the gas source was changed according to the load. Virtual Plant automatically calculates characteristics in the off-design mode.

4.1.3 Flownex Model

The double pressure model developed in Flownex is shown in Figure 42. Once again, the upper path shows the flow of gas and the lower one shows that of water/steam. Boundary conditions were used to set the temperature and pressure at the beginning of each stream. For gas, the boundary condition at the beginning of the stream was also used to set the 'Mass Source Fraction' and the one at the end of a stream set mass flow rate. For steam, the boundary condition at the end of the stream set the outlet pressure of the low-pressure turbine.

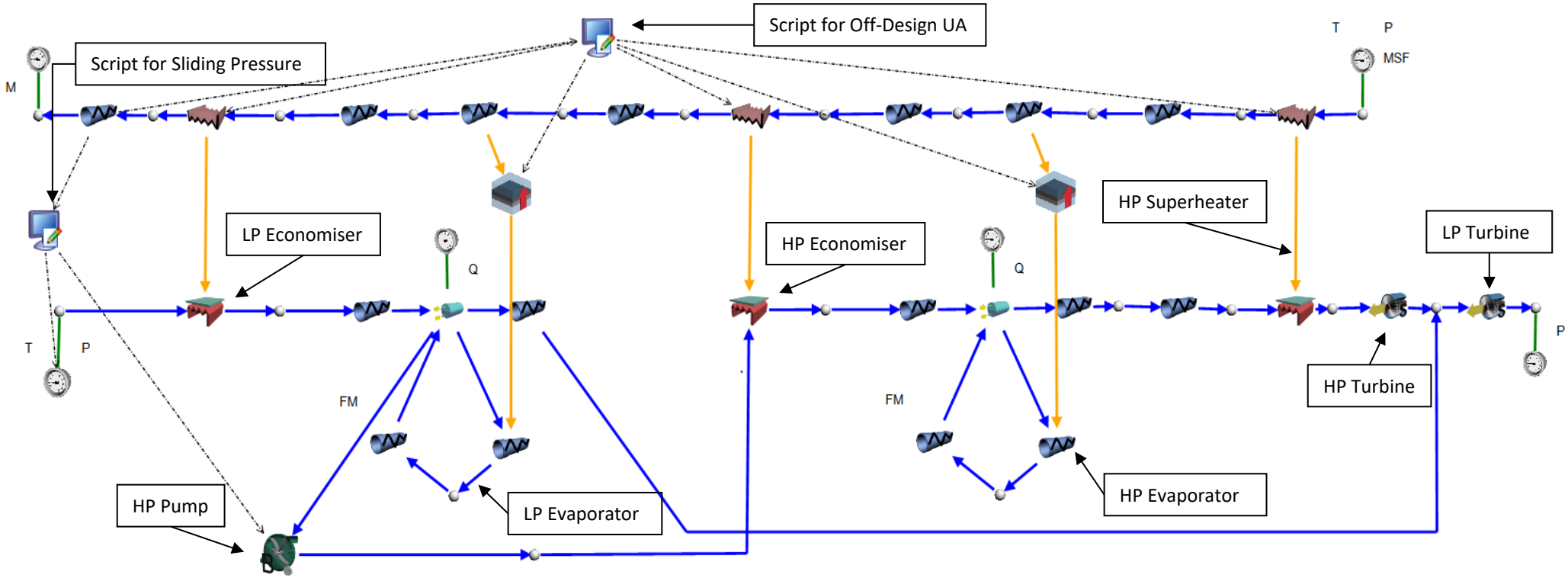

Figure 42: Double pressure Flownex model

The Flow Resistance elements were set to a high flow admittance to create a negligible pressure drop once again. The UA of the economisers and superheater were used as inputs to the Heat Exchangers. The coefficients for pressure drop in them were consistent with the single pressure model.

The evaporators were modelled the same as in the single pressure model. An area of $1m^2$ was used for the Composite heat Transfer Element and the convective heat transfer coefficients were calculated using the UA of the evaporators as in equation (3.12). A boundary condition maintained the quality of the drum at 0.2 and the mass flow rate in one of the Flow Resistances in the loop was fixed.

Water was extracted from the low-pressure drum for the high-pressure system. A Basic Centrifugal Pump was used for the high-pressure pump. The inputs required for the pump included the head at Best Efficiency Point and the volume flow at Best Efficiency Point. The head was calculated from the pressure rise equation shown in equation (4.3).

$$\Delta P = \rho \cdot g \cdot \Delta H \tag{4.3}$$

ΔP – pressure drop [Pa]

ρ – density of fluid [kg/m^3]

g – gravitational acceleration [m/s^2]

ΔH – fluid head [m]

The density of the water was found using steam tables and the known inlet pressure and temperature. Using this, the volume flow could also be calculated as shown in equation (4.4).

$$V_{pump} = \frac{\dot{m}_s}{\rho} \tag{4.4}$$

V_{pump} – Volume flow rate through the pump [m^3/s]

$\dot{m}_s$ – mass flow rate of water through the pump [kg/s]

The inputs to the pump are shown in Figure 43.

Pump Design/BEP Conditions		
Head at BEP	564.633	m
Volume flow at BEP	0.005511	m³/s
Dimensionless speed option	Apply reference chart	
Efficiency at BEP	0.75	0-1
Pump design criteria	Specify number of stages	
Number of stages	1	

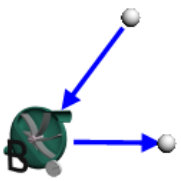

Figure 43: Inputs to the high-pressure pump

After exiting the high-pressure steam turbine, the high-pressure steam mixes with steam from the low-pressure drum to enter the low-pressure steam turbine.

Once again, scripts were used to account for off-design modelling. A script was used to calculate the UA of each heat exchanger for off-design cases. Another script was added to calculate the operational pressure for the low-pressure level as was done in the single pressure model. This script was also used to control the pressure in the high-pressure level by changing the pump head. The low-pressure value and pump head were found for various low loads. This was done by manually adjusting the water/steam pressure at the boundary condition for the low-pressure level as well as the pump head for the high-pressure level until the energy source for both drums were close to zero. The values for pressure and pump head were then plotted separately against gas mass flow which resulted in linear trends. The equations for the graphs were then used in the sliding pressure script in order to calculate the low-pressure value and pump head from gas mass flow.

4.2 Results

4.2.1 Design Model

The temperature profiles of water/steam and gas obtained from the double pressure models are shown in Figure 44. These results were also validated due to the fact that all data for the system was available from the textbook from which it was obtained, allowing all intermediate temperatures for gas and steam to be validated [31].

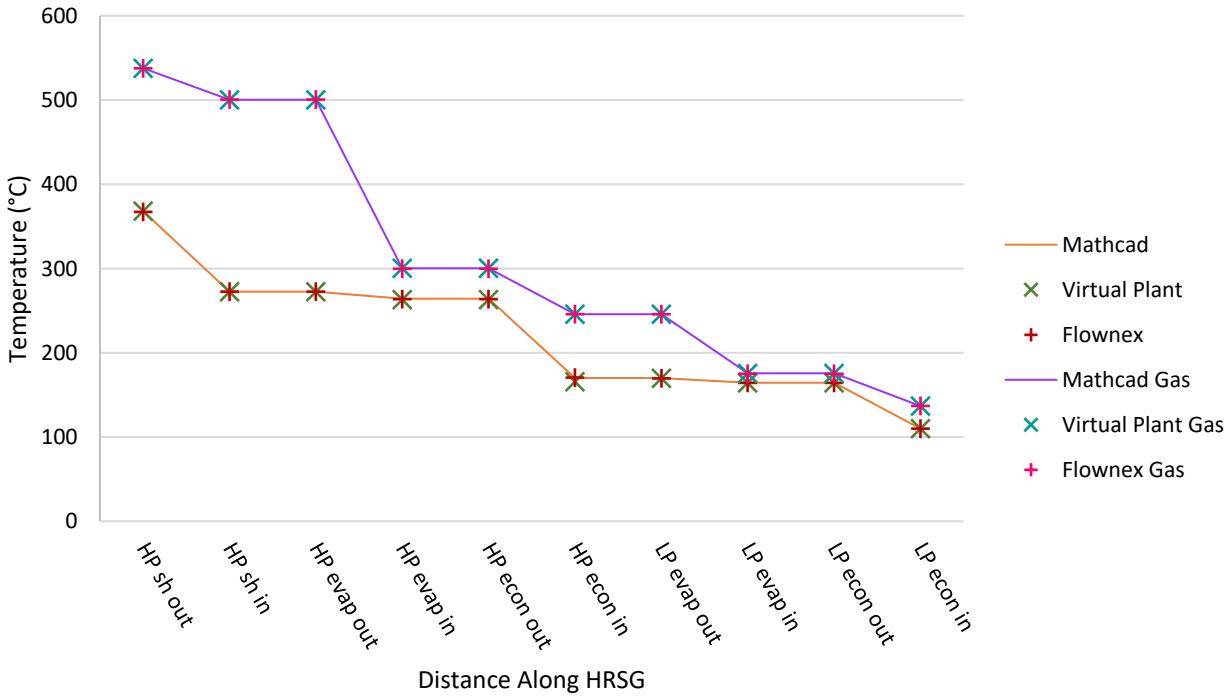

Figure 44: Graph showing comparison of double pressure models

There is a small difference in temperature at the inlet of the high-pressure economiser (HP econ in) of the Virtual Plant model. This occurred because Virtual Plant extracts water from the exit of the economiser (before it enters the drum) for the higher pressure level since the split to cycle is positioned at that point. If the split to cycle was set at the drum, it would lead to steaming in the high-pressure economiser. This was due to the fact that the connection point for the splitter to the drum could not be controlled in Virtual Plant as was done in Flownex (at a fraction of *0*). Thus, Virtual Plant extracts steam from the drum. This was not an issue for the analytical model since the temperature of the water entering the high-pressure level could be set to the drum temperature. The results closely agree with each other once again.

4.2.2 Off-Design Model

A comparison of the Virtual Plant and Flownex models run at 80% load are shown in Figure 45.

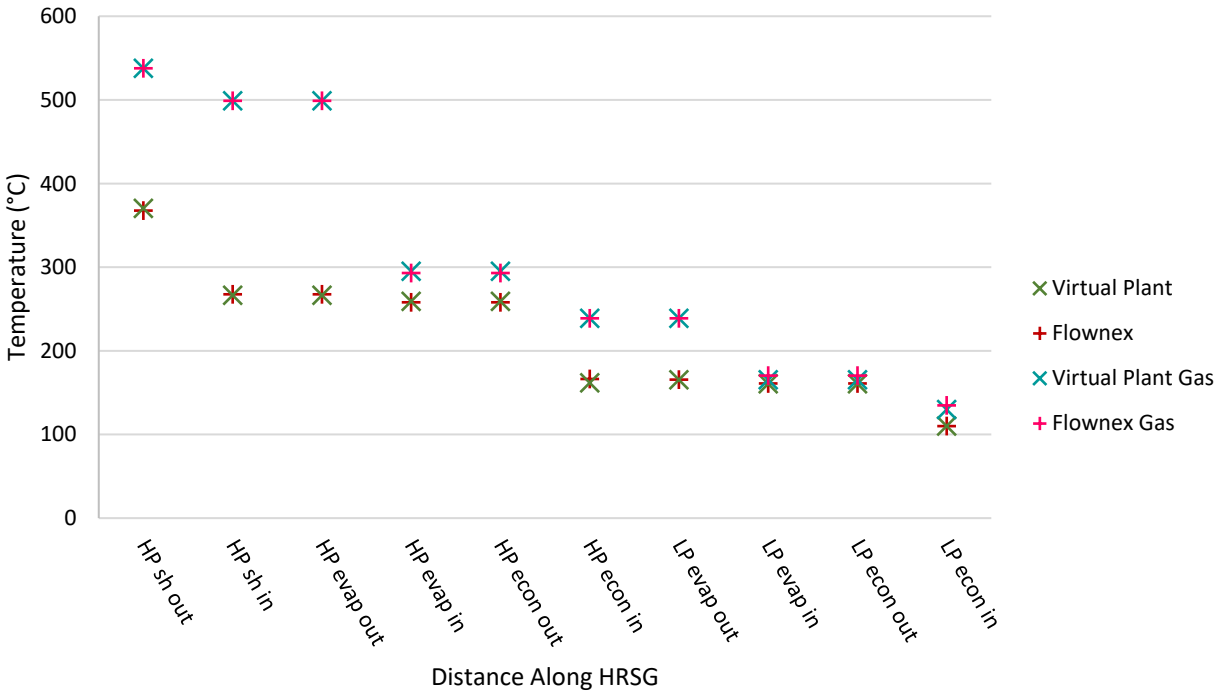

Figure 45: Graph showing comparison of double pressure models at 80% load

Results for the Virtual Plant and Flownex models run at 60% load are shown in Figure 46.

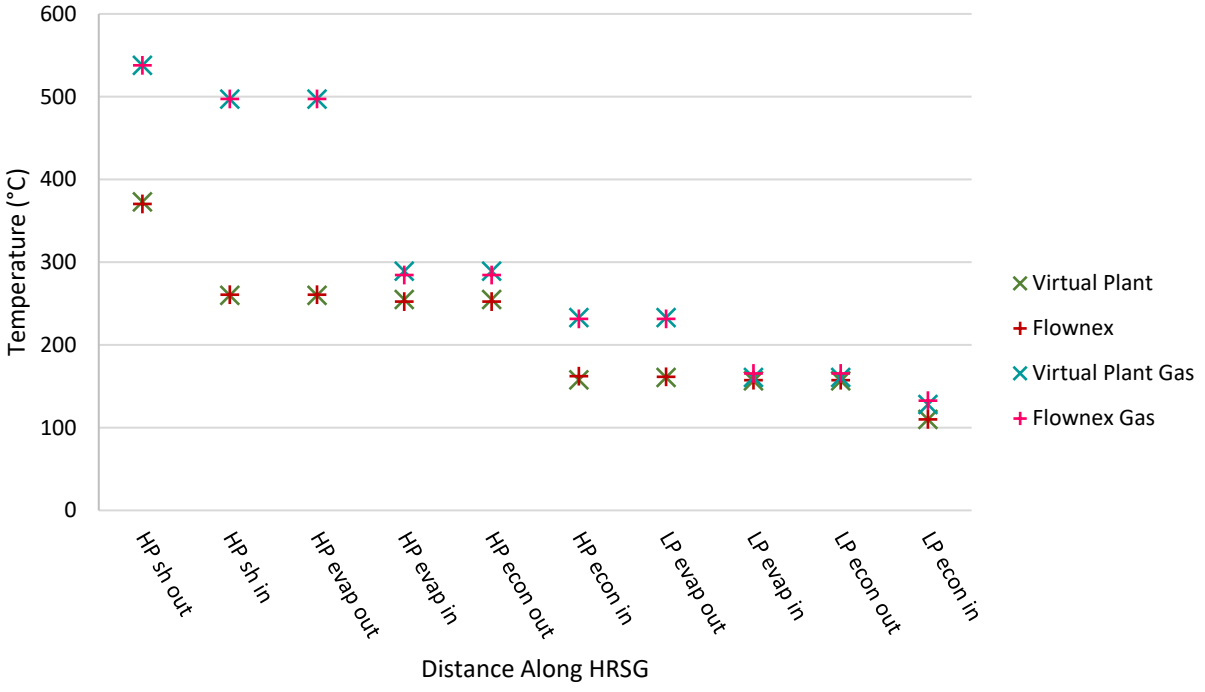

Figure 46: Graph showing comparison of double pressure models at 60% load

Only Virtual Plant and Flownex off-design results were compared for the double pressure model since the modelling of the off-design analytical model would have been too complex. The double pressure off-design results for Virtual Plant and Flownex agreed closely with one another. This showed that the added complexity of the system did not contribute to any errors or variations between models.

5. Triple Pressure Model

5.1 Methodology

This model was based on that of Alobaid et al [27]. Unlike the single and double pressure models, no results for intermediate water/steam and gas characteristics in the triple pressure model were available. This made the complexity of the modelling method much greater, especially considering the number of components in the system. This system was also highly optimised in order to increase efficiency, which made the results of the solution extremely susceptible to errors. The approach to modelling the triple pressure system was different to the single and double pressure systems. Firstly, the gas flow path no longer flowed through the pressure levels from high- to low-pressure consecutively. For example, the low-pressure (LP) components were ordered so that components from the intermediate- (IP) and high-pressure (HP) levels were positioned between them. Secondly, this model contained a reheating (RH) section following the intermediate-pressure section. Also, it included multiple economisers and superheaters in the high-pressure section, as well as locations where the gas would split through different heat exchangers that were at the same gas path location.

The schematic in Figure 47 shows the layout of the model with the initial known temperatures of water/steam represented by green circles. The only other knowns were the pressure of each drum, the mass flow rate of water/steam at each pressure level and the mass flow rate of gas. The sections that contain two heat exchangers (*IPECON/HPLTECON1* and *LPSH/IPSH*) represent components in parallel, i.e. gas flow is split between the components. Water from the low-pressure drum is extracted for the intermediate- and high-pressure systems. Steam from the intermediate-pressure superheater mixes with steam from the outlet of the high-pressure turbine to form the flow through the reheater section which flows to the intermediate-pressure turbine. Steam from the intermediate-pressure turbine outlet mixes with steam exiting the low-pressure superheater to enter the low-pressure turbine.

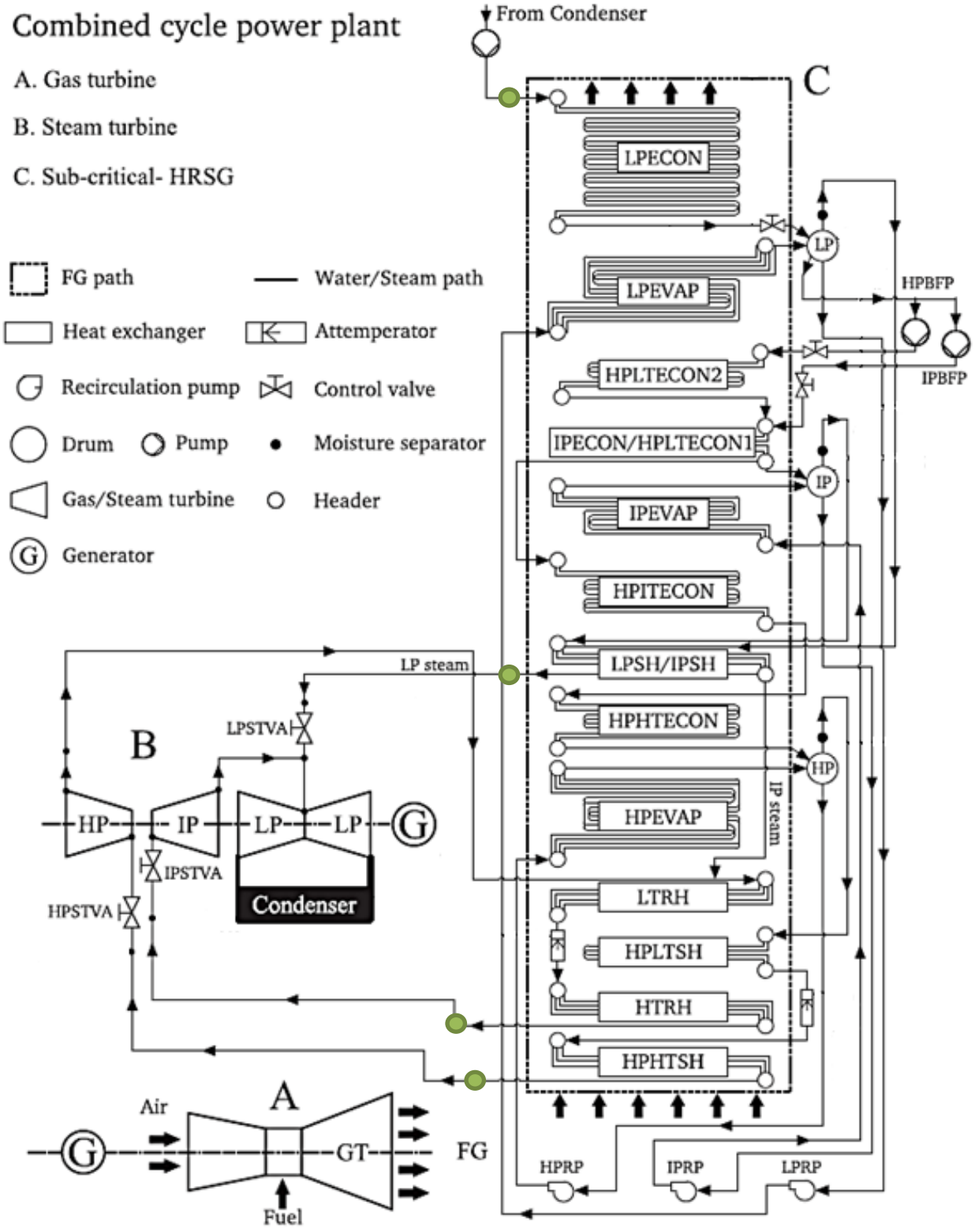

Figure 47: Schematic of triple-pressure model [27]

The isolated low-pressure system is shown in Figure 48 showing variable names (mass flow in green, water/steam temperature in blue and gas temperature in red). The red dashed line represents the omittance of components from other pressure levels. Water from the condenser first enters the HRSG to the low-pressure economiser (*LPECON*), it then flows to the low-pressure evaporator (*LPEVAP*). Water exits the low-pressure drum which splits into the intermediate- and high-pressure flows. Steam from the drum flows to the low-pressure superheater (*LPSH*) and then to the low-pressure turbine.

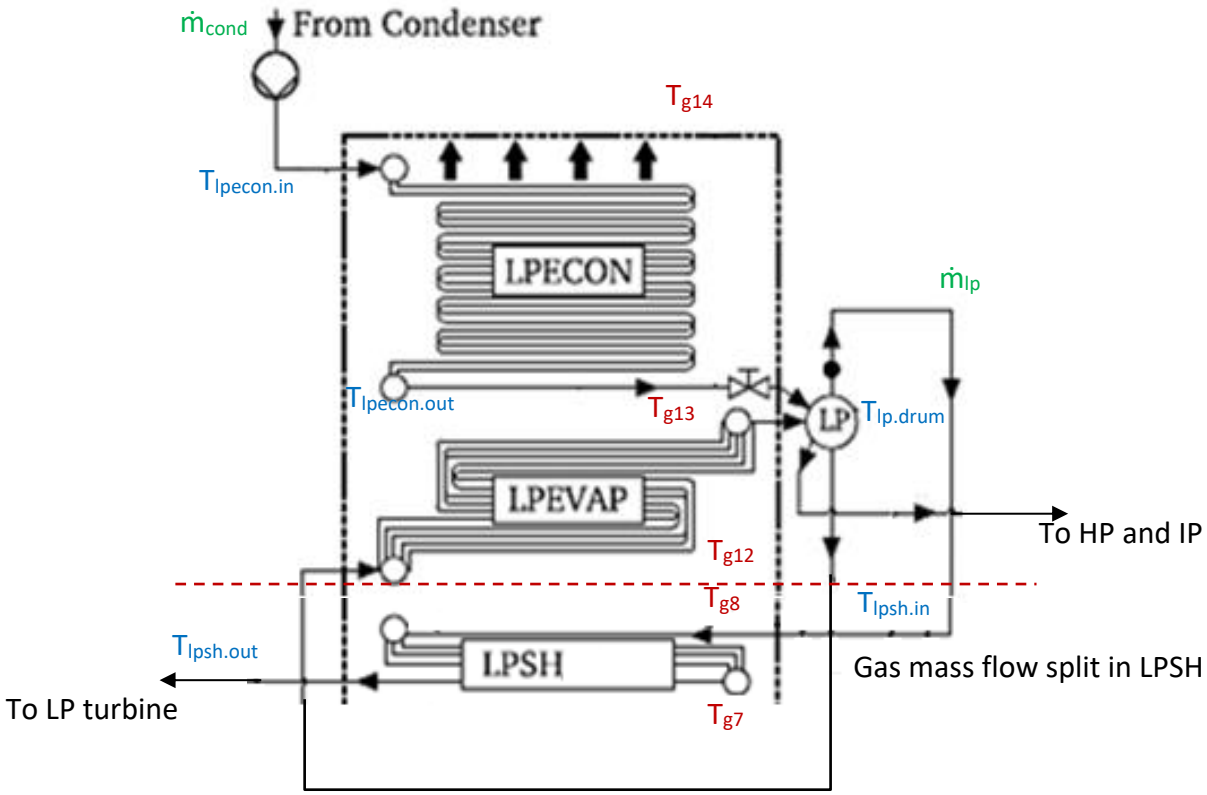

Figure 48: Schematic of low-pressure system

Figure 49 shows a schematic of the isolated intermediate-pressure system. Water enters the intermediate-pressure economiser (*IPECON*) from the low-pressure drum, which then flows to the intermediate-pressure evaporator (*IPEVAP*). Steam from the intermediate-pressure drum flows to the intermediate-pressure superheater (*IPSH*), which then mixes with steam from the high-pressure turbine to enter the low temperature reheater (*LTRH*). Thereafter, the steam enters the high temperature reheater (*HTRH*) and then flows to the intermediate-pressure turbine.

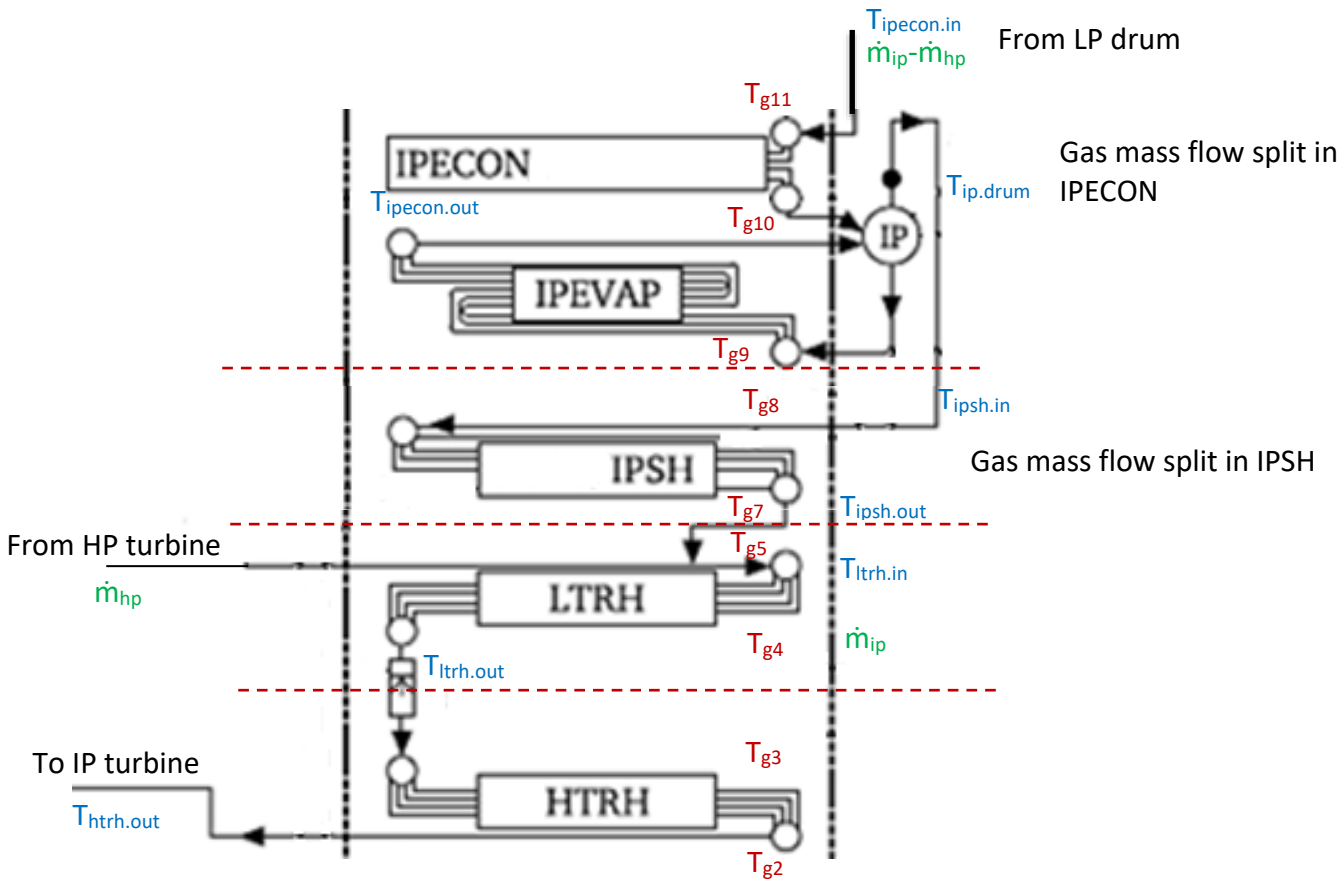

Figure 49: Schematic of intermediate-pressure system

The schematic in Figure 50 shows the layout of the isolated high-pressure system. Water from the low-pressure drum flows to the high-pressure low temperature economiser 2 (*HPLTECON2*), then the high-pressure low temperature economiser 1 (*HPLTECON1*), followed by the high-pressure intermediate temperature economiser (*HPITECON*) and, thereafter, the high-pressure high temperature economiser (*HPHTECON*). After the four economisers, the water flows to the high-pressure evaporator (*HPEVAP*). From the high-pressure drum, steam flows to the high-pressure low temperature superheater (*HPLTSH*) and, finally, the high-pressure high temperature superheater (*HPHTSH*) after which it flows to the high-pressure turbine.

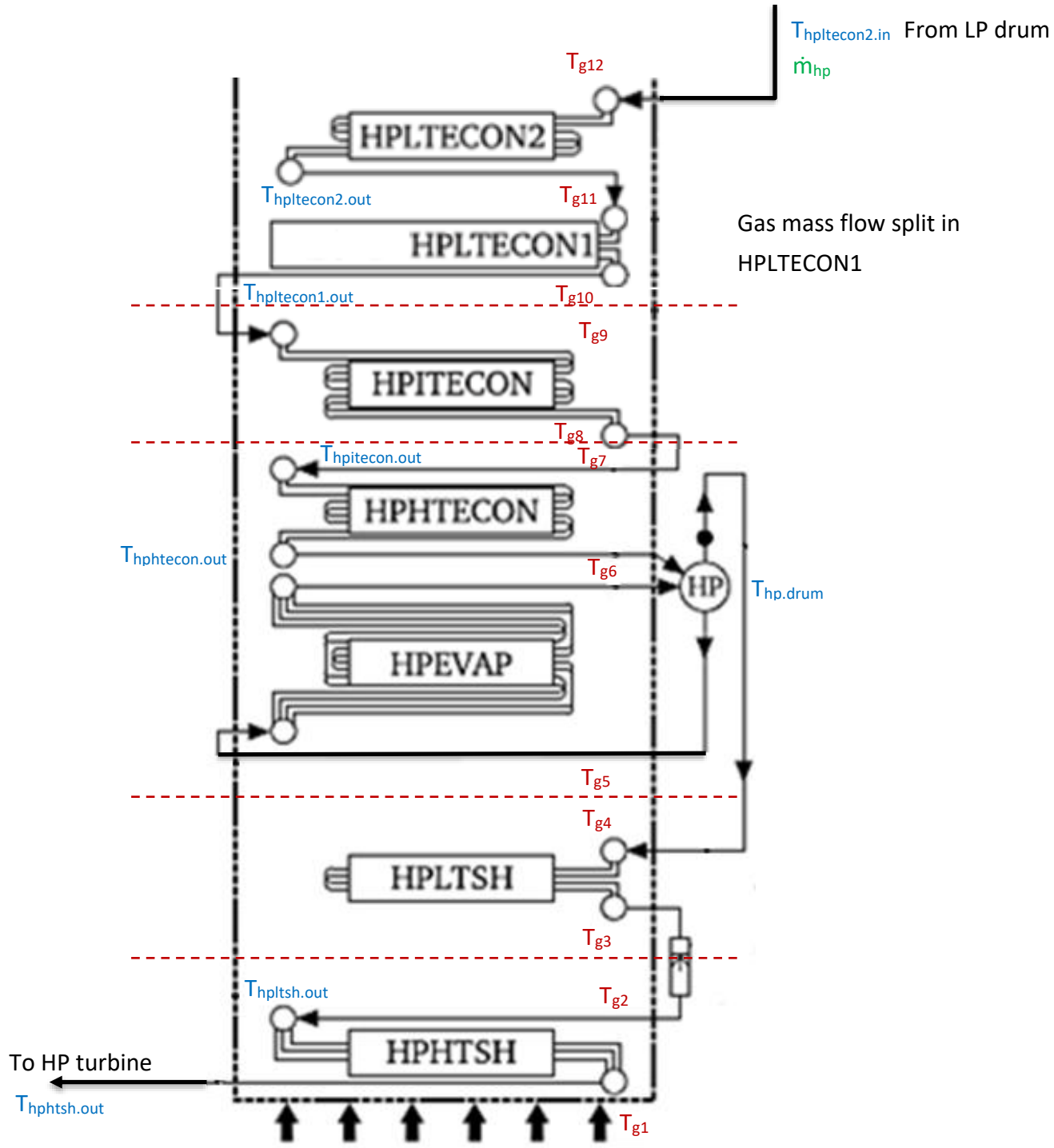

Figure 50: Schematic of high-pressure system

5.1.1 Analytical Model

Various approaches to the analytical model were made. Initially, an attempt was made to model the system starting from the inflow of water at the low-pressure economiser and working through it

systematically. However, due to the vast number of unknowns and the assumptions that had to be made, this model was unsuccessful. Steaming in the *HPHTECON* could not be avoided.

The gas composition used for this model was changed from the one used for the single and double pressure models. A more precise gas composition was used in order for the heat uptake to be similar to that of an actual gas to avoid any errors. This was because the composition, and therefore enthalpy calculation, used for the previous models was based on that of pure air which would cause a variation compared to flue gas. This variation would cause the highly optimised triple pressure model to fail. The gas used in the triple pressure model was made up of 75.37% nitrogen, 13.25% oxygen, 3.51% carbon dioxide, 0.9% argon and 6.97% steam. Therefore, the calculation of gas enthalpy had to be changed. In order for the enthalpy calculation to be consistent with that used by Virtual Plant, a specific heat capacity equation was extracted by running a single pressure Virtual Plant model at various gas inlet temperatures. The pinch point of the model was maximised in order to minimise the change in gas temperature over the HRSG. Thereafter, the model was run at multiple gas inlet temperatures and the specific heat capacity of gas was calculated at each data point using equation (5.1). The other variables were obtained from Virtual Plant results.

$$Q_{HRSG} = \dot{m}_g \cdot c_{pg} \cdot \Delta T_g \tag{5.1}$$

Q_{HRSG} – duty of the HRSG [W]

$\dot{m}_g$ – mass flow rate of gas through the HRSG [kg/s]

c_{pg} – specific heat capacity of gas [J/kg.K]

ΔT_g – change in gas temperature over the HRSG [K]

Table 3 shows a few of the data points obtained from Virtual Plant. The graph of specific heat capacity of gas vs average temperature resulted in a linear equation as shown in Figure 51. The enthalpy equation was then calculated as the integral of the specific heat equation.

Table 3: Data points for Cp calculation

Gas Inlet Temp. (°C)	Gas Outlet Temp. (°C)	HRSG Duty (W)	Ave. Temp (°C)	Cp (kJ/kg.K)
548.3	436.1	2405000	492.2	1.14338
555	435.2	2569000	495.1	1.143867
560	434.6	2690000	497.3	1.144255
565	434.1	2811000	499.55	1.145485
570	433.4	2934000	501.7	1.145718

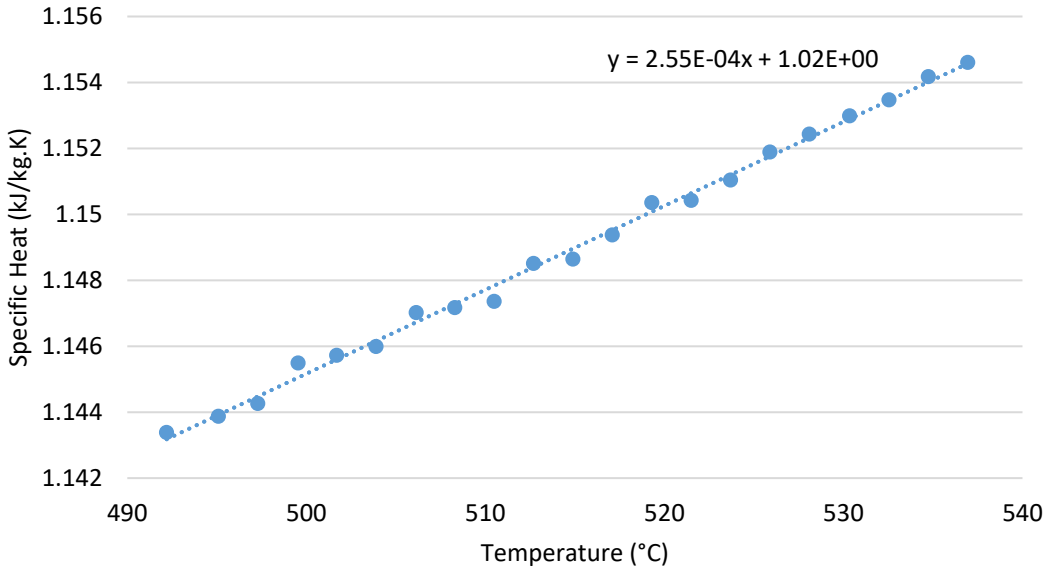

Figure 51: Graph of cp of gas vs. average temperature

Two deviations from the model obtained from Alobaid et al. had to be made [27]. Firstly, the steam temperature exiting the *LPSH* had to be decreased from 293°C to 280°C in order to prevent a temperature cross situation that, otherwise, could not be avoided. Secondly, the gas temperatures entering and exiting the HRSG could not be set according to that of Alobaid et al. but had to be calculated. The gas temperature entering the HRSG was decreased from 628°C to 625°C and that exiting the HRSG increased from 81°C to 101°C. This could have been due to the difference in gas composition or the difference in calculation of gas enthalpy.

It was found that the calculation had to start with an initial assumption (of 260°C) for the water temperature entering the *HPHTECON* in order to prevent steaming in this component. The high-pressure drum temperature was found using steam tables and the known pressure. Thereafter, the gas temperature (T_{g6}) exiting the *HPEVAP* and the water temperature ($T_{hphtecon.out}$) exiting the *HPHTECON* were found using assumed pinch and approach points of 2°C each. The duty of the *HPHTECON* was then found, which was used to calculate the gas temperature exiting the component (T_{g7}).

The enthalpy of steam exiting the high-pressure drum was calculated, which allowed for the duty of the *HPEVAP* to be calculated. This led to the calculation of the gas temperature entering the *HPEVAP* (T_{g5}). The calculation process up until this point is shown in Figure 52 with assumptions highlighted in orange and calculated values highlighted in green.

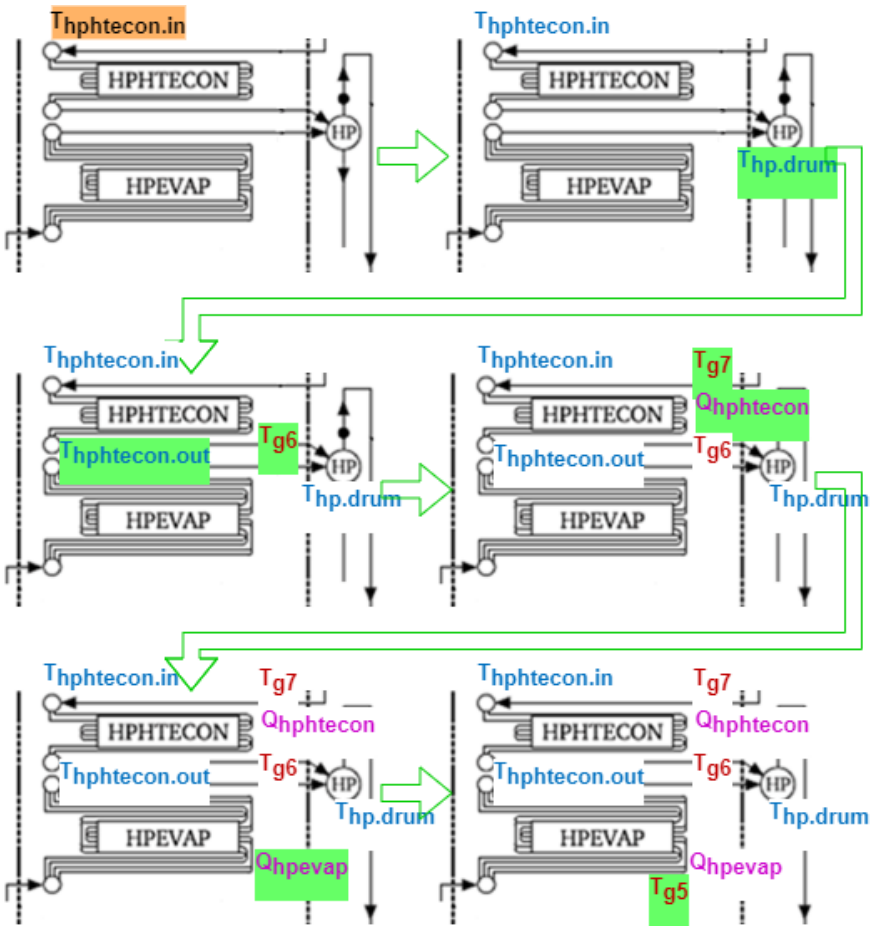

Figure 52: Calculation process for HPHTECON and HPEVAP

The temperature of the low-pressure drum was found using steam tables and the known pressure. The enthalpy of steam exiting the low-pressure drum and that of steam exiting the *LPSH* were calculated which allowed for the calculation of the *LPSH* duty. The temperature of gas exiting the *LPSH* (T_{g8}) was then calculated using an assumption of the fraction (0.8) of gas flowing through the *LPSH*. The assumption was based on the ratio of steam flowing through the *LPSH* to steam flowing through the *IPSH*, since these two components were in parallel, and then adjusted accordingly. This process is shown in Figure 53.

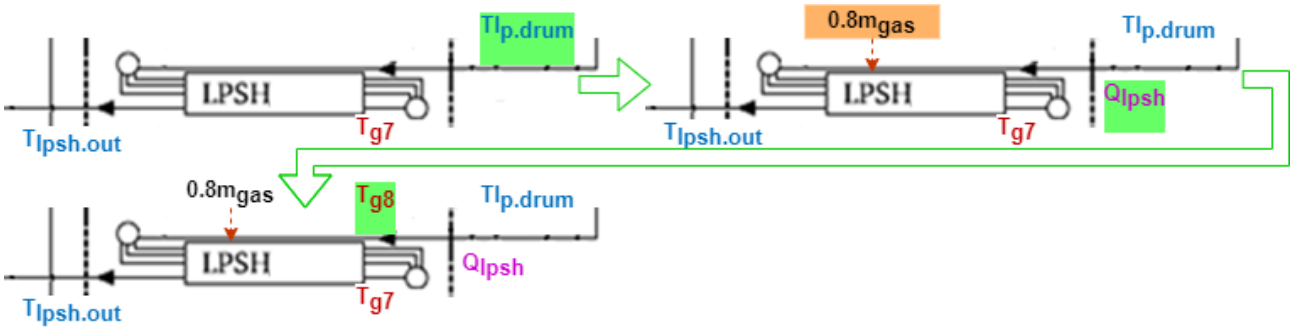

Figure 53: Process of calculation for the LPSH

The duty of the *IPSH* was found using the known change in gas temperature across it as well as the remaining fraction (0.2) of gas flowing through it. This allowed for the steam temperature exiting the component to be calculated ($T_{ipsh.out}$). The temperature of water entering the *LTRH* was found from the enthalpy of a mixture of steam exiting the *IPSH* and the high-pressure steam turbine, calculated as shown in equation (4.1) and (4.2). In order to move on, an assumption had to be made for the temperature of steam exiting the *LTRH*. Since the temperature of steam entering the *LTRH* (348.7°C) and exiting the *HTRH* (567°C) were known, these provided limits for the assumption, which was later adjusted to 427°C. The duty of the LTRH was calculated which allowed for the gas temperature entering the component (T_{g4}) to be calculated. This calculation is shown in Figure 54.

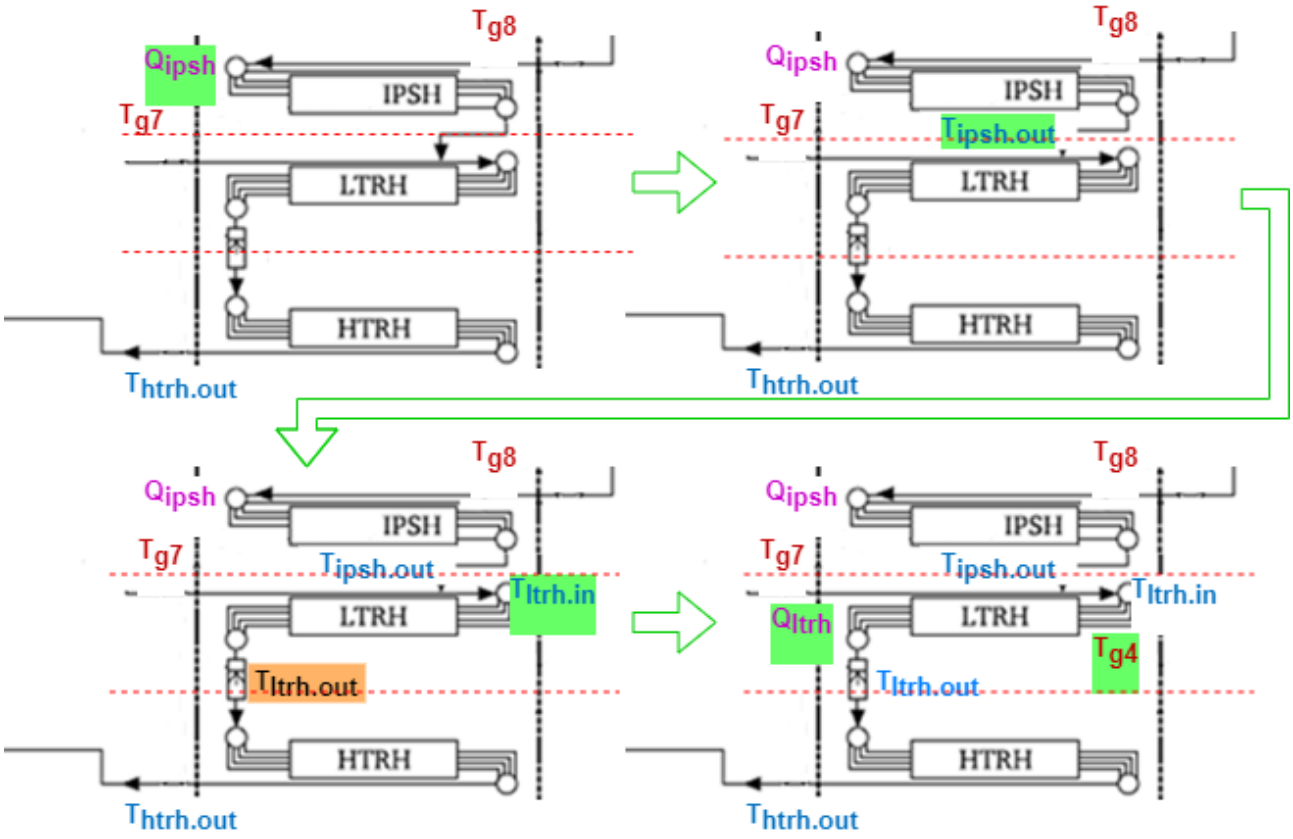

Figure 54: Process of calculation for IPSH and LTRH

Another assumption of 425°C had to be made (with limits of 309°C and 567°C) for the temperature of water exiting the *HPLTSH*. The duty of the *HPLTSH* was then calculated and thereafter, the gas temperature entering the component (T_{g3}). The duty of the *HPHTSH* could then be calculated from the known values of steam entering and exiting the component.

The duty of the *HTRH* was calculated using the known values of steam, which allowed for the gas temperature entering the component (T_{g2}) to be calculated. Using this, and the known value for the duty of the *HPHTSH*, T_{g1} was calculated (3°C lower than that of Alobaid et al). The calculation sequence for these components are shown in Figure 55.

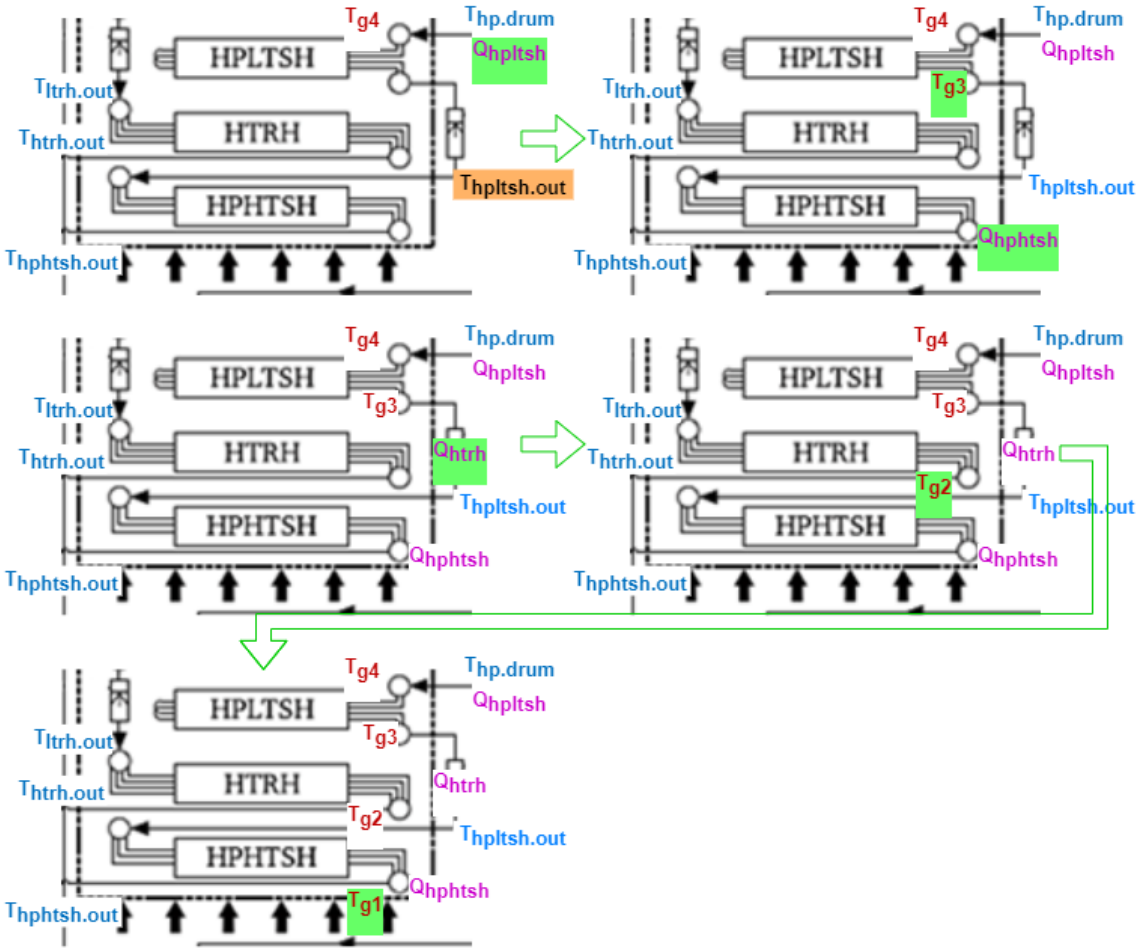

Figure 55: Process of calculation for the HPLTSH, HPHTSH and HTRH

The temperature of the gas exiting the *LPEVAP* (T_{g13}) and water exiting the *LPECON* were calculated using the low-pressure drum temperature and a pinch point of 15°C and approach point of 2°C. The duty of the *LPECON* was calculated which was used to calculate the gas temperature exiting the component (T_{g14}) (20°C higher than that of Alobaid et al.). The duty of the *LPEVAP* was then calculated, allowing for the gas temperature entering the component (T_{g12}) to be calculated. This process of calculation is shown in Figure 56.

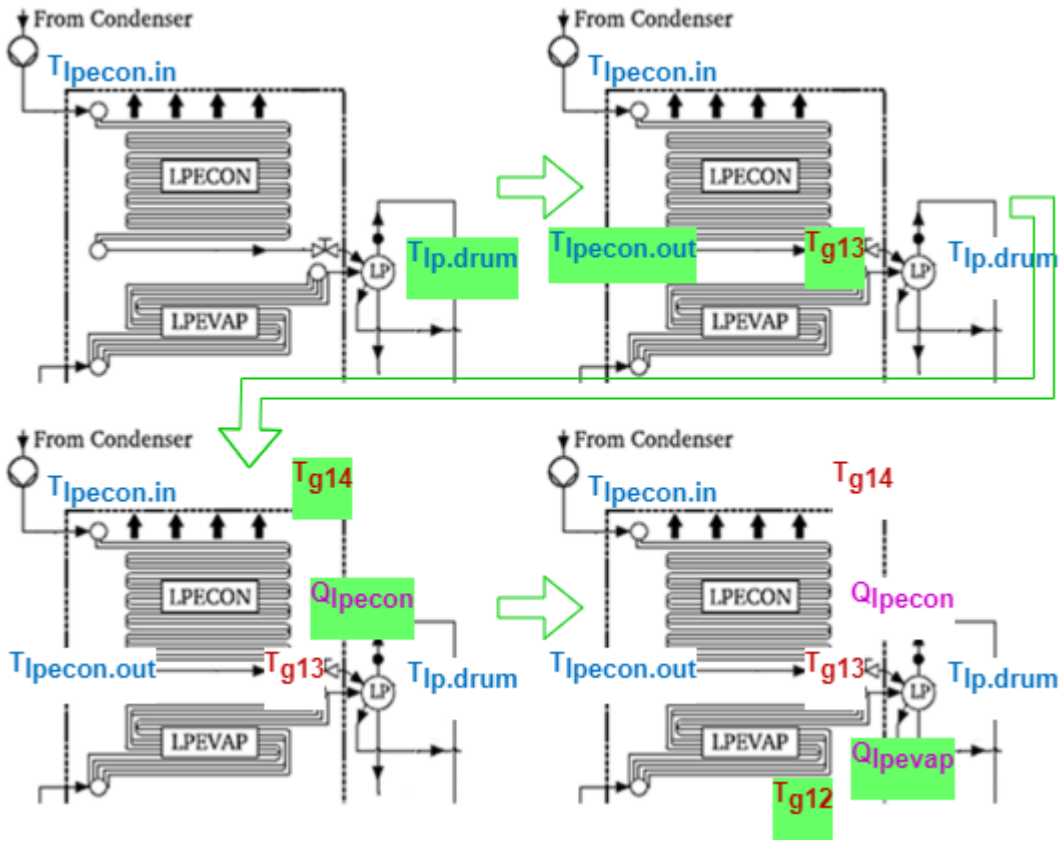

Figure 56: Process of calculation for the LPECON and LPEVAP

The temperature of the intermediate-pressure drum was calculated which led to the calculation of water temperature exiting the *IPECON* and the gas temperature entering the *IPECON* (T_{g10}) using pinch (20°C) and approach (2°C) points. The temperature of water entering the *IPECON* was known as it was extracted from the low-pressure drum, and the duty of the component could therefore be calculated. After making an assumption of the fraction (0.06) of gas flowing through the *IPECON*, the gas temperature exiting the component (T_{g11}) was calculated. The assumption was based on the ratio of steam flowing through the *IPECON* to steam flowing through the *HPLTECON1*. This fraction was small due to the fact that the flow through the *IPECON* was a small portion of the total IP flow as most of the flow is formed in the reheater section. The duty of the *IPEVAP* was calculated using the change in enthalpy of the water exiting the *IPECON* and steam exiting the drum. This was then used to calculate the gas temperature entering the *IPEVAP* (T_{g9}). This calculation is shown in Figure 57.

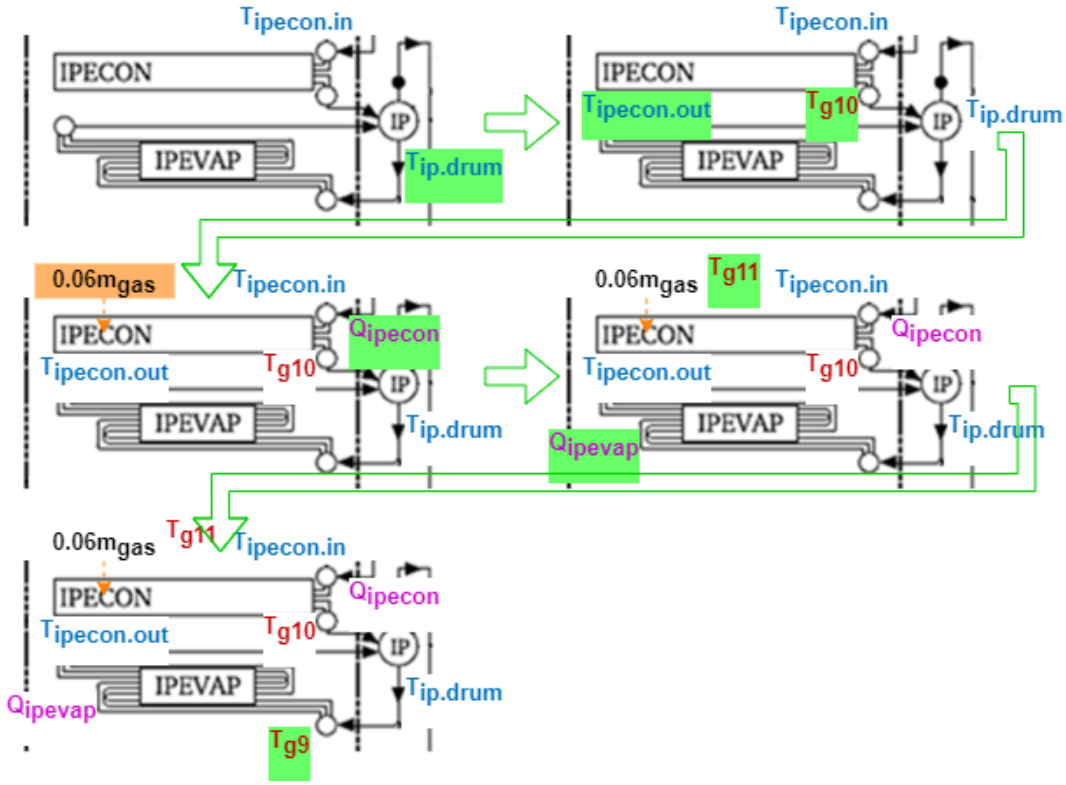

Figure 57: Process of calculation for the IPECON and IPEVAP

The duty of the *HPLTECON2* was calculated using known gas temperatures. Since the water entering the component was extracted from the low-pressure drum, the temperature of water exiting the *HPLTECON2* could be calculated. The duty of the *HPLTECON1* was calculated using known gas temperatures and fraction (0.94) of gas flowing through it. The temperature of the water exiting the component was then calculated. Finally, the duty of the *HPITECON* was calculated using known gas temperatures. The water temperature exiting the component was calculated which was used to iterate the assumption made for the inlet temperature of the *HPHTECON*. The process of this calculation is shown in Figure 58.

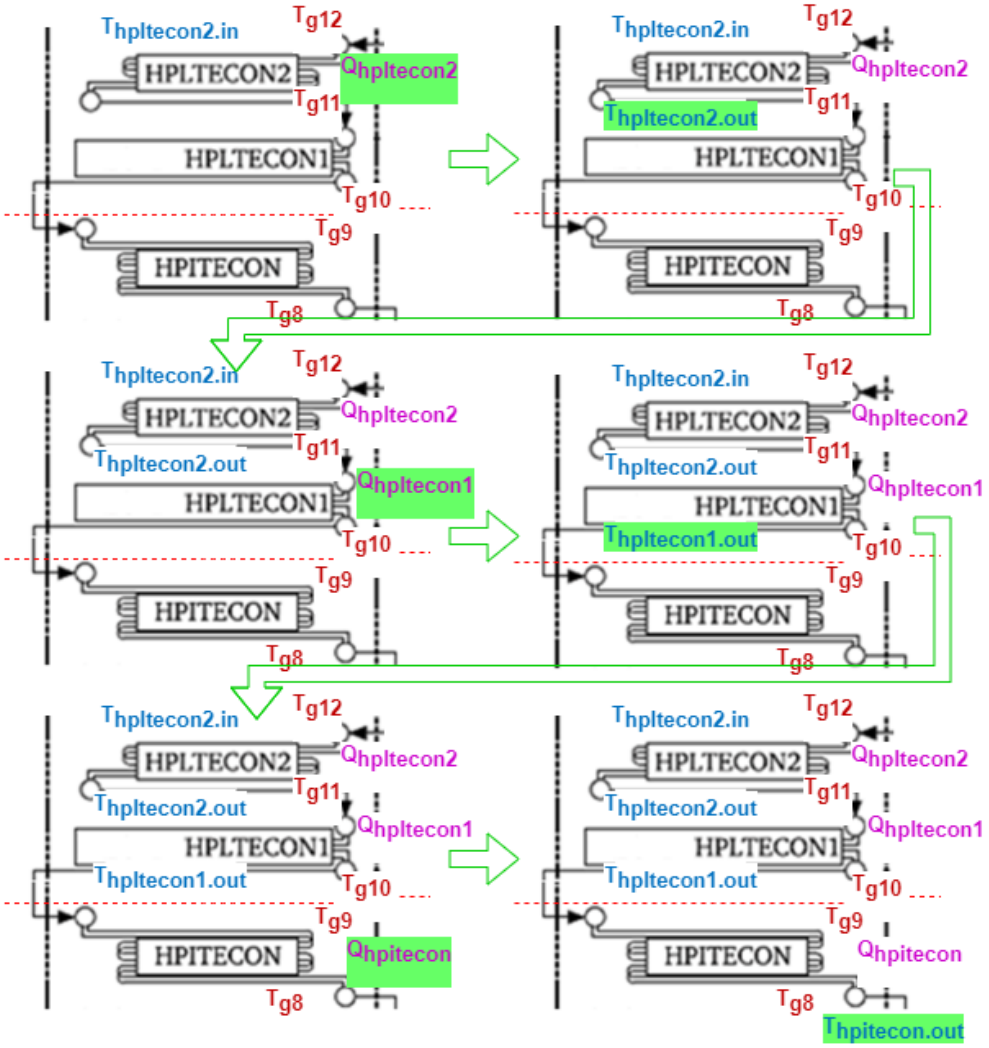

Figure 58: Process of calculation for the HPLTECON2, HPLTECON1 and HPITECON

Certain assumptions made in this model were critical. These included the pinch point of each pressure level (3), the 2 gas splits in the parallel components and the 2 water temperatures that had to be assumed. These 7 values had to be fine-tuned in the highly optimised system until there was no steaming or temperature cross situations in the system.

The pressure of steam exiting the low-pressure turbine was calculated as the saturated pressure of the feedwater. The enthalpy of steam entering the low-pressure turbine was calculated using the mixture equation shown in equation (4.1) and (4.2).

The UA of each component was calculated in order for them to be evaluated in off-design mode.

5.1.2 Virtual Plant Model

The results obtained from the analytical model were used as inputs to the Virtual Plant model shown in Figure 59.

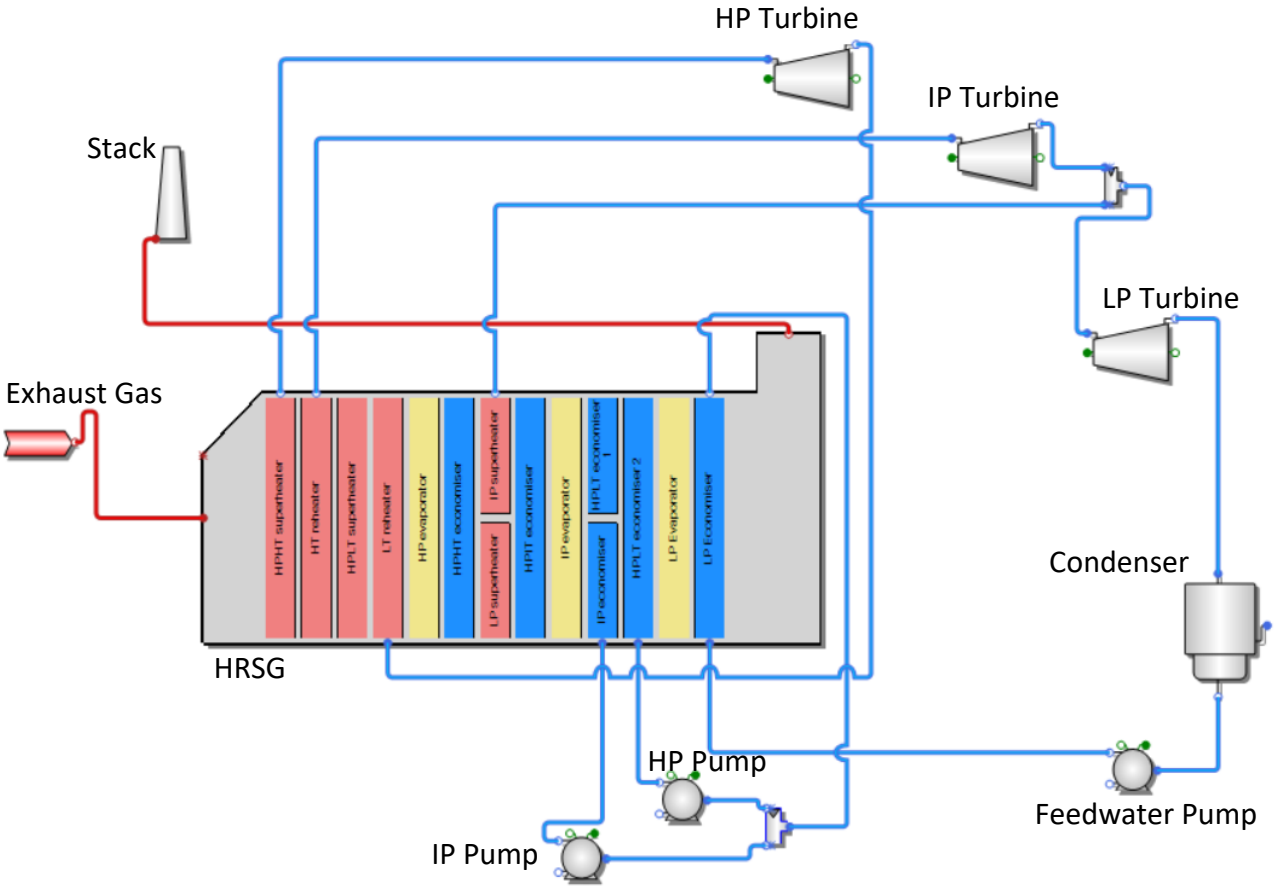

Figure 59: Triple pressure Virtual Plant model

The gas composition used was consistent with the analytical model. The 'Gas Path Arrangement' was set according to the triple pressure schematic in Figure 47 with the consideration of the parallel components. The fraction of gas mass flow through the parallel components was also set. For the 'Steam Side Arrangement', a split to the cycle was added after the *LPECON* to account for the water leaving the low-pressure drum. This was then split further to flow into the intermediate- and high-pressure pumps. A mix to the cycle was added before the *LTRH* in order to accommodate the steam exiting the high-pressure turbine. The characteristics of gas at the inlet of the HRSG and water/steam at each component were entered in 'HT Design Data'. All inputs to the HRSG are shown in Appendix E.

The inputs to the low-pressure turbine were set according to the mixture of the steam exiting the intermediate-pressure turbine and the *LPSH*.

For the off-design model, only the gas mass flow in the gas source was changed according to the load.

5.1.3 Flownex Model

The triple pressure Flownex model is shown in Figure 60. Due to the complexity of the model, it was separated onto 3 drawing pages and interconnected using projected nodes called View Nodes.

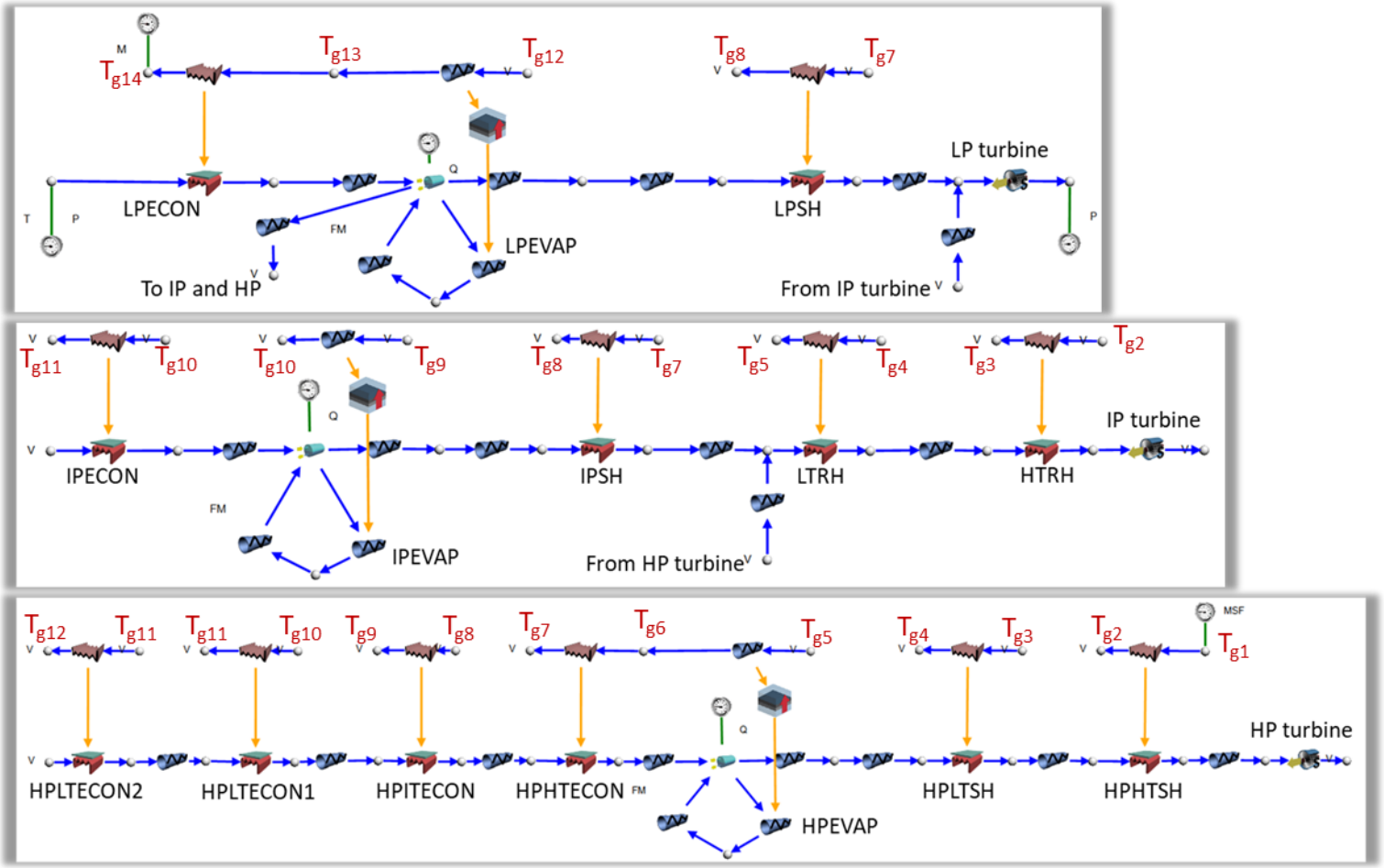

Figure 60: Triple pressure Flownex model

The connection of nodes between each pressure level was done by creating a page of Flow Resistance elements leading from a node projection of one pressure level to that of another pressure level. The gas was split where necessary by creating parallel Flow Resistance elements with flow admittances proportional to the fraction of gas flowing through them. The Flow Resistances were set to linear resistance behaviour. This means that the mass flow rate of fluid through them changes linearly with a change in admittance factor. The pressure drop over a Flow Resistance element with linear resistance behaviour is shown in equation (5.2).

$$\Delta P = \frac{\dot{m}}{A_f \cdot A_{sf} \cdot A_o} + \rho \cdot g \cdot \Delta z \tag{5.2}$$

ΔP – pressure drop over the component [Pa]

$\dot{m}$ – mass flow rate of fluid through the component [kg/s]

A_f – flow admittance

A_{sf} – admittance scaling factor

A_o – opening

ρ – fluid density [kg/m^3]

g – gravitational acceleration [m/s^2]

Δz – height difference between inlet and outlet [m]

An example of gas split at the entrance of parallel components is shown in Figure 61.

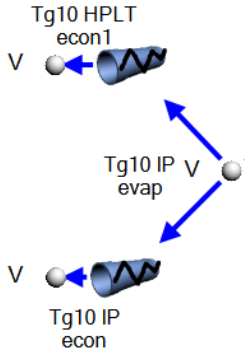

Figure 61: Gas split using projected nodes

The split of water exiting the low-pressure drum was done using parallel Flow Resistance elements connected to the respective pumps. This is shown in Figure 62. It was ensured that the Flow Resistance connected to the low-pressure drum, for flow to the higher pressure levels, was set at a fraction of *0* so that water exited from the bottom of the drum.

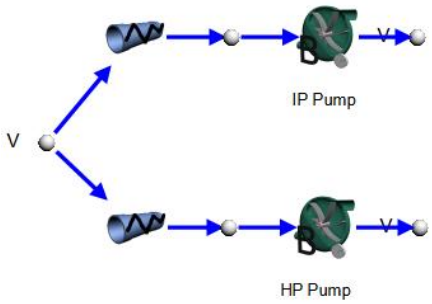

Figure 62: Water split using projected nodes

The inputs to both pumps were calculated using equations shown in equation (4.3) and (4.4). For off-design modelling, the input for each pump head was manually adjusted (along with the low-pressure value at the boundary condition) in order to find the operational pressure at each low load. The intermediate- and high-pressure values were controlled through the corresponding pump head values.

Boundary conditions were used to set the temperature and pressure at the beginning of each stream. For gas, the boundary condition at the beginning of the stream was also used to set the 'Mass Source Fraction' and the one at the end of a stream set mass flow rate. For steam, the boundary condition at the end of the stream set the outlet pressure of the low-pressure turbine.

The modelling of the economisers, evaporators and superheaters were similar to that of previous models.

For this model, a script for off-design modelling was not used for sliding pressure. This was because of the complexity of obtaining an operational pressure at each low load. The input low-pressure value and both pumps had to be manually adjusted until all three drums had an energy source close to zero, without causing any steaming in the economisers. Only two low load conditions were analysed (60% and 80%) as these were the only low loads at which information was available from Alobaid et al [27].

5.2 Results

The triple pressure model was analysed in design and off-design mode. The design case was analysed using a comparison between each model, as done previously. The design and off-design cases were then analysed by comparing results of the Virtual Plant and Flownex models to published plant data obtained from Alobaid et al [27].

5.2.1 Design Model

The comparisons between plant data and the analytical results for steam are shown in Table 4.

Table 4: Comparison between design base plant data and analytical results for steam

Component	Steam mass flow (kg/s)			Outlet temp. (°C)			Pressure (bar)		
	Plant	Analytical	Error %	Plant	Analytical	Error %	Plant	Analytical	Error %
HPSH outlet	78.2	78.2	0	567	567	0	97.7	97.7	0
RH outlet	83.2	83.2	0	567	567	0	21.4	21.4	0
LPSH outlet	9.8	9.8	0	293	280	4.44	4.1	4.1	0

The comparisons between plant data and the analytical results for gas variables are shown in Table 5.

Table 5: Comparisons between design base plant data and analytical results for gas

Gas Variable	Plant	Analytical	Error %
Mass flow (kg/s)	587	587	0
Tg1 – Inlet (°C)	628	624.8	0.51
Tg14 – Outlet (°C)	81	100.7	-24.32

The low-, intermediate- and high-pressure levels were plotted separately for the triple pressure model. The low-pressure water/steam and gas temperature profiles for each model is shown in Figure 63. The break in the gas flow line represents the omittance of components from other pressure levels.

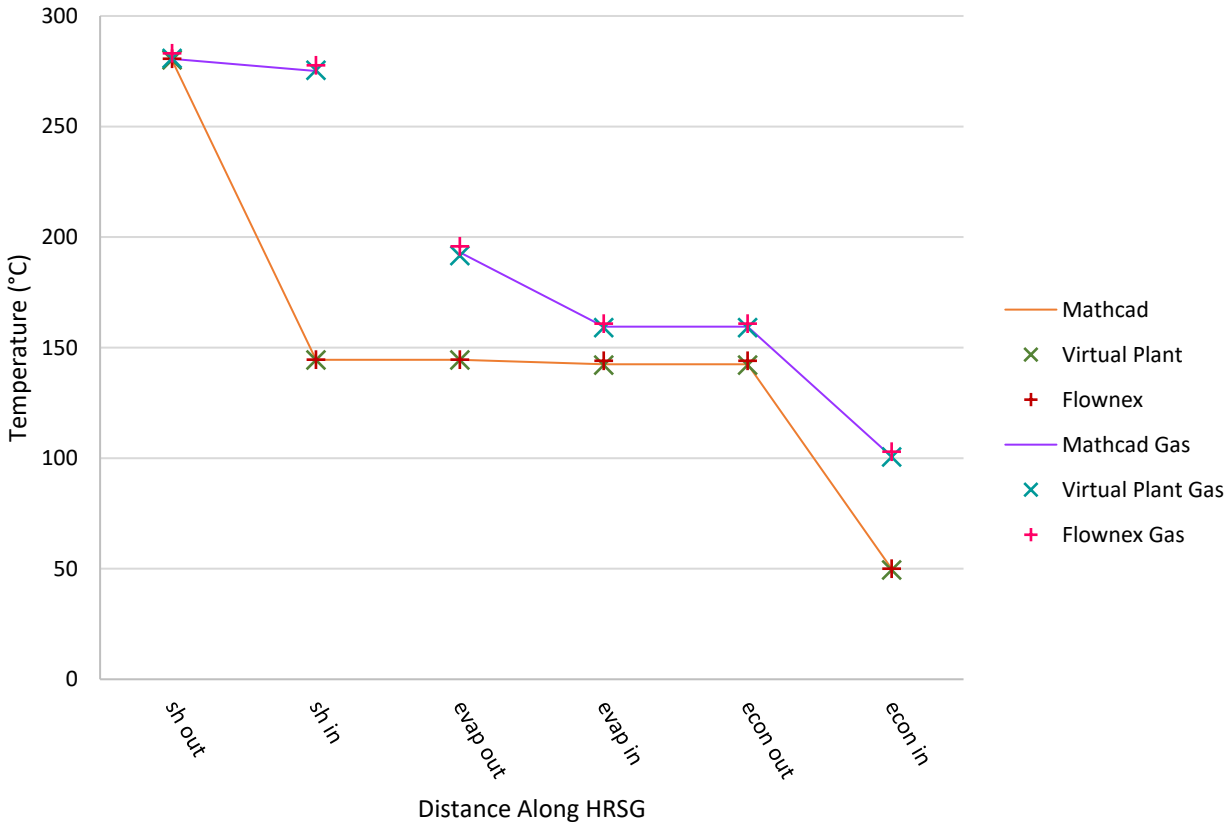

Figure 63: Graph showing comparison of triple pressure models (low-pressure)

The intermediate-pressure water/steam and gas temperature profiles for each model is shown in Figure 64.

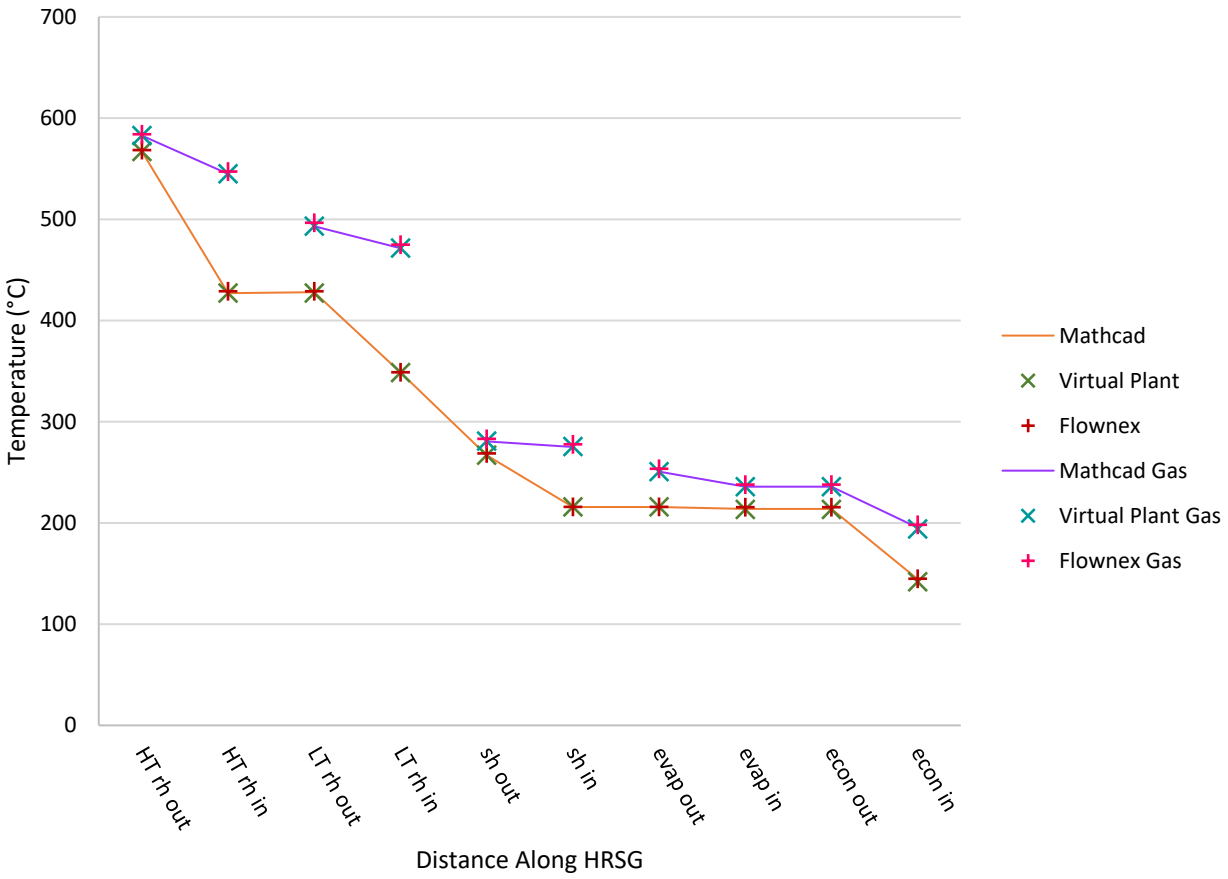

Figure 64: Graph showing comparison of triple pressure models (intermediate-pressure)

The high-pressure water/steam and gas temperature profiles for each model is shown in Figure 65.

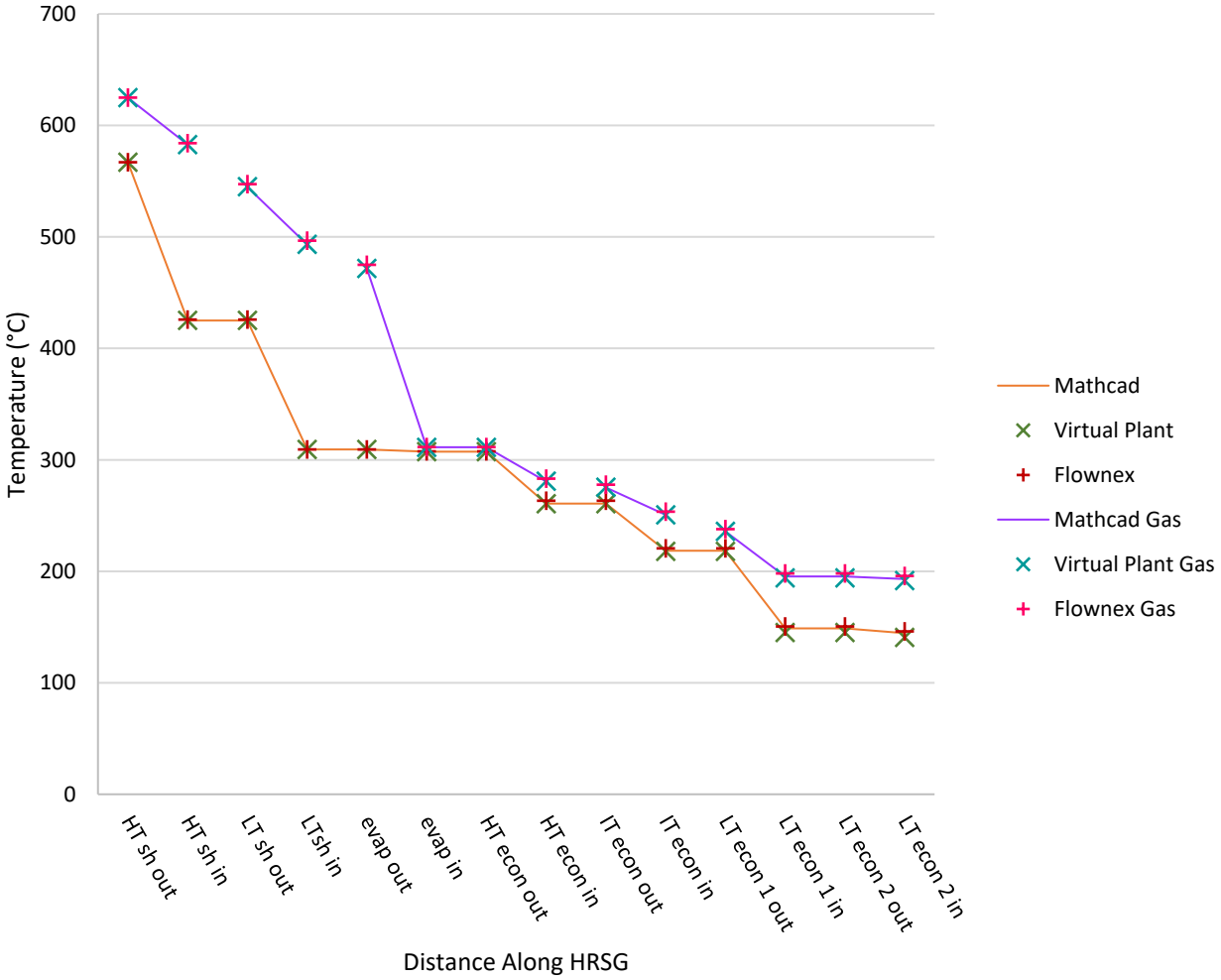

Figure 65: Graph showing comparison of triple pressure models (high-pressure)

Despite the fact that numerous assumptions had to be made for the triple pressure system, the results agree quite closely with one another. Considering the complexity of the system and the fact that a small difference at one point of the system could cause a larger difference down the line, the models produced successful results.

5.2.2 Off-Design Model

The Virtual Plant and Flownex models were run at 80% and 60% load. For Virtual Plant, the load was decreased by decreasing the gas mass flow accordingly. Other factors such as UA and steam pressure at each low load were automatically calculated by Virtual Plant. The gas mass flow for each load was obtained from Alobaid et al [27]. For Flownex, the gas mass flow, UA of each component and pressure of water/steam at each pressure level were changed for low load. The UA for each component was calculated, the low-pressure was manually adjusted using the boundary condition and the intermediate- and high-pressures were manually adjusted through the respective pump

heads. The pressures at each pressure level were adjusted until each drum had an energy source of close to zero (maximum 75.5 kW, which is less than 3% of the duties of the heat exchangers).

The results available from Alobaid et al. were the mass flow rate, temperature and pressure of the exiting steam for each pressure level i.e. the outlet of the *HPHTSH*, *HTRH* and *LPSH* [27]. Results for the outlet of the *HPHTSH* are shown in Table 6 with 'Expected' representing published plant data.

Table 6: Triple pressure off-design comparisons for HPHTSH outlet

Load%	HPHTSH steam mass flow (kg/s)			HPHTSH outlet temp. (°C)			HPHTSH pressure (bar)		
	Expected	Virtual Plant	Flownex	Expected	Virtual Plant	Flownex	Expected	Virtual Plant	Flownex
80	66.9	65.6	67.3	566.8	576.4	572.5	88	82.9	84.7
60	58.3	56.3	57.8	566.9	583.2	579.4	76.2	71.7	73.3

Results for the outlet of the *HTRH* are shown in Table 7.

Table 7: Triple pressure off-design comparisons for HTRH outlet

Load%	HTRH steam mass flow (kg/s)			HTRH outlet temp. (°C)			HTRH pressure (bar)		
	Expected	Virtual Plant	Flownex	Expected	Virtual Plant	Flownex	Expected	Virtual Plant	Flownex
80	74.7	69.7	71.6	567	571.3	569.4	20.6	18	18.5
60	64.9	59.8	61.6	566.9	574.5	572.4	17.7	15.5	15.9

Results for the outlet of the *LPSH* are shown in Table 8. Since the outlet steam temperature had to be decreased from 293°C to 280°C, a considerable difference in these results were expected.

Table 8: Triple pressure off-design comparisons for LPSH outlet

Load%	LPSH steam mass flow (kg/s)			LPSH outlet temp. (°C)			LPSH pressure (bar)		
	Expected	Virtual Plant	Flownex	Expected	Virtual Plant	Flownex	Expected	Virtual Plant	Flownex
80	7.7	7.7	8.1	289.9	271.4	271	3.9	3.4	3.5
60	6.4	6.4	6.8	281	264	263.3	3.3	2.9	3

The comparison of the plant data, Virtual Plant results and Flownex results for the mass flow rate of steam at design and low loads is depicted in Figure 66. This shows the mass flow rate of the outlet steam at low-, intermediate- and high-pressure levels.

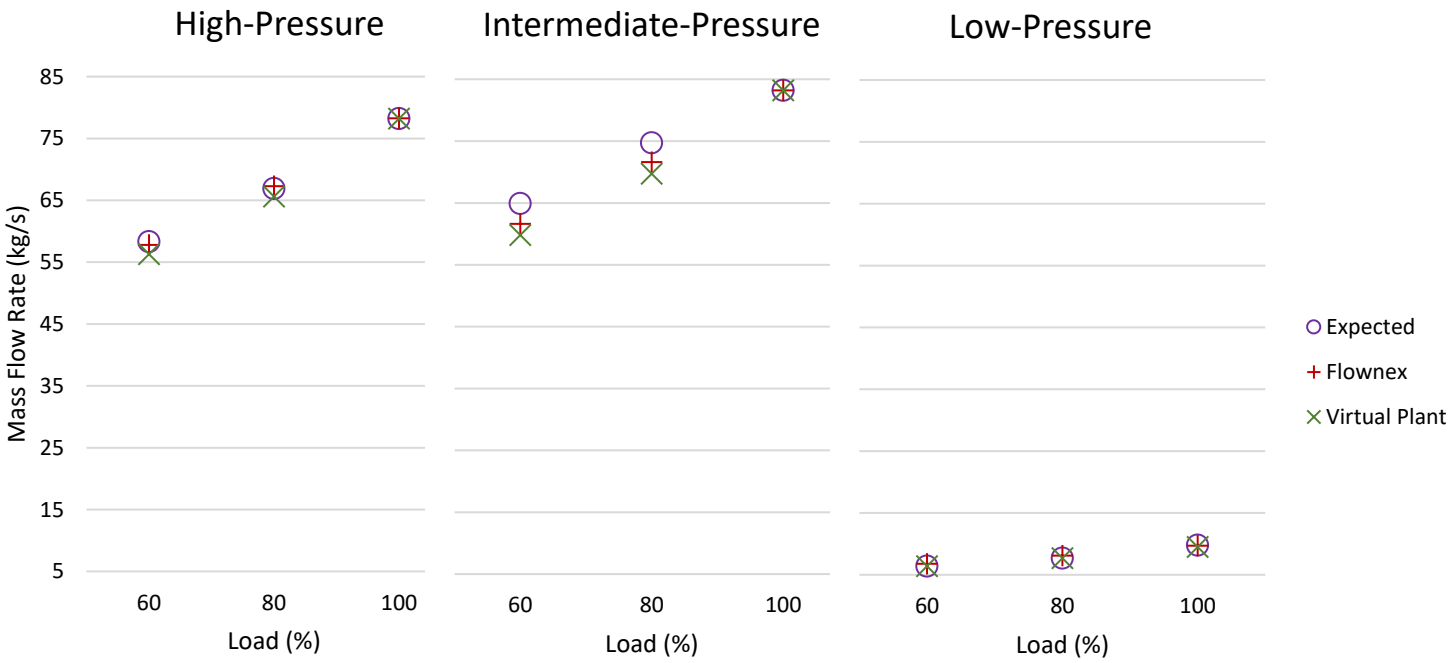

Figure 66: Graph showing comparisons of steam mass flow rate with a change in load

The comparison of the plant data, Virtual Plant results and Flownex results for the outlet temperature of steam at design and low loads is depicted in Figure 67. This shows the temperature of the outlet steam at low-, intermediate- and high-pressure levels.

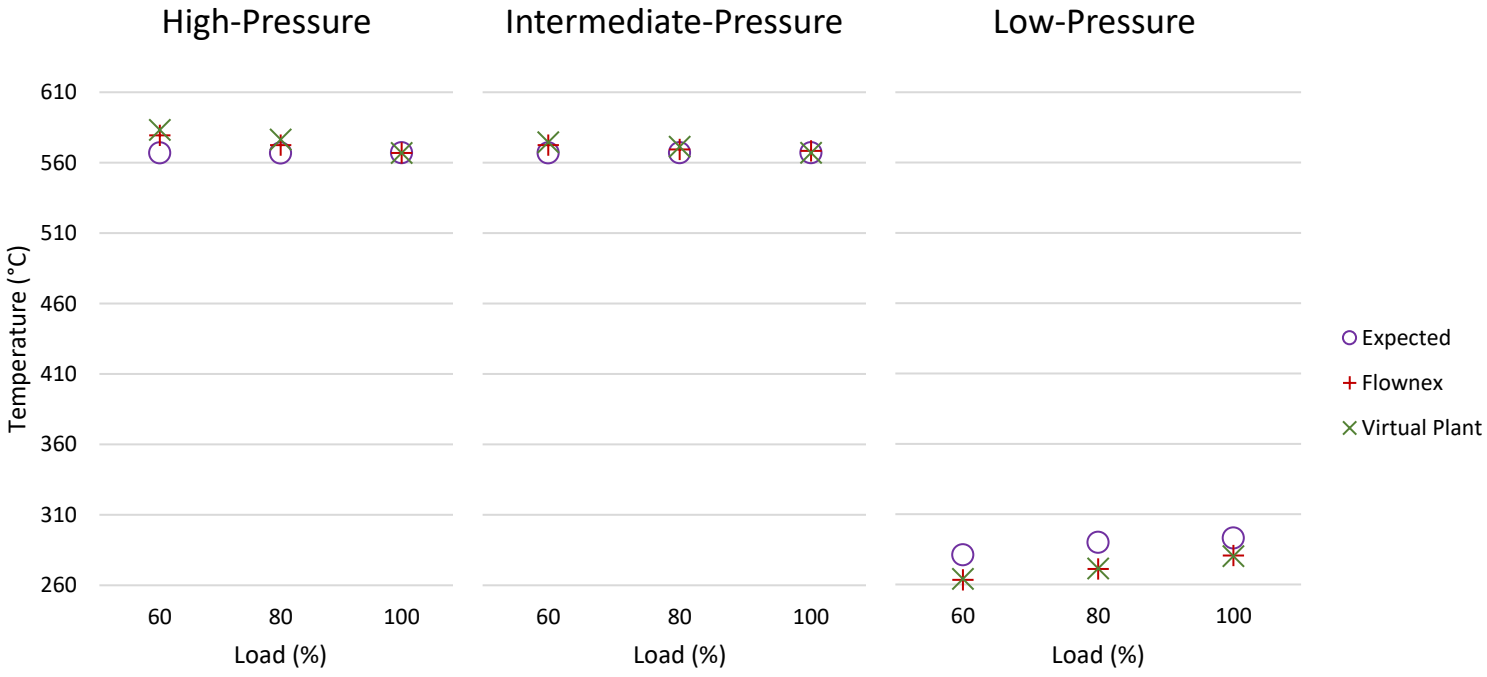

Figure 67: Graph showing comparisons of outlet temperature with a change in load

The comparison of the plant data, Virtual Plant results and Flownex results for the outlet pressure of steam at design and low loads is depicted in Figure 68. This shows the pressure of the steam at low-, intermediate- and high-pressure levels.

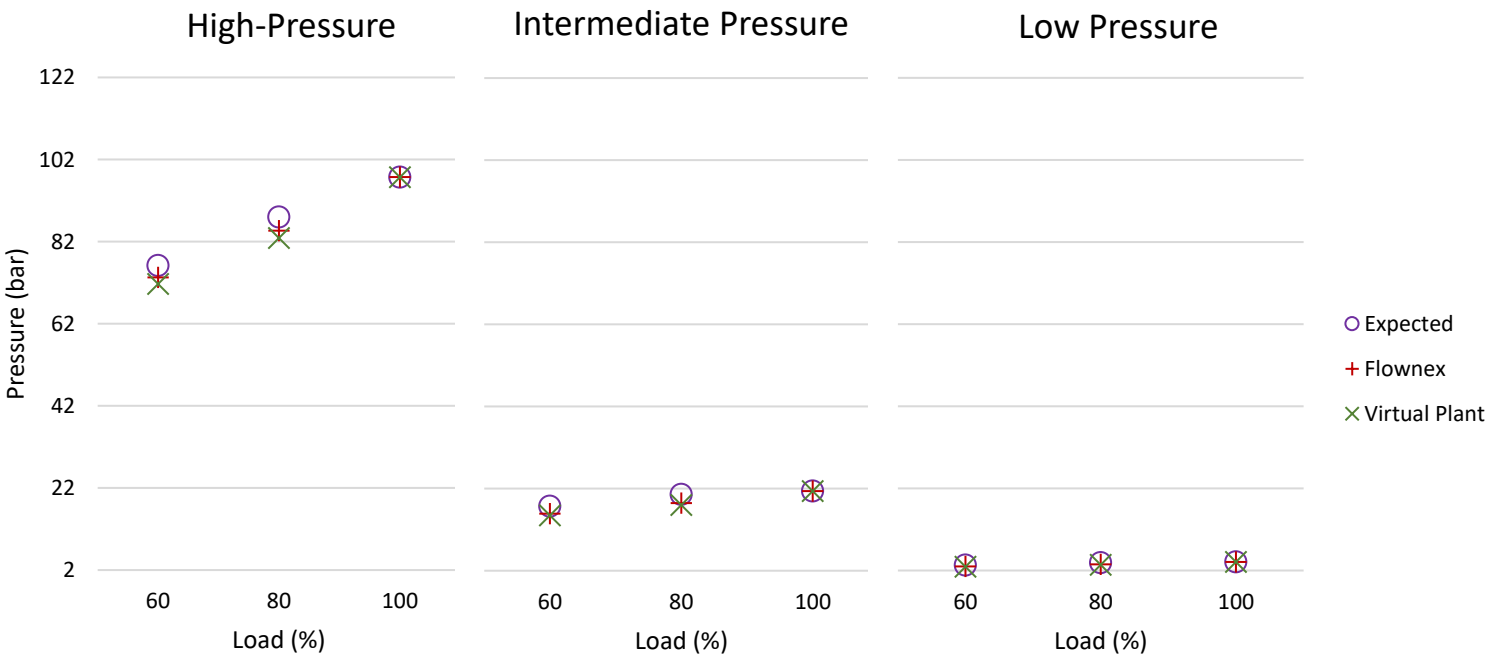

Figure 68: Graph showing comparisons of pressure with a change in load

The percentage error of the off-design Virtual Plant and Flownex results compared to plant data was calculated using equation (5.3).

$$\%error = \frac{expected - result}{expected} \cdot 100 \tag{5.3}$$

The graphs in Figure 69 and Figure 70 show the histograms of the percentage error in the Virtual Plant and Flownex models at low loads.

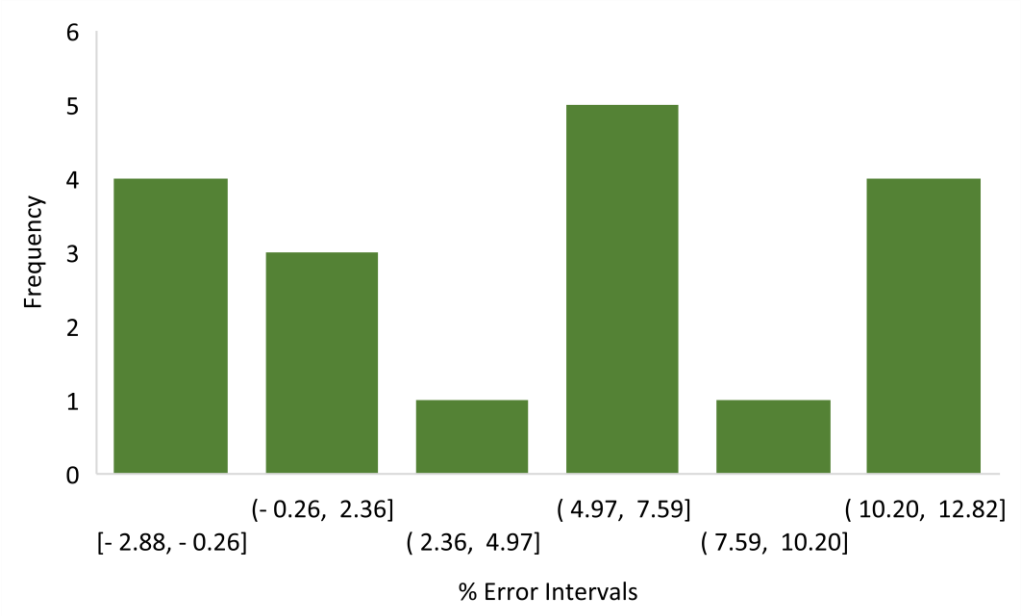

Figure 69: Histogram showing the frequency of % errors in the off-design Virtual Plant models

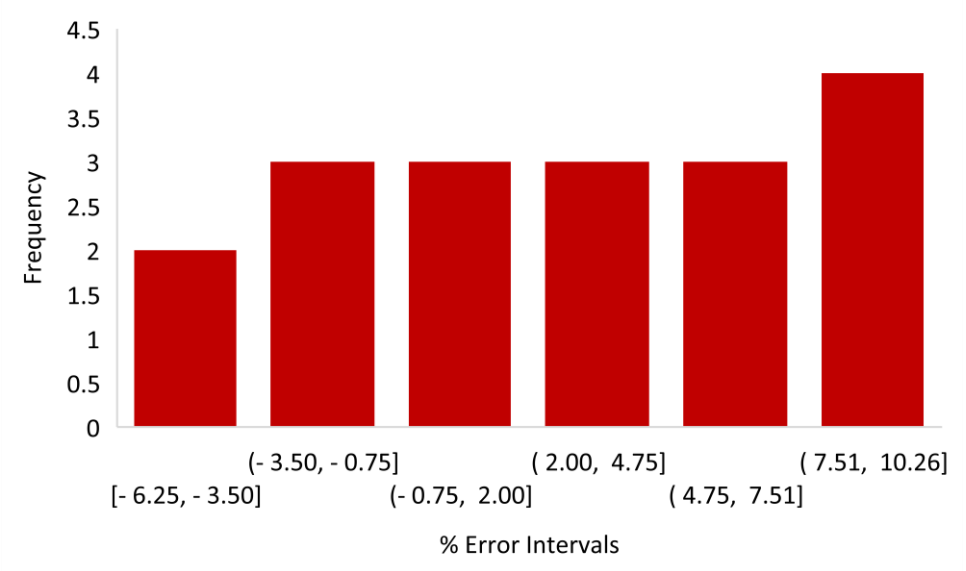

Figure 70: Histogram showing the frequency of % errors in the off-design Flownex models

The error of steam mass flow increases with the decrease in load and pressure level. The error in the high-pressure model is minimal, however, the intermediate- and low-pressure models produce fairly higher errors at low loads.

For the low-pressure steam outlet, there was a larger error in outlet temperature due to the temperature change that had to be made at this point to avoid a temperature cross situation.

Additionally, the error in temperature for all pressure levels is expected due to the absence of attemperation in the Flownex and Virtual Plant models as this was not modelled for. These variations meant that the Flownex and Virtual Plant models would behave differently to the plant under off-design conditions.

The errors between the models and plant data were expected due the changes in steam and gas temperature that were made as well as the amount of assumptions that had to be made. There was also the fact that attemperation was not modelled for in Flownex and Virtual Plant and the possibility of various other control mechanisms, such as supplementary firing; control valves; moisture separators; and bypass controls, used in the plant.

6. Conclusions and Recommendations

The primary objective of this study was to develop a model of a combined-cycle power plant in design and off-design conditions. This model was first done analytically, in Mathcad; then in Virtual Plant; and finally, in Flownex. These models analysed the steam side of a combined-cycle power plant. The Mathcad, Virtual Plant and Flownex models were compared to each other at each pressure level. This was done to verify them and ensure consistency.

6.1 Design

The architecture and design for the single and double pressure systems were obtained from a textbook by V. Ganapathy which provided detailed information of each system including the steam and gas temperatures at the inlet and outlet of each component in the HRSG [31]. Therefore, the modelling of these systems could be fact checked at intermediate points.

Unlike the single and double pressure systems, the resource used for the triple pressure model (Alobaid et al. [27]) did not provide detailed information or a modelling approach for the system. Only endpoint values were available, therefore, several assumptions had to be made without the option to validate them. Variations from the original system also had to be made to avoid complications due to the lack of information required for the solution.

The verification of the models was a success for the single, double and triple pressure models. Results obtained from each software were in close agreement with each other which showed that the modelling methodology for each software was consistent. The results of the single and double pressure model were also consistent with that of V. Ganapathy from which the inputs for each were obtained and were, therefore, validated [31].

In order to validate the triple-pressure model, it was compared to plant data obtained from Alobaid et al. at design and off-design conditions [27]. The design model showed close agreement to that of the plant data with the exception of changes that had to be made. These changes included a drop in the steam temperature exiting the *LPSH* to avoid a temperature cross situation and a variation in gas temperatures entering and exiting the HRSG. The changes made could not be avoided, which could have been due to the amount of assumptions that had to be made or a variation in gas composition which affects the calculation of gas enthalpy. Because of the complexity of the system, errors could not be easily pin pointed.

6.2 Off-Design

The mathematical modelling of off-design conditions in a combined-cycle power plant were first analysed and understood using the single pressure analytical model. The off-design cases were modelled for the single and double pressure models in Virtual Plant and Flownex. However, these were unable to be validated due to the lack of data for them. The textbook from which these systems were obtained did not provide the off-design results for them.

For the triple pressure model, the off-design case was able to be compared to plant data. Comparisons were made for steam mass flow rate, temperature and pressure at the exit of each pressure level at 60% and 80% load. The maximum error of the Virtual Plant model compared to plant data was 13% for off-design conditions. That of the Flownex model was 10%. This is acceptable due to the fact that multiple assumptions had to be made while modelling the triple pressure system as well as the changes in design temperatures. It also needs to be considered that the actual plant could have various control mechanisms and external factors incorporated in the system that were not modelled in this project, such as attemperation, control valves, moisture separators and bypass controls.

The results obtained show that Flownex is capable of modelling a combined-cycle power plant in design and off-design conditions.

6.3 Recommendations

It is recommended that more plant data be obtained for the triple pressure model in order to fine tune the results. This would help to perfect the calculation and design of the model. Modelling control elements of the system such as attemperation, control valves, moisture separators and bypass controls would also lead to a more accurate model. Once plant design data is obtained, all additional components in the system, that may not have been disclosed by Alobaid et al. [27], as well as control mechanisms can be analysed and modelled.

Using the ‘Designer’ function in Flownex would be a more efficient method of finding the operational pressure at low loads. It can, however, be unstable due to the two-phase nature of the problem. The transient controller should also be considered in order to increase efficiency. Manually adjusting the low-pressure boundary condition and intermediate- and high-pressure pumps in order to find the operational pressure at each low load can be tedious and lead to inaccuracies.

7. List of References

[1] M. S. Y. Ebaid and Q. Z. Al-hamdan, "Thermodynamic Analysis of Different Configurations of Combined Cycle Power Plants," *Mech. Eng. Res.*, vol. 5, no. 2, p. 89, 2015.

[2] C. Vandervort, T. Wetzel, and D. Leach, "Engineering And Validating A World Record Gas Turbine," *Mech. Eng.*, vol. 139, no. 12, 2017.

[3] T. K. Ibrahim and M. M. Rahman, "Effect of Compression Ratio on Performance of Combined Cycle Gas Turbine," *Int. J. Energy Eng.*, vol. 2, no. 1, pp. 9–14, 2012.

[4] Y. A. Cengel and M. A. Boles, *Thermodynamics An Engineering Approach*. 2011.

[5] P. K. Nag, *Power Plant Engineering*. 2008.

[6] M. P. Boyce, "Combined cycle power plants," *Comb. Cycle Syst. Near-Zero Emiss. Power Gener.*, pp. 1–43, 2012.

[7] A. D. Rao, *Combined Cycle Systems for Near-Zero Emission Power Generation*. Elsevier Ltd., 2012.

[8] R. Kehlhofer, F. Hannemann, B. Rukes, and F. Stirnimann, *Combined-Cycle Gas & Steam Turbine Power Plants*, 3rd ed. PennWell Corporation, 2009.

[9] V. Ganapathy, "Heat-recovery steam generators: Understand the basics," *Chem. Eng. Prog.*, vol. 92, no. 8, pp. 32–45, 1996.

[10] V. Ganapathy, *Steam Generators and Waste Heat Boilers for Process and Plant Engineers*. 2015.

[11] T. K. Ibrahim and M. M. Rahman, "Study on effective parameter of the triple-pressure reheat combined cycle performance," *Therm. Sci.*, vol. 17, no. 2, pp. 497–508, 2013.

[12] M. Mohagheghi and J. Shayegan, "Thermodynamic optimization of design variables and heat exchangers layout in HRSGs for CCGT , using genetic algorithm," *Appl. Therm. Eng.*, vol. 29, no. 2–3, pp. 290–299, 2009.

[13] A. T. Jarullah, "Heat Exchanger Effectiveness (NTU method)." [Online]. Available: http://ceng.tu.edu.iq/ched/images/lectures/chem-lec/st3/c2/Lec23.pdf. [Accessed: 23-Jul-2018].

[14] S. Cafaro, A. Traverso, and A. F. Massardo, "Monitoring of HRSG Performance in Large Size Combined Cycle Power Plants," no. January, 2008.

[15] R. Kehlhofer, *Combined-Cycle Gas & Steam Turbine Power Plants*. Oklahoma: PennWell Publishing Company, 1997.

[16] M. G. Zewge, T. A. Lemma, A. A. Ibrahim, and D. Sujan, "Modeling and Simulation of a Heat Recovery Steam Generator Using Partially Known Design Point Data," *Adv. Mater. Res.*, vol. 845, pp. 596–603, 2013.

[17] F. Haglind, "Variable geometry gas turbines for improving the part-load performance of marine combined cycles - Combined cycle performance," *Appl. Therm. Eng.*, vol. 31, no. 4, pp. 467–476, 2011.

[18] A. Tica, H. Guéguen, D. Dumur, D. Faille, and F. Davelaar, “Design of a combined cycle power plant model for optimization,” vol. 98, pp. 256–265, 2012.

[19] M. P. Polsky, “Sliding Pressure Operation in Combined Cycles,” *Am. Soc. Mech. Eng.*, 1982.

[20] A. Stodola, *Steam and Gas Turbines*, Vol. 1. New York: Peter Smith, 1945.

[21] W. F. Fuls, “Enhancement to the Traditional Ellipse Law for More Accurate Modeling of a Turbine With a Finite Number of Stages,” 2017.

[22] D. Lindsley, *Power-plant Control and Instrumentation - The Control of Boilers and HRSG Systems*. Institution of Engineering and Technology, 2000.

[23] N. A. Ali and A. Y. Abdalla, “Modeling Combined Cycle Performance At Full and Part Loads,” *9th Int. Conf. Heat Transf. Fluid Mech. Thermodyn.*, no. July, pp. 1211–1221, 2012.

[24] M. Rauch, A. Galović, and Z. Virag, “Optimization of combined brayton-rankine cycle with respect to the total thermal efficiency,” *Trans. Famena*, vol. 40, no. 1, pp. 1–10, 2016.

[25] D. Kumar Mohanty and V. Venkatesh, “Performance Analysis of a Combined Cycle Gas Turbine Under Varying Operating Conditions,” *Mech. Eng. An Int. J. (MEIJ)*, vol. 1, no. 2, pp. 11–25, 2014.

[26] T. Srinivas, A. V. S. S. K. S. Gupta, and B. V. Reddy, “Thermodynamic simulation of a combined cycle power plant at part-load operation,” *Cogener. Distrib. Gener. J.*, vol. 23, no. 4, pp. 50–63, 2008.

[27] F. Alobaid, R. Starkloff, S. Pfeiffer, K. Karner, B. Epple, and H. Kim, “A comparative study of different dynamic process simulation codes for combined cycle power plants – Part A : Part loads and off-design operation,” *Fuel*, vol. 153, pp. 692–706, 2015.

[28] “Mathcad.” [Online]. Available: https://www.mathcad.com/en.

[29] “VirtualPlant.” [Online]. Available: https://www.gpstrategies.com/solution/technical-engineering/etapro/etapro-virtualplant-thermal-performance/.

[30] “Flownex.” [Online]. Available: https://www.flownex.com/.

[31] V. Ganapathy, *Industrial Boilers and Heat Recovery Steam Generators*. CRC Press, 2002.

[32] P. Rousseau and W. F. Fuls, “Power Plant Systems Analysis.” 2018.

[33] J. I. Manassaldi, S. F. Mussati, and N. J. Scenna, “Optimal synthesis and design of Heat Recovery Steam Generation (HRSG) via mathematical programming,” *Energy*, 2011.

Appendix A. Single Pressure Analytical Model – Design Case

Design Case

This model will calculate the temperatures, mass flow rates, duties and other variables for design conditions of a combined-cycle power plant

Known Variables

The known variables of the system are as follows

$m_{gas} := 148788 \frac{lb}{h} = 18.747 \frac{kg}{s}$ gas mass flow rate entering HRSG

$T_{g.1} := 1019\,°F = 548.333\,°C$ gas temperature entering HRSG

$P_{so} := 615psi = 4.24\,MPa$ pressure of steam generated

$T_{so} := 600\,°F = 315.556\,°C$ temperature of steam generated

$T_{w.1} := 230\,°F = 110\,°C$ Temperature of water entering HRSG

The following schematic provides the representation of each variable name

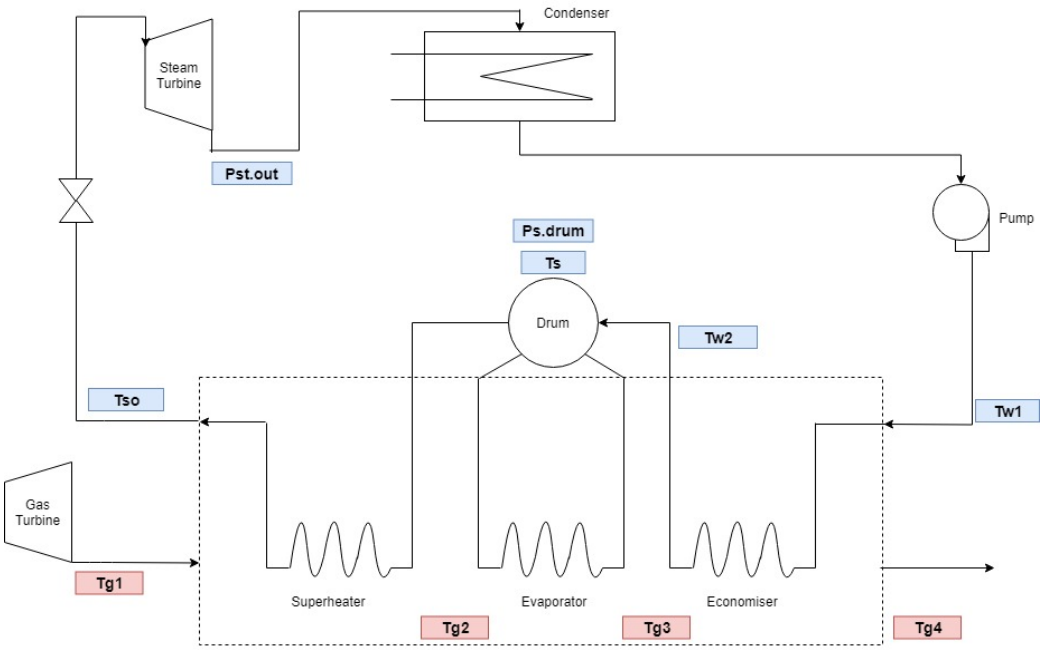

Calculation

HRSG

Assumptions

Initially, a pinch point and approach point need to be chosen in order to form the basis of the HRSG design

$PP := 15\Delta°F = 8.333K$ Pinch point

$AP := 15\Delta°F = 8.333K$ Approach point

The formula for the enthalpy of air is used as an estimate to calculate the enthalpy of gas at certain temperatures

$$h_{gas}(T) := \left[0.9816 \cdot T/°C + 1.245 \cdot 10^{-4} \cdot (T/°C)^2 - 1.308 \cdot 10^{-8} \cdot (T/°C)^3 - 2.154 \cdot 10^{-12} \cdot (T/°C)^4\right] \frac{kJ}{kg}$$

The drum pressure will be equal to the pressure of steam generated as the pressure through the HRSG remains constant

$P_{s.drum} := P_{so} = 4.24 \cdot MPa$ Drum pressure

Therefore, the saturated steam temperature can be calculated using steam tables

$T_s := T_{steam}(P_{s.drum}, "", "", "") = 253.84 \cdot °C$ Saturation temperature

Using the temperature profile as reference, the following temperatures can be calculated

$T_{g.3} := T_s + PP = 262.174 \cdot °C$ gas temperature leaving evaporator

$T_{w.2} := T_s - AP = 245.507 \cdot °C$ water temperature entering evaporator

The duty of the superheater and evaporator combined can be calculated using the gas mass flow and change in enthalpy

$Q_{sh.ev} := m_{gas} \cdot (h_{gas}(T_{g.1}) - h_{gas}(T_{g.3})) = 5.768 \cdot MW$ heat absorbed by the superheater and evaporator

This can then be used to calculate the steam mass flow rate using enthalpies of steam

$h_{so} := h_{steam}(P_{so}, T_{so}, "", "", "") = 2.997 \times 10^3 \cdot \frac{kJ}{kg}$ enthalpy of superheated steam

$h_{w.2} := h_{steam}(P_{s.drum}, T_{w.2}, "", "", "") = 1.064 \times 10^3 \cdot \frac{kJ}{kg}$ enthalpy of water entering evaporator

$m_{steam} := \frac{Q_{sh.ev}}{(h_{so} - h_{w.2})} = 2.984 \cdot \frac{kg}{s}$ steam mass flow rate

The duty of the superheater can be calculated using the steam mass flow rate

$h_s := h_{steam}(P_{s.drum}, "", "", 1, "") = 2799.622 \cdot \frac{kJ}{kg}$ vapor enthalpy at drum pressure

$Q_{sh} := m_{steam} \cdot (h_{so} - h_s) = 589.3 \cdot kW$ energy absorbed by superheater

This can be used to calculate the change in enthalpy over the superheater and the enthalpy formula can be used to calculate the temperature of the gas exiting the superheater

$\Delta h_{12} := \frac{Q_{sh}}{m_{gas}} = 31.434 \cdot \frac{kJ}{kg}$ change in gas enthalpy over the superheater

$h_{g1} := h_{gas}(T_{g.1}) = 573.326 \cdot \frac{kJ}{kg}$ enthalpy of gas entering the superheater

$h_{g2} := h_{g1} - \Delta h_{12} = 541.892 \cdot \frac{kJ}{kg}$ enthalpy of gas exiting the superheater

$T_{g.2} := root(h_{gas}(T_{g.1}) - h_{g2}, T_{g.1}) = 519.81 \cdot °C$ gas temperature leaving superheater

The evaporator and economiser duties are calculated as follows

$Q_{ev} := Q_{sh.ev} - Q_{sh} = 5.178 \cdot MW$ evaporator duty

$h_{w.1} := h_{steam}(P_{s.drum}, T_{w.1}, "", "", "") = 464.348 \cdot \frac{kJ}{kg}$ enthalpy of water entering HRSG

$Q_{ec} := m_{steam} \cdot (h_{w.2} - h_{w.1}) = 1.789 \cdot MW$ economiser duty

Finally, the enthalpy formula can be used to calculate the temperature of gas exiting the economiser

$\Delta h_{34} := \frac{Q_{ec}}{m_{gas}} = 95.426 \cdot \frac{kJ}{kg}$ change in gas enthalpy over the economiser

$h_{g3} := h_{gas}(T_{g.3}) = 265.661 \cdot \frac{kJ}{kg}$ enthalpy of gas entering the economiser

$h_{g4} := h_{g3} - \Delta h_{34}$ enthalpy of gas exiting the economiser

$T_{g.4} := root(h_{gas}(T_{g.3}) - h_{g4}, T_{g.3}) = 169.835 \cdot °C$ exit gas temperature from economiser

UA

UA (overall conductance) calculations are made in order for the system to be evaluated in off-design mode
The log mean temperature over each component is first calculated so that the UA of each component may be calculated

$LMTD_{sh} := \frac{(T_{g.1} - T_{so}) - (T_{g.2} - T_s)}{\ln\left[\frac{(T_{g.1} - T_{so})}{(T_{g.2} - T_s)}\right]} = 249.005 \cdot K$ Log mean temperature difference over the superheater

$LMTD_{ev} := \frac{(T_{g.2} - T_s) - (T_{g.3} - T_s)}{\ln\left[\frac{(T_{g.2} - T_s)}{(T_{g.3} - T_s)}\right]} = 74.394 \cdot K$ Log mean temperature difference over the evaporator

$LMTD_{ec} := \frac{(T_{g.3} - T_{w.2}) - (T_{g.4} - T_{w.1})}{\ln\left[\frac{(T_{g.3} - T_{w.2})}{(T_{g.4} - T_{w.1})}\right]} = 33.773 \cdot K$ Log mean temperature difference over the economiser

$UA_{sh.d} := \frac{Q_{sh}}{LMTD_{sh}} = 2.367 \cdot \frac{kW}{K}$ Overall conductance of the superheater

$UA_{ev.d} := \frac{Q_{ev}}{LMTD_{ev}} = 69.609 \cdot \frac{kW}{K}$ Overall conductance of the evaporator

$UA_{ec.d} := \frac{Q_{ec}}{LMTD_{ec}} = 52.969 \cdot \frac{kW}{K}$ Overall conductance of the economiser

Condenser

$P_{con} := p_{steam}(T_{w.1}, "", "", "") = 143.376 \cdot kPa$ Saturated water pressure in the condenser

Pressure drop over steam turbine

$P_{st.out} := P_{con} = 143.376 \cdot kPa$ Pressure of steam exiting the steam turbine

$\Delta P_{st.d} := -P_{st.out} + P_{so} = 4.097 \times 10^3 \cdot kPa$ Pressure drop across the steam turbine

Mass Flow in Evaporator

$h_{ev.in} := h_{steam}(P_{s.drum}, "", "", 0, "") = 1.104 \times 10^3 \cdot \frac{kJ}{kg}$ enthalpy of water entering the evaporator

$h_{ev.out} := h_{steam}(P_{s.drum}, "", "", 0.5, "") = 1.952 \times 10^3 \cdot \frac{kJ}{kg}$ enthalpy of water exiting the evaporator

$m_{ev} := \frac{Q_{ev}}{h_{ev.out} - h_{ev.in}} = 6.11 \frac{kg}{s}$ mass flow rate in the evaporator

Steam Turbine Calculations

$P_{so} - P_{con} = 4.097 \cdot MPa$ Pressure drop over the turbine

$\rho_w := \rho_{steam}(P_{so}, T_{so}, "", "", "") = 17.411 \frac{kg}{m^3}$ Density of steam entering the turbine

$V_w := \frac{m_{steam}}{\rho_w} = 0.171 \frac{m^3}{s}$ Volumetric flow rate of steam through the turbine

Results

$m_{steam} = 2.984 \frac{kg}{s}$

$m_{gas} = 18.747 \frac{kg}{s}$

$Q_{sh} = 589.3 \cdot kW$

$Q_{ev} = 5.178 \times 10^3 \cdot kW$

$Q_{ec} = 1.789 \times 10^3 \cdot kW$

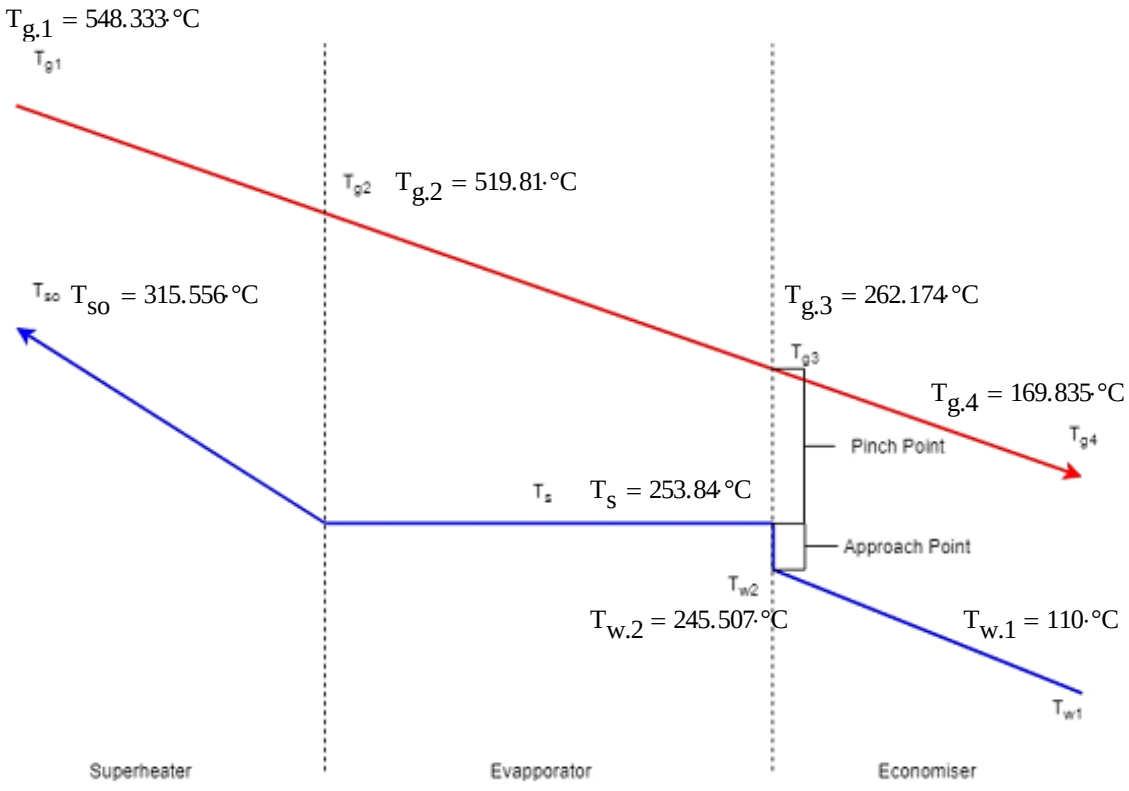
$T_{g.1} = 548.333 \cdot °C$
T_{g1}
T_{g2} $T_{g.2} = 519.81 \cdot °C$
T_{so} $T_{so} = 315.556 \cdot °C$
$T_{g.3} = 262.174 \cdot °C$
T_{g3}
$T_{g.4} = 169.835 \cdot °C$
T_{g4}
Pinch Point
T_s $T_S = 253.84 \cdot °C$
Approach Point
T_{w2}
$T_{w.2} = 245.507 \cdot °C$
$T_{w.1} = 110 \cdot °C$
T_{w1}
Superheater
Evapporator
Economiser

Appendix B. Single Pressure Analytical Model – Off-Design Case

Off-Design Case

This model will calculate the temperatures, mass flow rate, duties and other variables for off-design conditions of a combined-cycle power plant. Factors from the design case will be used in order to make certain calculations. The off-design mode is carried out at 45% load

Known Variables

The known variables of the off-design case are as follows

The gas mass flow and inlet temperature are controlled in the off-design so that they follow a trend. This is done to prevent steaming in the economiser. Initially, mass flow remains constant while temperature increases up until 50% load, after which the temperature remains constant while mass flow increases. The following calculations plot this concept on a graph which allows for the calculation of temperature and mass flow at any load

$$data := \begin{pmatrix} 40 & 866.15 & 111591 \\ 50 & 1019 & 111591 \\ 100 & 1019 & 148788 \end{pmatrix}$$

3 points on the graph at 40%, 50% and 100% load

$$Mflow(load) := linterp\left(data^{\langle 0 \rangle}, data^{\langle 2 \rangle}, load\right) \cdot \frac{lb}{h}$$

Plotting of mass flow

$$Tflow(load) := linterp\left(data^{\langle 0 \rangle}, data^{\langle 1 \rangle}, load\right) °F$$

Plotting of temperature

$$load := 0, 10 .. 100$$

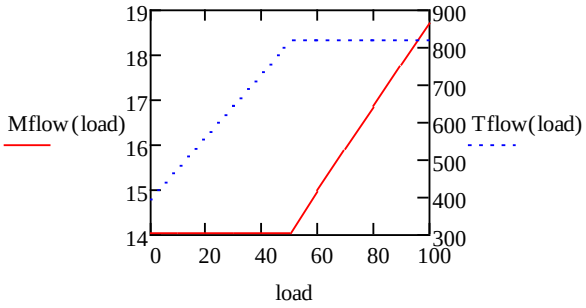

Graph of mass flow and temperature over various loads

$m_{gas} := Mflow(45) = 14.06 \frac{kg}{s}$ gas flow rate entering HRSG at 45% load

$T_{g.1} := Tflow(45) = 505.875 °C$ gas temperature entering HRSG at 45% load

$P_{so} := 423.5 psi = 29.199 bar$ pressure of steam generated

$T_{so} := 600 °F = 315.556 °C$ temperature of steam generated

$T_{w.1} := 230 °F = 110 °C$ Temperature of water entering HRSG

$m_{gas.d} := 148788 \frac{lb}{h} = 18.747 \frac{kg}{s}$ gas mass flow rate in the design case

$UA_{sh.d} := 2.367 \frac{kW}{K}$ Overall conductance of the superheater in the design case

$UA_{ev.d} := 69.609 \frac{kW}{K}$ Overall conductance of the evaporator in the design case

$UA_{ec.d} := 52.969 \frac{kW}{K}$ Overall conductance of the economiser in the design case

Calculation

HRSG

Assumptions for the specific heat capacities of gas and steam/water had to be made due to the face that temperatures are not yet known

$c_{p.g.sh} := 0.277\frac{kcal}{kg\cdot K} = 1.16\cdot\frac{kJ}{kg\cdot K}$ specific heat capacity of gas in the superheater

$c_{p.g.ev} := 0.269\frac{kcal}{kg\cdot K} = 1.126\cdot\frac{kJ}{kg\cdot K}$ specific heat capacity of gas in the evaporator

$c_{p.g.ec} := 0.259\frac{kcal}{kg\cdot K} = 1.084\cdot\frac{kJ}{kg\cdot K}$ specific heat capacity of gas in the economiser

$C_{gas.sh} := m_{gas}\cdot c_{p.g.sh} = 16.306\cdot\frac{kJ}{s\cdot K}$ Fluid heat capacity of gas in the superheater

$C_{gas.ev} := m_{gas}\cdot c_{p.g.ev} = 15.835\cdot\frac{kJ}{s\cdot K}$ Fluid heat capacity of gas in the evaporator

$C_{gas.ec} := m_{gas}\cdot c_{p.g.ec} = 15.247\cdot\frac{kJ}{s\cdot K}$ Fluid heat capacity of gas in the economiser

$c_{p.s.sh} := 0.764\frac{kcal}{kg\cdot K} = 3.199\cdot\frac{kJ}{kg\cdot K}$ specific heat capacity of steam in the superheater

$c_{p.s.ev} := 49.747\frac{kcal}{kg\cdot K} = 208.281\cdot\frac{kJ}{kg\cdot K}$ specific heat capacity of steam/water in the evaporator

$c_{p.s.ec} := 1.057\frac{kcal}{kg\cdot K} = 4.425\cdot\frac{kJ}{kg\cdot K}$ specific heat capacity of water in the economiser

An assumption also had to be made for the steam mass flow which was then iterated

$m_{steam.a} \equiv 2.096\frac{kg}{s}$ Assumed mass flow rate of steam

$C_{steam.sh} := m_{steam.a}\cdot c_{p.s.sh} = 6.705\cdot\frac{kJ}{s\cdot K}$ Fluid heat capacity of steam in the superheater

$C_{steam.ev} := m_{steam.a}\cdot c_{p.s.ev} = 436.556\cdot\frac{kJ}{s\cdot K}$ Fluid heat capacity of steam/water in the evaporator

$C_{steam.ec} := m_{steam.a}\cdot c_{p.s.ec} = 9.276\cdot\frac{kJ}{s\cdot K}$ Fluid heat capacity of water in the economiser

The overall conductance (UA) of each component in the off design case were calculated using the UA's of the components in the design case and the gas mass flow in both design and off-design case. This could be done using a simplification of the relationship between the UA's in design and off-design modes

$UA_{sh} := UA_{sh.d}\cdot\left(\frac{m_{gas}}{m_{gas.d}}\right)^{0.65} = 1.963\cdot\frac{kW}{K}$ Overall conductance of the superheater

$UA_{ev} := UA_{ev.d}\cdot\left(\frac{m_{gas}}{m_{gas.d}}\right)^{0.65} = 57.737\cdot\frac{kW}{K}$ Overall conductance of the evaporator

$UA_{ec} := UA_{ec.d}\cdot\left(\frac{m_{gas}}{m_{gas.d}}\right)^{0.65} = 43.935\cdot\frac{kW}{K}$ Overall conductance of the economiser

The effectiveness of each component is found using the number of transfer units (NTU) and the fluid heat capacities of gas and steam/water in that component

First, the minimum and maximum fluid heat capacities between the gas and water/steam need to be identified. Thereafter, NTU and effectiveness may be calculated

Superheater

$C_{min.sh} := \min(C_{steam.sh}, C_{gas.sh}) = 6.705 \cdot \frac{kW}{K}$ — Minimum fluid heat capacity in the superheater

$C_{max.sh} := \max(C_{steam.sh}, C_{gas.sh}) = 16.306 \cdot \frac{kW}{K}$ — Maximum fluid heat capacity in the superheater

$NTU_{sh} := \frac{UA_{sh}}{C_{min.sh}} = 0.293$ — Number of transfer units in the superheater

$R_{sh} := \frac{C_{min.sh}}{C_{max.sh}} = 0.411$ — Ratio of minimum to maximum fluid heat capacities in the superheater

$\varepsilon_{sh} := \frac{1 - e^{-NTU_{sh} \cdot (1 - R_{sh})}}{1 - R_{sh} \cdot e^{-NTU_{sh} \cdot (1 - R_{sh})}} = 0.242$ — Effectiveness of the superheater

Evaporator

$C_{min.ev} := \min(C_{steam.ev}, C_{gas.ev}) = 15.835 \cdot \frac{kW}{K}$ — Minimum fluid heat capacity in the evaporator

$C_{max.ev} := \max(C_{steam.ev}, C_{gas.ev}) = 436.556 \cdot \frac{kW}{K}$ — Maximum fluid heat capacity in the evaporator

$NTU_{ev} := \frac{UA_{ev}}{C_{min.ev}} = 3.646$ — Number of transfer units in the evaporator

$\varepsilon_{ev} := 1 - e^{-NTU_{ev}} = 0.974$ — Effectiveness of the evaporator

The effectiveness formla for the evaporator is different due to R approaching zero. This is because a phase change occurs and Cmax becomes immense

Economiser

$C_{min.ec} := \min(C_{steam.ec}, C_{gas.ec}) = 9.276 \cdot \frac{kW}{K}$ — Minimum fluid heat capacity in the economiser

$C_{max.ec} := \max(C_{steam.ec}, C_{gas.ec}) = 15.247 \cdot \frac{kW}{K}$ — Maximum fluid heat capacity in the economiser

$NTU_{ec} := \frac{UA_{ec}}{C_{min.ec}} = 4.737$ — Number of transfer units in the economiser

$R_{ec} := \frac{C_{min.ec}}{C_{max.ec}} = 0.608$ — Ratio of minimum to maximum fluid heat capacities in the economiser

$\varepsilon_{ec} := \frac{1 - e^{-NTU_{ec} \cdot (1 - R_{ec})}}{1 - R_{ec} \cdot e^{-NTU_{ec} \cdot (1 - R_{ec})}} = 0.932$ — Effectiveness of the economiser

The effectiveness formula used is that of a cross flow heat exchanger
Thereafter, the effectiveness of each component can be used to calculate the duties of the respective component. The pinch and approach points can no longer be chosen in order to calculate the gas temperature leaving the evaporator and the water temperature entering the evaporator

The drum pressure will be equal to the pressure of steam generated as the pressure through the HRSG remains constant

$P_{s.drum} := P_{so} = 2.92 \cdot MPa$ Drum pressure

Therefore, the saturated steam temperature can be calculated using steam tables

$T_s := T_{steam}(P_{s.drum}, "", "", "") = 232.363 \cdot °C$ Saturation temperature

The duty of the superheater can be calculated using the effectiveness, minimum fluid head capacity and difference in temperature between the gas and steam entering the superheater (maximum temperature difference between the fluids in the superheater)

$Q_{sh} := \varepsilon_{sh} \cdot C_{min.sh} \cdot (T_{g.1} - T_s) = 444.124 \cdot kW$ Energy absorbed by superheater

The temperature of gas can then be calculated using an energy balance across the superheater

$T_{g.2} := T_{g.1} - \frac{Q_{sh}}{m_{gas} \cdot c_{p.g.sh}} = 478.639 \cdot °C$ Temperature of gas exiting superheater

The duty of the evaporater was calculated using the same concept as that of the superheater

$Q_{ev} := \varepsilon_{ev} \cdot C_{min.ev} \cdot (T_{g.2} - T_s) = 3.798 \cdot MW$ Energy absorbed in evaporator

The temperature of water entering the evaporator had to initially be assumed, this was then iterated

$T_{w.2} := 447 °F = 230.556 \cdot °C$ Assumed temperature of water entering evaporator

This was used to calculate the enthalpy of water at that point. Thereafter, the mass flow rate of steam was calculated using an energy balance across the evaporator with steam/water enthalpies

$h_s := h_{steam}(P_{s.drum}, "", "", 1, "") = 2.803 \times 10^3 \cdot \frac{kJ}{kg}$ vapor enthalpy at drum pressure

$h_{w.2} := h_{steam}(P_{s.drum}, T_{w.2}, "", "", "") = 992.835 \cdot \frac{kJ}{kg}$ enthalpy of water entering the evaporator

$m_{steam} := \frac{Q_{ev}}{(h_s - h_{w.2})} = 2.098 \cdot \frac{kg}{s}$ steam mass flow rate

The temperature of gas exiting the evaporator could also be calculated using an energy balance across the evaporator

$T_{g.3} := T_{g.2} - \frac{Q_{ev}}{m_{gas} \cdot c_{p.g.ev}} = 238.789 \cdot °C$ Temperature of gas exiting evaporator

The duty of the economiser was calculated using the same concept as that of the superheater and evaporator

$Q_{ec} := \varepsilon_{ec} \cdot C_{min.ec} \cdot (T_{g.3} - T_{w.1}) = 1.114 \cdot MW$ Energy absorbed in economiser

The assumption of water temperature entering the evaporator then needed to be tested in order for iteration. This was done using an energy balance across the economiser by calculating the enthalpies of water entering and exiting it and using steam tables to find the temperature

$h_{w.1} := h_{steam}(P_{s.drum}, T_{w.1}, "", "", "") = 463.385 \cdot \frac{kJ}{kg}$ enthalpy of water entering economiser

$h_{w.2.test} := \frac{Q_{ec}}{m_{steam}} + h_{w.1} = 994.237 \cdot \frac{kJ}{kg}$ enthalpy of water exiting economiser

$T_{w.2.test} := T_{steam}(P_{s.drum}, "", h_{w.2.test}, "") = 230.838 \cdot °C$ Check for water temperature entering evaporator

Q

entering evaporator

$T_{g.4} := T_{g.3} - \frac{Q_{ec}}{m_{gas} \cdot c_{p.g.ec}} = 165.742 \cdot °C$ Temperature of gas exiting HRSG

The temperature of steam generated was calculated in order to compare it to the desired temperature of steam

$h_{so} := \frac{Q_{sh}}{m_{steam}} + h_s = 3.015 \times 10^3 \cdot \frac{kJ}{kg}$ Enthalpy of steam generated

$T_{so.test} := T_{steam}(P_{so}, "", h_{so}, "") = 307.203 \cdot °C$ Temperature of steam generated

Attemperation

The attemperation required would ideally be zero due to sliding pressure. However, a calclation was done in order for testing. The mass flow rate of attemperation can be calculated using the conservation of energy

$m_{att} \cdot h_{cool} + m_{steam} \cdot h_{so} = m_{steam} \cdot h_{desired} + m_{att} \cdot h_{desired}$ Energy balance before and after attemperation

$h_{desired} := h_{steam}(P_{so}, T_{so}, "", "", "") = 3.035 \times 10^3 \cdot \frac{kJ}{kg}$ Enthalpy of steam after attemperation

$h_{cool} := h_{w.1}$ water used for attemperation will be the same as feedwater

$m_{att} := \frac{m_{steam} \cdot (h_{so} - h_{desired})}{(h_{desired} - h_{cool})} = -0.017 \frac{kg}{s}$ mass flow rate of attemperation

Condenser

$P_{con} := p_{steam}(T_{w.1}, "", "", "") = 1.434 \times 10^5 Pa$ Saturated water pressure in the condenser

Turbine Pressure

The flow coefficient allows for the turbine swallowing capacity to be maintained. It relates the mass flow rate of steam in the design condition to that of the off-design condition. Using this, the pressure entering the steam turbine can be calculated so that the pressure drop over the turbine can be calculated

$P_{so.d} := 4.24 \times 10^3 \, kPa$ Pressure of steam generated in the design condition

$m_{steam.d} := 3.106 \frac{kg}{s}$ mass flow rate of steam in the design condition

$\rho_{st.in.d} := 17.411 \frac{kg}{m^3}$ Density of water entering the steam turbine in the design condition

$\rho_{st.in} := \rho_{steam}(P_{so}, T_{so}, "", "", "") = 11.537 \frac{kg}{m^3}$ density of water entering the steam turbine

$m_{steam} = m_{steam.d} \cdot \frac{\sqrt{P_{in} \cdot \rho_{st.in}}}{\sqrt{P_{so.d} \cdot \rho_{st.in.d}}}$ mass flow rate of steam

$P_{in} := \frac{P_{so.d} \cdot m_{steam}^2 \cdot \rho_{st.in.d}}{m_{steam.d}^2 \cdot \rho_{st.in}} = 2.919 \cdot MPa$ pressure entering the steam turbine as a result of the equation above

Ideally, the control valve before the steam turbine should be fully open, so the pressure drop over the valve should be zero. This was used to adjust the steam pressure in order to find the operational pressure at each low load

$\Delta P_{valve} := P_{so} - P_{in} = 0.562 \cdot kPa$ Valve pressure drop

$P_{st.out} := P_{con} = 143.376 \cdot kPa$ Pressure of steam exiting the steam turbine

$\Delta P_{st} := P_{in} - P_{st.out} = 2.776 \cdot MPa$ Steam turbine pressure drop

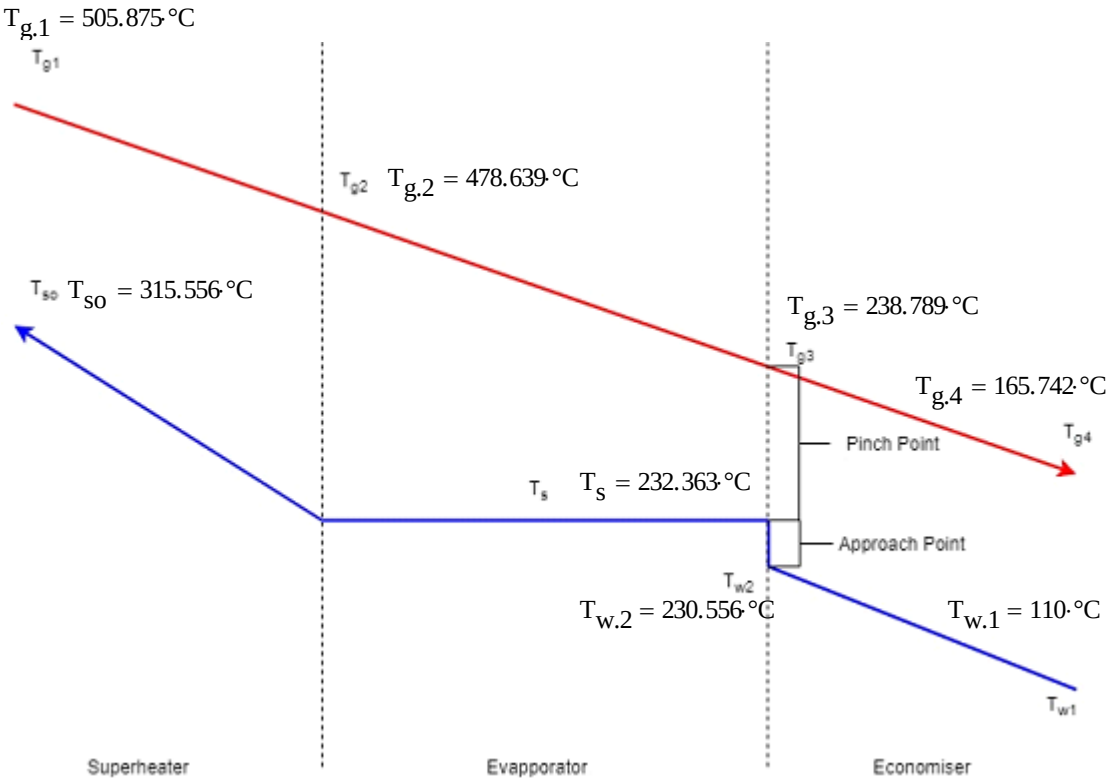

Appendix C. Double Pressure Analytical Model

Double Pressure

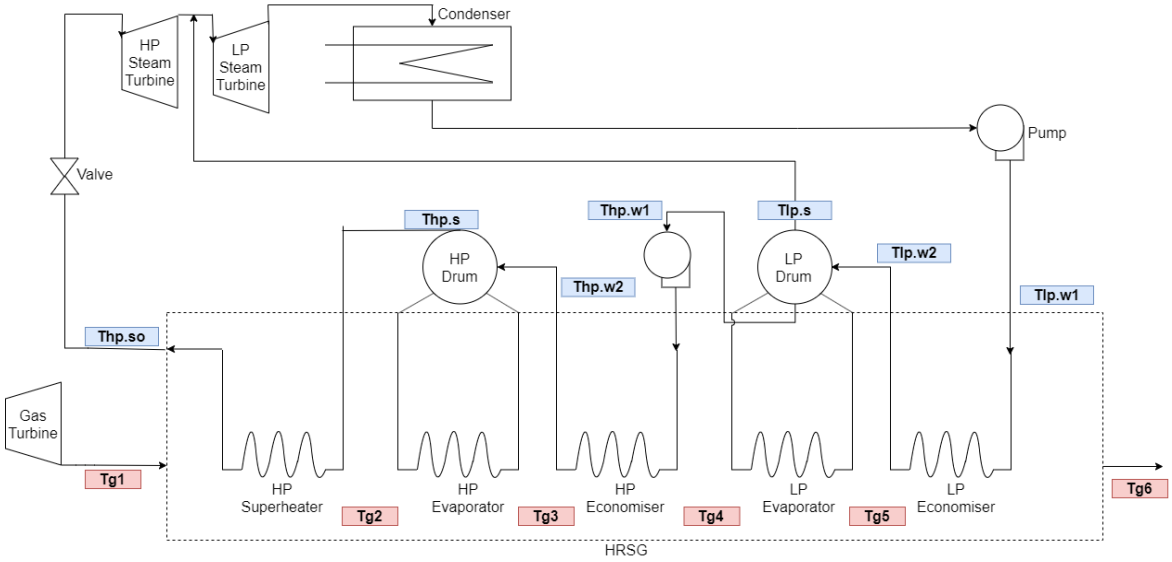

Known Variables

$m_{steam.hp} := 39500\frac{lb}{h} = 4.977\frac{kg}{s}$ mass flow of HP steam required

$m_{steam.lp} := 50842\frac{lb}{h} = 6.406\frac{kg}{s}$ mass flow of LP steam required

$P_{hp} := 830psi = 57.226\cdot bar$ HP steam pressure

$P_{lp} := 115psi = 7.929\cdot bar$ LP steam pressure

$m_{gas} := 300000\frac{lb}{h} = 37.799\frac{kg}{s}$ gas mass flow

$T_{g1} := 1000\,°F = 537.778\cdot °C$ gas temperature entering HRSG

$PP_{hp} := 50\Delta°F = 27.778K$ Pinch points

$PP_{lp} := 10\Delta°F = 5.556K$

$AP_{hp} := 15\Delta°F = 8.333K$ Approach points

$AP_{lp} := 10\Delta°F = 5.556K$

$T_{lp.w1} := 230\,°F = 110\cdot °C$ Temperature of water entering HRSG

Solution

$$h_{gas}(T) := \left[0.9816\cdot T/°C + 1.245\cdot 10^{-4}\cdot (T/°C)^2 - 1.308\cdot 10^{-8}\cdot (T/°C)^3 - 2.154\cdot 10^{-12}\cdot (T/°C)^4\right]\frac{kJ}{kg}$$

High Pressure

$T_{hp.s} := T_{steam}(P_{hp}, "", "", "") = 272.516°C$ HP Saturation temperature

$T_{g.3} := T_{hp.s} + PP_{hp} = 300.293\cdot °C$ gas temperature leaving HP evaporator

$T_{hp.w2} := T_{hp.s} - AP_{hp} = 264.182\cdot °C$ water temperature entering HP evaporator

$Q_{hp.sh.ev} := m_{gas}\cdot\left(h_{gas}(T_{g1}) - h_{gas}(T_{g.3})\right) = 9.679\cdot MW$ heat absorbed by the superheater and HP evaporator

$h_{hp.w2} := h_{steam}(P_{hp}, T_{hp.w2}, "", "", "") = 1.156 \times 10^3 \cdot \frac{kJ}{kg}$ enthalpy of water entering HP evaporator

$h_{hp.s} := h_{steam}(P_{hp}, "", "", 1, "") = 2.787 \times 10^3 \cdot \frac{kJ}{kg}$ vapor enthalpy at HP drum pressure

$h_{so} := h_{hp.w2} + \frac{Q_{hp.sh.ev}}{m_{steam.hp}} = 3.1 \times 10^3 \cdot \frac{kJ}{kg}$ enthalpy of superheated steam

$T_{so} := T_{steam}(P_{hp}, "", h_{so}, "") = 368.004\,°C$ Temperature of superheated steam

$Q_{hp.sh} := m_{steam.hp} \cdot (h_{so} - h_{hp.s}) = 1.556\,MW$ energy absorbed by superheater

$\Delta h_{12} := \frac{Q_{hp.sh}}{m_{gas}} = 41.176 \frac{kJ}{kg}$ change in gas enthalpy over the superheater

$h_{g1} := h_{gas}(T_{g1}) = 561.674 \frac{kJ}{kg}$ Enthalpy of gas entering superheater

$h_{g2} := h_{g1} - \Delta h_{12} = 520.498 \frac{kJ}{kg}$ Enthalpy of gas exiting superheater

$T_{g.2} := root(h_{gas}(T_{g1}) - h_{g2}, T_{g1}) = 500.313\,°C$ gas temperature exiting superheater

$Q_{hp.ev} := Q_{hp.sh.ev} - Q_{hp.sh} = 8.122\,MW$ HP evaporator duty

$T_{lp.s} := T_{steam}(P_{lp}, "", "", "") = 170.044\,°C$ LP Saturation temperature

$T_{hp.w1} := T_{lp.s} = 170.044\,°C$ Temperature entering HP economiser

$h_{hp.w1} := h_{steam}(P_{hp}, T_{hp.w1}, "", "", "") = 722.111 \frac{kJ}{kg}$ enthalpy of water entering HP economizer

$Q_{hp.ec} := m_{steam.hp} \cdot (h_{hp.w2} - h_{hp.w1}) = 2.157\,MW$ HP economiser duty

$\Delta h_{34} := \frac{Q_{hp.ec}}{m_{gas}} = 57.068 \frac{kJ}{kg}$ change in gas enthalpy over HP economiser

$h_{g3} := h_{gas}(T_{g.3}) = 305.623 \frac{kJ}{kg}$ gas enthaply entering HP economiser

$h_{g4} := h_{g3} - \Delta h_{34} = 248.555 \frac{kJ}{kg}$ gas enthaply exiting HP economiser

$T_{g.4} := root(h_{gas}(T_{g.3}) - h_{g4}, T_{g.3}) = 245.76\,°C$ exit gas temperature from economiser

Low Pressure

$T_{g.5} := T_{lp.s} + PP_{lp} = 175.6\,°C$ gas temperature leaving LP evaporator

$T_{lp.w2} := T_{lp.s} - AP_{lp} = 164.489\,°C$ water temperature entering LP evaporator

$h_{lp.w2} := h_{steam}(P_{lp}, T_{lp.w2}, "", "", "") = 695.175 \frac{kJ}{kg}$ enthalpy of water entering LP evaporator

$h_{lp.w1} := h_{steam}(P_{lp}, T_{lp.w1}, "", "", "") = 461.836 \frac{kJ}{kg}$ enthalpy of water entering LP economizer

$Q_{lp.ec} := m_{steam.lp} \cdot (h_{lp.w2} - h_{lp.w1}) = 1.495\,MW$ LP economiser duty

$\Delta h_{56} := \frac{Q_{lp.ec}}{m_{gas}} = 39.545 \frac{kJ}{kg}$ gas enthalpy change over LP economiser

$h_{g5} := h_{gas}(T_{g.5}) = 176.135 \cdot \frac{kJ}{kg}$ gas enthalpy entering LP economiser

$h_{g6} := h_{g5} - \Delta h_{56}$ gas enthalpy exiting LP economiser

$T_{g.6} := root(h_{gas}(T_{g.5}) - h_{g6}, T_{g.5}) = 136.811 \cdot °C$ exit gas temperature from LP economiser

$Q_{lp.ev} := m_{gas} \cdot (h_{gas}(T_{g.4}) - h_{gas}(T_{g.5})) = 2.737 \cdot MW$ LP evaporator duty

$h_{lp.s} := h_{steam}(P_{lp}, "", "", 1, "") = 2.768 \times 10^3 \cdot \frac{kJ}{kg}$ enthalpy of steam exiting LP drum

Turbines

$P_{lp.st.out} := p_{steam}(T_{lp.w1}, "", "", "") = 1.434 \cdot bar$ condenser pressure

$s_{hp.in} := s_{steam}(P_{hp}, T_{so}, "", "", "") = 6.444 \cdot \frac{kJ}{kg \cdot K}$ entropy of HP steam exiting superheater

$h_{hp.out.isen} := h_{steam}(P_{lp}, "", "", "", s_{hp.in}) = 2.67 \times 10^3 \cdot \frac{kJ}{kg}$ isentropic enthalpy of steam exiting HP turbine

$h_{hp.out.actual} := (h_{hp.out.isen} - h_{so}) \cdot 0.85 + h_{so} = 2.735 \times 10^3 \cdot \frac{kJ}{kg}$ actual enthalpy of steam exiting HP turbine

$h_{lp.st} := \frac{m_{steam.hp} \cdot h_{hp.out.actual} + (m_{steam.lp} - m_{steam.hp}) \cdot h_{lp.s}}{m_{steam.lp}} = 2.742 \times 10^3 \cdot \frac{kJ}{kg}$

enthalpy of steam entering LP turbine

$T_{lp.st} := T_{steam}(P_{lp}, "", h_{lp.st}, "") = 170.044 \cdot °C$ temperature of steam entering LP turbine

$\rho_{hp} := \rho_{steam}(P_{hp}, "", "", h_{so}, "") = 21.459 \frac{kg}{m^3}$ density of steam entering HP turbine

$P_{hp} - P_{lp} = 4.93 \cdot MPa$ pressure drop over HP turbine

$V_{hp} := \frac{m_{steam.hp}}{\rho_{hp}} = 0.232 \frac{m^3}{s}$ volume flow rate through HP turbine

$\rho_{lp} := \rho_{steam}(P_{lp}, "", "", h_{lp.st}, "") = 4.178 \frac{kg}{m^3}$ density of steam entering LP turbine

$P_{lp} - P_{lp.st.out} = 649.521 \cdot kPa$ pressure drop over LP turbine

$V_{lp} := \frac{m_{steam.lp}}{\rho_{lp}} = 1.533 \frac{m^3}{s}$ volume flow rate through LP turbine

HP Pump

$\Delta P = \rho g \Delta H_T$

$\rho_p := \rho_{steam}(P_{lp}, "", 0, "", "") = 897.41 \frac{kg}{m^3}$ density of water entering HP pump

$\Delta H_T := \frac{P_{hp} - P_{lp}}{\rho_p \cdot g} = 560.162 m$ HP pump head

$V_{pump} := \frac{m_{steam.hp}}{\rho_p} = 5.546 \times 10^{-3} \frac{m^3}{s}$ Volume flow rate through HP pump

Overall Conductance

High Pressure

$$LMTD_{sh.hp} := \frac{\left(T_{g1} - T_{so}\right) - \left(T_{g.2} - T_{hp.s}\right)}{\ln\left[\frac{\left(T_{g1} - T_{so}\right)}{\left(T_{g.2} - T_{hp.s}\right)}\right]} = 197.366\,K$$

Log mean temperature difference over the HP superheater

$$LMTD_{ev.hp} := \frac{\left(T_{g.2} - T_{hp.s}\right) - \left(T_{g.3} - T_{hp.s}\right)}{\ln\left[\frac{\left(T_{g.2} - T_{hp.s}\right)}{\left(T_{g.3} - T_{hp.s}\right)}\right]} = 95.056\,K$$

Log mean temperature difference over the HP evaporator

$$LMTD_{ec.hp} := \frac{\left(T_{g.3} - T_{hp.w2}\right) - \left(T_{g.4} - T_{hp.w1}\right)}{\ln\left[\frac{\left(T_{g.3} - T_{hp.w2}\right)}{\left(T_{g.4} - T_{hp.w1}\right)}\right]} = 53.492\,K$$

Log mean temperature difference over the HP economiser

$$UA_{sh.hp} := \frac{Q_{hp.sh}}{LMTD_{sh.hp}} = 7.886\,\frac{kW}{K}$$

Overall conductance of the HP superheater

$$UA_{ev.hp} := \frac{Q_{hp.ev}}{LMTD_{ev.hp}} = 85.445\,\frac{kW}{K}$$

Overall conductance of the HP evaporator

$$UA_{ec.hp} := \frac{Q_{hp.ec}}{LMTD_{ec.hp}} = 40.326\,\frac{kW}{K}$$

Overall conductance of the HP economiser

Low Pressure

$$LMTD_{ev.lp} := \frac{\left(T_{g.4} - T_{lp.s}\right) - \left(T_{g.5} - T_{lp.s}\right)}{\ln\left[\frac{\left(T_{g.4} - T_{lp.s}\right)}{\left(T_{g.5} - T_{lp.s}\right)}\right]} = 26.859\,K$$

Log mean temperature difference over the LP evaporator

$$LMTD_{ec.lp} := \frac{\left(T_{g.5} - T_{lp.w2}\right) - \left(T_{g.6} - T_{lp.w1}\right)}{\ln\left[\frac{\left(T_{g.5} - T_{lp.w2}\right)}{\left(T_{g.6} - T_{lp.w1}\right)}\right]} = 17.823\,K$$

Log mean temperature difference over the LP economiser

$$UA_{ev.lp} := \frac{Q_{lp.ev}}{LMTD_{ev.lp}} = 101.92\,\frac{kW}{K}$$

Overall conductance of the LP evaporator

$$UA_{ec.lp} := \frac{Q_{lp.ec}}{LMTD_{ec.lp}} = 83.866\,\frac{kW}{K}$$

Overall conductance of the LP economiser

Mass Flow in Evaporators

$$h_{hp.ev.in} := h_{steam}\left(P_{hp}, "", "", 0, ""\right) = 1.198 \times 10^3\,\frac{kJ}{kg}$$

enthalpy of water entering the HP evaporator

$$h_{hp.ev.out} := h_{steam}\left(P_{hp}, "", "", 0.5, ""\right) = 1.993 \times 10^3\,\frac{kJ}{kg}$$

enthalpy of water exiting the HP evaporator

$$m_{hp.ev} := \frac{Q_{hp.ev}}{h_{hp.ev.out} - h_{hp.ev.in}} = 10.219\,\frac{kg}{s}$$

mass flow rate in the HP evaporator

$$h_{lp.ev.in} := h_{steam}\left(P_{lp}, "", "", 0, ""\right) = 719.399\,\frac{kJ}{kg}$$

enthalpy of water entering the LP evaporator

$h_{lp.ev.out} := h_{steam}\left(P_{lp}, "", "", 0.5, ""\right) = 1.744 \times 10^{3} \cdot \frac{kJ}{kg}$ enthalpy of water exiting the LP evaporator

$m_{lp.ev} := \frac{Q_{lp.ev}}{h_{lp.ev.out} - h_{lp.ev.in}} = 2.673 \frac{kg}{s}$ mass flow rate in the LP evaporator

Appendix D. Triple Pressure Analytical Model

Known Variables

$P_{hp} := 97.7\,bar$ — High Pressure

$P_{ip} := 21.4\,bar$ — Intermediate Pressure

$P_{lp} := 4.1\,bar$ — Low Pressure

$m_{cond} := 93\,\frac{kg}{s}$ — Mass Flow through condenser

$m_{hp} := 78.2\,\frac{kg}{s}$ — HP mass flow

$m_{ip} := 83.2\,\frac{kg}{s}$ — IP Mass Flow

$m_{lp} := 9.8\,\frac{kg}{s}$ — LP Mass Flow

$m_{gas} := 587\,\frac{kg}{s}$ — Mass Flow of gas

Low Pressure
Intermediate Pressure
High Pressure
Gas

$T_{lpec.in} := 50\,°C$ — Temp of water entering LP economiser

$T_{lpsh.out} := 280\,°C$ — Temp of steam exiting LP superheater

$T_{htrh.out} := 567\,°C$ — Temp of water exiting high temp reheater

$T_{hphtsh.out} := 567\,°C$ — Temp of steam exiting HP high temp superheater

Assumptions

$AP := 2K$ — Approach Point

$PP_{lp} := 15K$ — LP pinch point

$PP_{ip} := 20K$ — IP pinch point

$PP_{hp} := 2K$ — HP pinch point

$f_{g.lpsh} := 0.8$ — Fraction of gas flowing through the LP superheater

$f_{g.ipec} := 0.06$ — Fraction of gas flowing through the IP economiser

$T_{hphtec.in} := 260\,°C$ — Temp. of water entering HP high temp. economiser

$T_{ltrh.out} := 427\,°C$ — Temp. of steam exiting low temp. reheater

$T_{hpltsh.out} := 425\,°C$ — Temp. of steam exiting HP low temp. superheater

Solution

$T_0 := 0\,°C$ — Reference temp for gas enthalpy calcs.

$$h_{gas}(T) := \left[\left[0.00025464 \cdot \frac{(T/°C)^2}{2} + 1.0178 \cdot T/°C\right] - \left[0.00025464 \cdot \frac{(T_0/°C)^2}{2} + 1.0178 \cdot T_0/°C\right]\right] \cdot \frac{kJ}{kg}$$

$T_{hp.drum} := T_{steam}(P_{hp}, "", "", "") = 309.294\,°C$ — HP drum temp.

$T_{g6} := T_{hp.drum} + PP_{hp} = 311.294\,°C$ — Temp. of gas exiting HP evaporator

$h_{g6} := h_{gas}(T_{g6}) = 329.172\,\frac{kJ}{kg}$ — Enthalpy of gas exiting HP evaporator

$h_{hphtec.in} := h_{steam}(P_{hp}, T_{hphtec.in}, "", "", "") = 1.134 \times 10^3 \cdot \frac{kJ}{kg}$ Enthalpy of water entering HP high temp. economiser

$T_{hphtec.out} := T_{hp.drum} - AP = 307.294 \cdot °C$ Temp of water exiting HP high temp. economiser

$h_{hphtec.out} := h_{steam}(P_{hp}, T_{hphtec.out}, "", "", "") = 1.386 \times 10^3 \cdot \frac{kJ}{kg}$ Enthalpy of water exiting HP high temp. economiser

$Q_{hphtec} := m_{hp} \cdot (h_{hphtec.out} - h_{hphtec.in}) = 19.683 \cdot MW$ Duty of HP high temp. economiser

$Q_{hphtec} = m_{gas} \cdot (h_{g6} - h_{g7})$

$h_{g7} := \frac{-Q_{hphtec}}{m_{gas}} + h_{gas}(T_{g6}) = 295.641 \cdot \frac{kJ}{kg}$ Enthalpy of gas exiting HP high temp. economiser

$T_{g7} := root(h_{g7} - h_{gas}(T_{g6}), T_{g6}) = 280.62 \cdot °C$ Temp of gas exiting HP high temp. economiser

$h_{hp.drum.out} := h_{steam}(P_{hp}, "", "", 1, "") = 2.73 \times 10^3 \cdot \frac{kJ}{kg}$ Enthalpy of steam exiting HP drum

$Q_{hpev} := m_{hp} \cdot (h_{hp.drum.out} - h_{hphtec.out}) = 105.083 \cdot MW$ Duty of HP evaporator

$Q_{hpev} = m_{gas} \cdot (h_{g5} - h_{g6})$

$h_{g5} := \frac{Q_{hpev}}{m_{gas}} + h_{gas}(T_{g6}) = 508.19 \cdot \frac{kJ}{kg}$ Enthalpy of gas entering HP evaporator

$T_{g5} := root(h_{g5} - h_{gas}(T_{g6}), T_{g6}) = 471.494 \cdot °C$ Temp of gas entering HP evaporator

$T_{lp.drum} := T_{steam}(P_{lp}, "", "", "") = 144.505 \cdot °C$ LP drum temp.

$T_{lpsh.in} := T_{lp.drum}$ Temp. of steam entering LP superheater

$h_{lpsh.in} := h_{steam}(P_{lp}, "", "", 1, "") = 2.739 \times 10^3 \cdot \frac{kJ}{kg}$ Enthalpy of steam entering LP superheater

$h_{lpsh.out} := h_{steam}(P_{lp}, T_{lpsh.out}, "", "", "") = 3.026 \times 10^3 \cdot \frac{kJ}{kg}$ Enthalpy of steam exiting LP superheater

$Q_{lpsh} := m_{lp} \cdot (h_{lpsh.out} - h_{lpsh.in}) = 2.809 \cdot MW$ Duty of LP superheater

$Q_{lpsh} = f_{g.lpsh}\, m_{gas} \cdot (h_{g7} - h_{g8})$

$h_{g8} := \frac{-Q_{lpsh}}{m_{gas} \cdot f_{g.lpsh}} + h_{gas}(T_{g7})$ Enthalpy of gas exiting LP superheater

$T_{g8} := root(h_{g8} - h_{gas}(T_{g7}), T_{g7}) = 275.125 \cdot °C$ Temp of gas exiting LP superheater

$Q_{ipsh} := (1 - f_{g.lpsh}) m_{gas} \cdot (h_{gas}(T_{g7}) - h_{gas}(T_{g8})) = 0.702 \cdot MW$ Duty of IP superheater

$Q_{ipsh} = (m_{ip} - m_{hp}) \cdot (h_{ipsh.out} - h_{ipdrum.out})$

$h_{ipdrum.out} := h_{steam}(P_{ip}, "", "", 1, "") = 2.8 \times 10^3 \cdot \frac{kJ}{kg}$ Enthalpy of steam exiting IP drum

$h_{ipsh.out} := \frac{Q_{ipsh}}{(m_{ip} - m_{hp})} + h_{ipdrum.out} = 2.94 \times 10^3 \cdot \frac{kJ}{kg}$ Enthalpy of steam exiting IP superheater

$T_{ipsh.out} := T_{steam}(P_{ip}, "", h_{ipsh.out}, "") = 266.846 \cdot °C$ Temp. of steam exiting IP superheater

$P_{hpst.out} := P_{ip} = 21.4 \cdot bar$ Pressure of steam exiting HP turbine

$s_{hp.in} := s_{steam}(P_{hp}, T_{hphtsh.out}, "", "", "") = 6.822 \cdot \frac{kJ}{kg \cdot K}$ Entropy of steam entering HP turbine

$h_{hp.out.isen} := h_{steam}(P_{hpst.out}, "", "", "", s_{hp.in}) = 3.073 \times 10^3 \cdot \frac{kJ}{kg}$ Isentropic enthalpy of steam exiting HP turbine

$h_{hphtsh.out} := h_{steam}(P_{hp}, T_{hphtsh.out}, "", "", "") = 3.546 \times 10^3 \cdot \frac{kJ}{kg}$ Enthalpy of steam exiting HP high temp. superheater

$h_{hp.out.actual} := 0.85 \cdot (h_{hp.out.isen} - h_{hphtsh.out}) + h_{hphtsh.out} = 3.144 \times 10^3 \cdot \frac{kJ}{kg}$ Actual enthalpy of steam exiting HP turbine

$T_{hp.out} := T_{steam}(P_{ip}, "", h_{hp.out.actual}, "") = 354.115 \cdot °C$ Temperature of steam exiting HP turbine

$h_{ltrh.in} := \frac{m_{hp} \cdot h_{hp.out.actual} + (m_{ip} - m_{hp}) \cdot h_{ipsh.out}}{m_{ip}} = 3.132 \times 10^3 \cdot \frac{kJ}{kg}$ Enthalpy of steam entering low temp reheater

$T_{ltrh.in} := T_{steam}(P_{ip}, "", h_{ltrh.in}, "") = 348.66 \cdot °C$ Temp. of steam entering low temp reheater

$h_{ltrh.out} := h_{steam}(P_{ip}, T_{ltrh.out}, "", "", "") = 3.306 \times 10^3 \cdot \frac{kJ}{kg}$ Enthalpy of steam exiting low temp. reheater

$Q_{ltrh} := m_{ip} \cdot (h_{ltrh.out} - h_{ltrh.in}) = 14.463 \cdot MW$ Duty of low temp. reheater

$Q_{ltrh} = m_{gas} \cdot (h_{g4} - h_{g5})$

$h_{g4} := \frac{Q_{ltrh}}{m_{gas}} + h_{gas}(T_{g5})$ Enthalpy of gas entering low temp. reheater

$T_{g4} := root(h_{g4} - h_{gas}(T_{g5}), T_{g5}) = 493.095 \cdot °C$ Temp. of gas entering low temp. reheater

$T_{hpltsh.in} := T_{hp.drum} = 309.294 \cdot °C$ Temp. of steam entering HP low temp. superheater

$h_{hpltsh.out} := h_{steam}(P_{hp}, T_{hpltsh.out}, "", "", "") = 3.176 \times 10^3 \cdot \frac{kJ}{kg}$ Enthalpy of steam exiting HP low temp. superheater

$h_{hpltsh.in} := h_{steam}(P_{hp}, "", "", 1, "") = 2.73 \times 10^3 \cdot \frac{kJ}{kg}$ Enthalpy of steam entering HP low temp. superheater

$Q_{hpltsh} := m_{hp} \cdot (h_{hpltsh.out} - h_{hpltsh.in}) = 34.921 \cdot MW$ Duty of HP low temp. superheater

$Q_{hpltsh} = m_{gas} \cdot (h_{g3} - h_{g4})$

$h_{g3} := \frac{Q_{hpltsh}}{m_{gas}} + h_{gas}(T_{g4}) = 592.319 \cdot \frac{kJ}{kg}$ Enthalpy of gas entering HP low temp. superheater

$T_{g3} := root(h_{g3} - h_{gas}(T_{g4}), T_{g4}) = 544.828 \cdot °C$ Temp. of gas entering HP low temp. superheater

$T_{hphtsh.in} := T_{hpltsh.out}$ Temp. of steam entering HP high temp. superheater

$h_{hphtsh.in} := h_{steam}(P_{hp}, T_{hphtsh.in}, "", "", "") = 3.176 \times 10^3 \cdot \frac{kJ}{kg}$ Enthalpy of steam entering HP high temp. superheater

$Q_{hphtsh} := m_{hp} \cdot (h_{hphtsh.out} - h_{hphtsh.in}) = 28.956 \cdot MW$ Duty of HP high temp. superheater

$h_{htrh.out} := h_{steam}(P_{ip}, T_{htrh.out}, "", "", "") = 3.616 \times 10^3 \cdot \frac{kJ}{kg}$ Enthalpy of steam exiting high temp. reheater

$Q_{htrh} := m_{ip} \cdot (h_{htrh.out} - h_{ltrh.out}) = 25.795 \cdot MW$ Duty of high temp. reheater

$Q_{htrh} = m_{gas} \cdot (h_{g2} - h_{g3})$

$h_{g2} := \frac{Q_{htrh}}{m_{gas}} + h_{g3} = 636.264 \cdot \frac{kJ}{kg}$ Enthalpy of gas entering high temp. reheater

$T_{g2} := root(h_{g2} - h_{gas}(T_{g3}), T_{g3}) = 582.667 \cdot °C$ Temp. of gas entering high temp. reheater

$Q_{hphtsh} = m_{gas} \cdot \left(h_{gas}\left(T_{g1}\right) - h_{gas}\left(T_{g2}\right)\right)$

$h_{g1} := \frac{Q_{hphtsh}}{m_{gas}} + h_{gas}\left(T_{g2}\right)$ — Enthalpy of gas entering HP high temp. superheater

$T_{g1} := \text{root}\left(h_{g1} - h_{gas}\left(T_{g2}\right), T_{g2}\right) = 624.773 \cdot °C$ — Temp. of gas entering HP high temp. superheater

$T_{lp.drum} = 144.505 \cdot °C$ — LP drum temp.

$T_{lpec.out} := T_{lp.drum} - AP = 142.505 \cdot °C$ — Temp. of water exiting LP economiser

$h_{lpec.in} := h_{steam}\left(P_{lp}, T_{lpec.in}, "", "", ""\right) = 209.679 \cdot \frac{kJ}{kg}$ — Enthalpy of water entering LP economiser

$h_{lpec.out} := h_{steam}\left(P_{lp}, T_{lpec.out}, "", "", ""\right) = 599.975 \cdot \frac{kJ}{kg}$ — Enthalpy of water exiting LP economiser

$Q_{lpec} := m_{cond} \cdot \left(h_{lpec.out} - h_{lpec.in}\right) = 36.297 \cdot MW$ — Duty of the LP econmiser

$Q_{lpec} = m_{gas} \cdot \left(h_{g13} - h_{g14}\right)$

$T_{g13} := T_{lp.drum} + PP_{lp} = 159.505 \cdot °C$ — Gas temp. exiting LP evaporator

$h_{g14} := \frac{-Q_{lpec}}{m_{gas}} + h_{gas}\left(T_{g13}\right) = 103.748 \cdot \frac{kJ}{kg}$ — Enthalpy of gas exiting LP economiser

$T_{g14} := \text{root}\left(h_{g14} - h_{gas}\left(T_{g13}\right), T_{g13}\right) = 100.666 \cdot °C$ — Temp. of gas exiting LP economiser

$h_{lpdrum.out} := h_{steam}\left(P_{lp}, "", "", 1, ""\right) = 2.739 \times 10^{3} \cdot \frac{kJ}{kg}$ — Enthalpy of steam exiting LP drum

$Q_{lpev} := m_{lp} \cdot \left(h_{lpdrum.out} - h_{lpec.out}\right) = 20.964 \cdot MW$ — Duty of LP evaporator

$Q_{lpev} = m_{gas} \cdot \left(h_{g12} - h_{g13}\right)$

$h_{g12} := h_{gas}\left(T_{g13}\right) + \frac{Q_{lpev}}{m_{gas}} = 201.297 \cdot \frac{kJ}{kg}$ — Enthalpy of gas entering LP evaporator

$T_{g12} := \text{root}\left(h_{g12} - h_{gas}\left(T_{g13}\right), T_{g13}\right) = 193.112 \cdot °C$ — Temp. of gas entering LP evaporator

$T_{ip.drum} := T_{steam}\left(P_{ip}, "", "", ""\right) = 215.832 \cdot °C$ — Temp. of IP drum

$T_{ipec.in} := T_{lp.drum}$ — Temp. of water entering IP economiser

$T_{ipec.out} := T_{ip.drum} - AP = 213.832 \cdot °C$ — Temp. of water exiting IP economiser

$h_{ipec.in} := h_{steam}\left(P_{ip}, T_{ipec.in}, "", "", ""\right) = 609.662 \cdot \frac{kJ}{kg}$ — Enthalpy of water entering IP economiser

$h_{ipec.out} := h_{steam}\left(P_{ip}, T_{ipec.out}, "", "", ""\right) = 915.275 \cdot \frac{kJ}{kg}$ — Enthalpy of water exiting IP economiser

$Q_{ipec} := \left(m_{ip} - m_{hp}\right) \cdot \left(h_{ipec.out} - h_{ipec.in}\right) = 1.528 \cdot MW$ — Duty of IP economiser

$Q_{ipec} = f_{g.ipec}\, m_{gas} \cdot \left(h_{g10} - h_{g11}\right)$

$T_{g10} := T_{ip.drum} + PP_{ip} = 235.832 \cdot °C$ — Temp. of gas exiting IP evaporator

$h_{g11} := \frac{-Q_{ipec}}{m_{gas} \cdot f_{g.ipec}} + h_{gas}\left(T_{g10}\right)$ — Enthalpy of gas exiting IP economiser

$T_{g11} := \text{root}\left(h_{g11} - h_{gas}\left(T_{g10}\right), T_{g10}\right) = 195.386 \cdot °C$ — Temp. of gas exiting IP economiser

$T_{hpltec2.in} := T_{lp.drum}$ — Temp. of water entering HP low temp. economiser 2

$Q_{hpltec2} := m_{gas} \cdot \left(h_{gas}\left(T_{g11}\right) - h_{gas}\left(T_{g12}\right)\right) = 1.425 \cdot MW$ Duty of HP low temp. economiser 2

$Q_{hpltec2} = \left(m_{hp}\right) \cdot \left(h_{hpltec2.out} - h_{hpltec2.in}\right)$

$h_{hpltec2.in} := h_{steam}\left(P_{hp}, T_{hpltec2.in}, "", "", ""\right) = 614.548 \cdot \frac{kJ}{kg}$ Enthalpy of water entering HP low temp. economiser 2

$h_{hpltec2.out} := \frac{Q_{hpltec2}}{m_{hp}} + h_{hpltec2.in} = 632.765 \cdot \frac{kJ}{kg}$ Enthalpy of water exiting HP low temp. economiser 2

$T_{hpltec2.out} := T_{steam}\left(P_{hp}, "", h_{hpltec2.out}, ""\right) = 148.782 \cdot °C$ Temp. of water exiting HP low temp. economiser 2

$T_{hpltec1.in} := T_{hpltec2.out}$ Temp. of water entering HP low temp. economiser 1

$Q_{hpltec1} := \left(1 - f_{g.ipec}\right) m_{gas} \cdot \left(h_{gas}\left(T_{g10}\right) - h_{gas}\left(T_{g11}\right)\right) = 23.94 \cdot MW$ Duty of HP low temp. economiser 1

$Q_{hpltec1} = \left(m_{hp}\right) \cdot \left(h_{hpltec1.out} - h_{hpltec1.in}\right)$

$h_{hpltec1.in} := h_{steam}\left(P_{hp}, T_{hpltec1.in}, "", "", ""\right) = 632.827 \cdot \frac{kJ}{kg}$ Enthalpy of water entering HP low temp. economiser 1

$h_{hpltec1.out} := \frac{Q_{hpltec1}}{m_{hp}} + h_{hpltec1.in} = 938.961 \cdot \frac{kJ}{kg}$ Enthalpy of water exiting HP low temp. economiser 1

$T_{hpltec1.out} := T_{steam}\left(P_{hp}, "", h_{hpltec1.out}, ""\right) = 218.495 \cdot °C$ Temp. of water exiting HP low temp. economiser 1

$Q_{ipev} := \left(m_{ip} - m_{hp}\right) \cdot \left(h_{ipdrum.out} - h_{ipec.out}\right) = 9.422 \cdot MW$ Duty of IP evaporator

$Q_{ipev} = m_{gas} \cdot \left(h_{g9} - h_{g10}\right)$

$h_{g9} := \frac{Q_{ipev}}{m_{gas}} + h_{gas}\left(T_{g10}\right) = 263.162 \cdot \frac{kJ}{kg}$ Enthalpy of gas entering IP evaporator

$T_{g9} := root\left(h_{g9} - h_{gas}\left(T_{g10}\right), T_{g10}\right) = 250.698 \cdot °C$ Temp. of gas entering IP evaporator

$T_{hpitec.in} := T_{hpltec1.out}$ Temp. of water entering HP intermediate temp. economiser

$Q_{hpitec} := m_{gas} \cdot \left(h_{gas}\left(T_{g8}\right) - h_{gas}\left(T_{g9}\right)\right) = 15.554 \cdot MW$ Duty of HP intermediate temp. economiser

$Q_{hpitec} = \left(m_{hp} - m_{extract}\right) \cdot \left(h_{hpitec.out} - h_{hpltec1.out}\right)$

$h_{hpitec.out} := \frac{Q_{hpitec}}{m_{hp}} + h_{hpltec1.out} = 1.138 \times 10^{3} \cdot \frac{kJ}{kg}$ Enthalpy of water exiting HP intermediate temp. economiser

$T_{hpitec.out} := T_{steam}\left(P_{hp}, "", h_{hpitec.out}, ""\right) = 260.739 \cdot °C$ Temp. of water exiting HP intermediate temp. economiser (used for to iterate T.hphtec.in)

Turbines

$P_{lpst.out} := p_{steam}\left(T_{lpec.in}, "", "", ""\right) = 0.124 \cdot bar$ Pressure of steam exiting LP turbine

$s_{ip.in} := s_{steam}\left(P_{ip}, T_{htrh.out}, "", "", ""\right) = 7.586 \cdot \frac{kJ}{kg \cdot K}$ Entropy of steam entering IP turbine

$h_{ip.out.isen} := h_{steam}\left(P_{lp}, "", "", "", s_{ip.in}\right) = 3.084 \times 10^{3} \cdot \frac{kJ}{kg}$ Isentropic enthalpy of steam exiting IP turbine

$h_{ip.out.actual} := \left(h_{ip.out.isen} - h_{htrh.out}\right) \cdot 0.85 + h_{htrh.out} = 3.164 \times 10^{3} \cdot \frac{kJ}{kg}$ Actual enthalpy of steam exiting IP turbine

$T_{ip.out} := T_{steam}\left(P_{lp}, "", h_{ip.out.actual}, ""\right) = 347.026 \cdot °C$ Temp. of steam exiting IP turbine

$$h_{lp.st} := \frac{m_{ip} \cdot h_{ip.out.actual} + m_{lp} \cdot h_{lpsh.out}}{m_{ip} + m_{lp}} = 3.149 \times 10^{3} \cdot \frac{kJ}{kg}$$ Enthalpy of steam entering LP turbine

$$T_{lp.st.in} := T_{steam}\left(P_{lp}, "", h_{lp.st}, ""\right) = 339.99 \cdot °C$$ Temp. of steam entering LP turbine

$$P_{lp} - P_{lpst.out} = 397.649 \cdot kPa$$ Pressure drop over LP turbine

$$\rho_{lp} := \rho_{steam}\left(P_{lp}, "", "", h_{lp.st}, ""\right) = 1.46 \frac{kg}{m^3}$$ Density of steam entering LP turbine

$$V_{lp} := \frac{m_{cond}}{\rho_{lp}} = 63.696 \frac{m^3}{s}$$ Volume flow rate of steam entering LP turbine

$$P_{ip} - P_{lp} = 1.73 \times 10^{3} \cdot kPa$$ Pressure drop over IP turbine

$$\rho_{ip} := \rho_{steam}\left(P_{ip}, "", "", h_{htrh.out}, ""\right) = 5.584 \frac{kg}{m^3}$$ Density of steam entering IP turbine

$$V_{ip} := \frac{m_{ip}}{\rho_{ip}} = 14.899 \frac{m^3}{s}$$ Volume flow rate of steam entering IP turbine

$$P_{hp} - P_{ip} = 7.63 \cdot MPa$$ Pressure drop over HP turbine

$$\rho_{hp} := \rho_{steam}\left(P_{hp}, "", "", h_{hphtsh.out}, ""\right) = 26.662 \frac{kg}{m^3}$$ Density of steam entering HP turbine

$$V_{hp} := \frac{m_{hp}}{\rho_{hp}} = 2.933 \frac{m^3}{s}$$ Volume flow rate of steam entering HP turbine

Pumps

$$\Delta P = \rho g \Delta H_T$$

$$\rho := \rho_{steam}\left(P_{lp}, "", 0, "", ""\right) = 922.074 \frac{kg}{m^3}$$ Density of water exiting LP drum

$$\Delta H_{T.IP} := \frac{P_{ip} - P_{lp}}{\rho \cdot g} = 191.32 m$$ IP pump head

$$V_{pump.IP} := \frac{m_{ip} - m_{hp}}{\rho} = 5.423 \times 10^{-3} \frac{m^3}{s}$$ Volume flow rate through IP pump

$$\Delta H_{T.HP} := \frac{P_{hp} - P_{lp}}{\rho \cdot g} = 1.035 \times 10^{3} m$$ HP pump head

$$V_{pump} := \frac{m_{hp}}{\rho} = 0.08481 \frac{m^3}{s}$$ Volume flow rate through HP pump

Overall Conductance

Low Pressure

$$LMTD_{lpec} := \frac{\left(T_{g13} - T_{lpec.out}\right) - \left(T_{g14} - T_{lpec.in}\right)}{\ln\left(\frac{T_{g13} - T_{lpec.out}}{T_{g14} - T_{lpec.in}}\right)} = 30.828 \cdot K$$ Log mean temperature difference over the LP economiser

$$LMTD_{lpev} := \frac{(T_{g12} - T_{lp.drum}) - (T_{g13} - T_{lp.drum})}{\ln\left[\frac{(T_{g12} - T_{lp.drum})}{(T_{g13} - T_{lp.drum})}\right]} = 28.584\,K$$

Log mean temperature difference over the LP evaporator

$$LMTD_{lpsh} := \frac{(T_{g7} - T_{lpsh.out}) - (T_{g8} - T_{lpsh.in})}{\ln\left[\frac{(T_{g7} - T_{lpsh.out})}{(T_{g8} - T_{lpsh.in})}\right]} = 24.3\,K$$

Log mean temperature difference over the LP superheater

$$UA_{lpec} := \frac{Q_{lpec}}{LMTD_{lpec}} = 1.1774 \times 10^3 \cdot \frac{kW}{K}$$

Overall conductance of the LP economiser

$$UA_{lpev} := \frac{Q_{lpev}}{LMTD_{lpev}} = 733.416 \cdot \frac{kW}{K}$$

Overall conductance of the LP evaporator

$$UA_{lpsh} := \frac{Q_{lpsh}}{LMTD_{lpsh}} = 115.602 \cdot \frac{kW}{K}$$

Overall conductance of the LP superheater

Intermediate Pressure

$$LMTD_{ipec} := \frac{(T_{g10} - T_{ipec.out}) - (T_{g11} - T_{ipec.in})}{\ln\left(\frac{T_{g10} - T_{ipec.out}}{T_{g11} - T_{ipec.in}}\right)} = 34.446\,K$$

Log mean temperature difference over the IP economiser

$$LMTD_{ipev} := \frac{(T_{g9} - T_{ip.drum}) - (T_{g10} - T_{ip.drum})}{\ln\left(\frac{T_{g9} - T_{ip.drum}}{T_{g10} - T_{ip.drum}}\right)} = 26.748\,K$$

Log mean temperature difference over the IP evaporator

$$LMTD_{ipsh} := \frac{(T_{g7} - T_{ipsh.out}) - (T_{g8} - T_{ip.drum})}{\ln\left(\frac{T_{g7} - T_{ipsh.out}}{T_{g8} - T_{ip.drum}}\right)} = 31.184\,K$$

Log mean temperature difference over the IP superheater

$$LMTD_{ltrh} := \frac{(T_{g4} - T_{ltrh.out}) - (T_{g5} - T_{ltrh.in})}{\ln\left(\frac{T_{g4} - T_{ltrh.out}}{T_{g5} - T_{ltrh.in}}\right)} = 91.553\,K$$

Log mean temperature difference over the LT reheater

$$LMTD_{htrh} := \frac{(T_{g2} - T_{htrh.out}) - (T_{g3} - T_{ltrh.out})}{\ln\left(\frac{T_{g2} - T_{htrh.out}}{T_{g3} - T_{ltrh.out}}\right)} = 50.633\,K$$

Log mean temperature difference over the HT reheater

$$UA_{ipec} := \frac{Q_{ipec}}{LMTD_{ipec}} = 44.361 \cdot \frac{kW}{K}$$

Overall conductance of the IP economiser

$$UA_{ipev} := \frac{Q_{ipev}}{LMTD_{ipev}} = 352.258 \cdot \frac{kW}{K}$$

Overall conductance of the IP evaporator

$$UA_{ipsh} := \frac{Q_{ipsh}}{LMTD_{ipsh}} = 22.52 \cdot \frac{kW}{K}$$ Overall conductance of the IP superheater

$$UA_{ltrh} := \frac{Q_{ltrh}}{LMTD_{ltrh}} = 157.974 \cdot \frac{kW}{K}$$ Overall conductance of the LT reheater

$$UA_{htrh} := \frac{Q_{htrh}}{LMTD_{htrh}} = 509.454 \cdot \frac{kW}{K}$$ Overall conductance of the LT reheater

High Pressure

$$LMTD_{hpltec2} := \frac{\left(T_{g11} - T_{hpltec2.out}\right) - \left(T_{g12} - T_{hpltec2.in}\right)}{\ln\left(\frac{T_{g11} - T_{hpltec2.out}}{T_{g12} - T_{hpltec2.in}}\right)} = 47.598 \cdot K$$ Log mean temperature difference over the HPLT economiser 2

$$LMTD_{hpltec1} := \frac{\left(T_{g10} - T_{hpltec1.out}\right) - \left(T_{g11} - T_{hpltec1.in}\right)}{\ln\left(\frac{T_{g10} - T_{hpltec1.out}}{T_{g11} - T_{hpltec1.in}}\right)} = 29.597 \cdot K$$ Log mean temperature difference over the HPLT economiser 1

$$LMTD_{hpitec} := \frac{\left(T_{g8} - T_{hpitec.out}\right) - \left(T_{g9} - T_{hpitec.in}\right)}{\ln\left(\frac{T_{g8} - T_{hpitec.out}}{T_{g9} - T_{hpitec.in}}\right)} = 22.111 \cdot K$$ Log mean temperature difference over the HPIT economiser

$$LMTD_{hphtec} := \frac{\left(T_{g6} - T_{hphtec.out}\right) - \left(T_{g7} - T_{hphtec.in}\right)}{\ln\left(\frac{T_{g6} - T_{hphtec.out}}{T_{g7} - T_{hphtec.in}}\right)} = 10.134 \cdot K$$ Log mean temperature difference over the HPHT economiser

$$LMTD_{hpev} := \frac{\left(T_{g5} - T_{hp.drum}\right) - \left(T_{g6} - T_{hp.drum}\right)}{\ln\left(\frac{T_{g5} - T_{hp.drum}}{T_{g6} - T_{hp.drum}}\right)} = 36.445 \cdot K$$ Log mean temperature difference over the HP evaporator

$$LMTD_{hpltsh} := \frac{\left(T_{g3} - T_{hpltsh.out}\right) - \left(T_{g4} - T_{hpltsh.in}\right)}{\ln\left(\frac{T_{g3} - T_{hpltsh.out}}{T_{g4} - T_{hpltsh.in}}\right)} = 149.541 \cdot K$$ Log mean temperature difference over the HPLT superheater

$$LMTD_{hphtsh} := \frac{\left(T_{g1} - T_{hphtsh.out}\right) - \left(T_{g2} - T_{hphtsh.in}\right)}{\ln\left(\frac{T_{g1} - T_{hphtsh.out}}{T_{g2} - T_{hphtsh.in}}\right)} = 99.5 \cdot K$$ Log mean temperature difference over the HPHT superheater

$$UA_{hpltec2} := \frac{Q_{hpltec2}}{LMTD_{hpltec2}} = 29.929 \cdot \frac{kW}{K}$$ Overall conductance of the HPLT economiser 2

$$UA_{hpltec1} := \frac{Q_{hpltec1}}{LMTD_{hpltec1}} = 808.853 \cdot \frac{kW}{K}$$ Overall conductance of the HPLT economiser 1

$$UA_{hpitec} := \frac{Q_{hpitec}}{LMTD_{hpitec}} = 703.46 \cdot \frac{kW}{K}$$

Overall conductance of the HPIT economiser

$$UA_{hphtec} := \frac{Q_{hphtec}}{LMTD_{hphtec}} = 1.94215 \times 10^{3} \cdot \frac{kW}{K}$$

Overall conductance of the HPHT economiser

$$UA_{hpev} := \frac{Q_{hpev}}{LMTD_{hpev}} = 2.883 \times 10^{3} \cdot \frac{kW}{K}$$

Overall conductance of the HP evaporator

$$UA_{hpltsh} := \frac{Q_{hpltsh}}{LMTD_{hpltsh}} = 233.521 \cdot \frac{kW}{K}$$

Overall conductance of the HPLT superheater

$$UA_{hphtsh} := \frac{Q_{hphtsh}}{LMTD_{hphtsh}} = 291.0155 \cdot \frac{kW}{K}$$

Overall conductance of the HPHT superheater

Appendix E. Triple Pressure Virtual Plant Inputs

The data shown in this section depicts the inputs to the Virtual Plant triple pressure model. Figure 71 shows the gas path arrangement for the HRSG with components ordered from hot to cold flow. Pressure level 1 was the high-pressure system, pressure level 2 was intermediate-pressure and pressure level 3 was low-pressure. The parallel components were accounted for, as well as the percentage of gas flowing through them. The flow arrangement for all components were set as counter flow except for the evaporators which were cross flow.

Gas Path - Hot to Cold

	Section Type	Pressure Level	Parallel With Previous	% of Gas	Flow Arrangement	Description
Sect #1	Superheater	1	No	100	Counter Flow	HPHT superheater
Sect #2	Superheater	2	No	100	Counter Flow	HT reheater
Sect #3	Superheater	1	No	100	Counter Flow	HPLT superheater
Sect #4	Superheater	2	No	100	Counter Flow	LT reheater
Sect #5	Evaporator (Dru...	1	No	100	Cross Flow	HP evaporator
Sect #6	Economizer	1	No	100	Counter Flow	HPHT economiser
Sect #7	Superheater	2	No	20	Counter Flow	IP superheater
Sect #8	Superheater	3	Parallel	80	Counter Flow	LP superheater
Sect #9	Economizer	1	No	100	Counter Flow	HPIT economiser
Sect #10	Evaporator (Dru...	2	No	100	Cross Flow	IP evaporator
Sect #11	Economizer	1	No	94	Counter Flow	HPLT economiser 1
Sect #12	Economizer	2	Parallel	6	Counter Flow	IP economiser
Sect #13	Economizer	1	No	100	Counter Flow	HPLT economiser 2
Sect #14	Evaporator (Dru...	3	No	100	Cross Flow	LP Evaporator
Sect #15	Economizer	3	No	100	Counter Flow	LP Economiser

Figure 71: Virtual Plant inputs for gas path

The steam side arrangement for each pressure level is shown in Figure 72, Figure 73 and Figure 74.

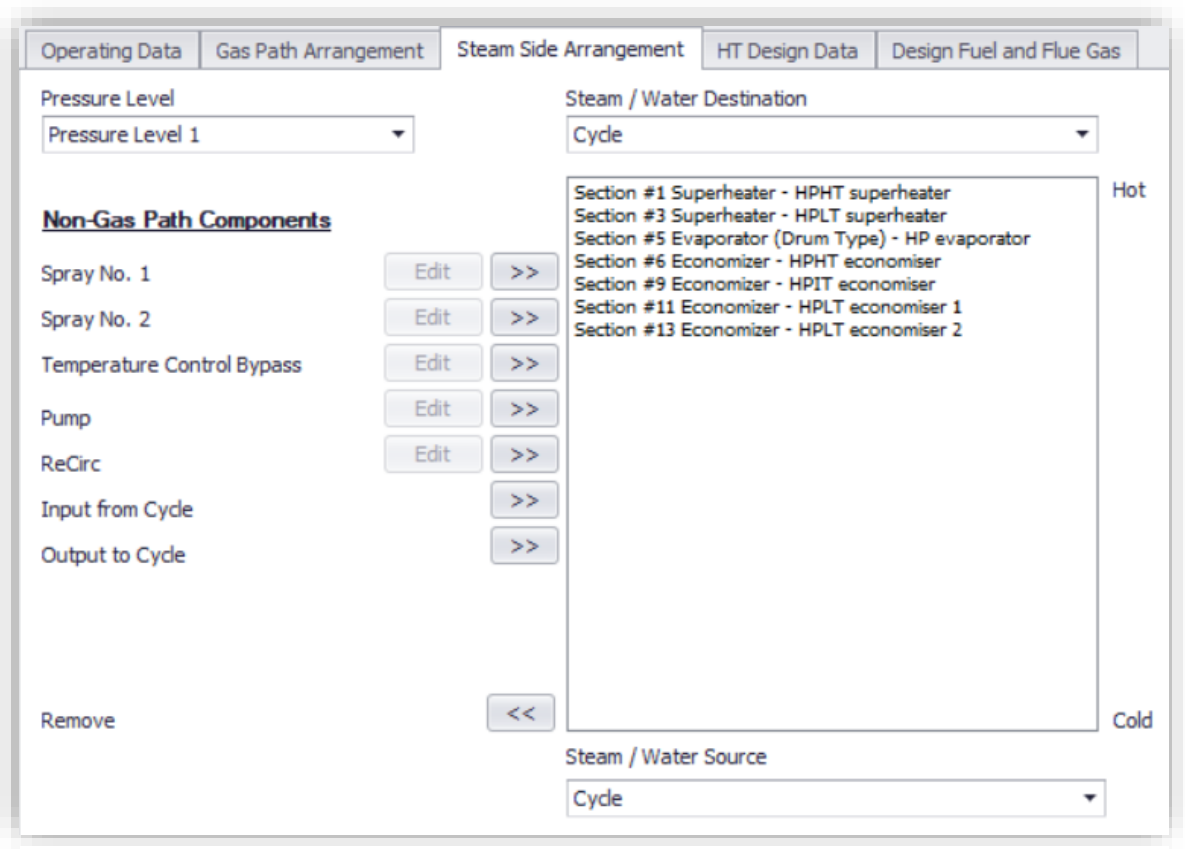

Figure 72: High-pressure arrangement

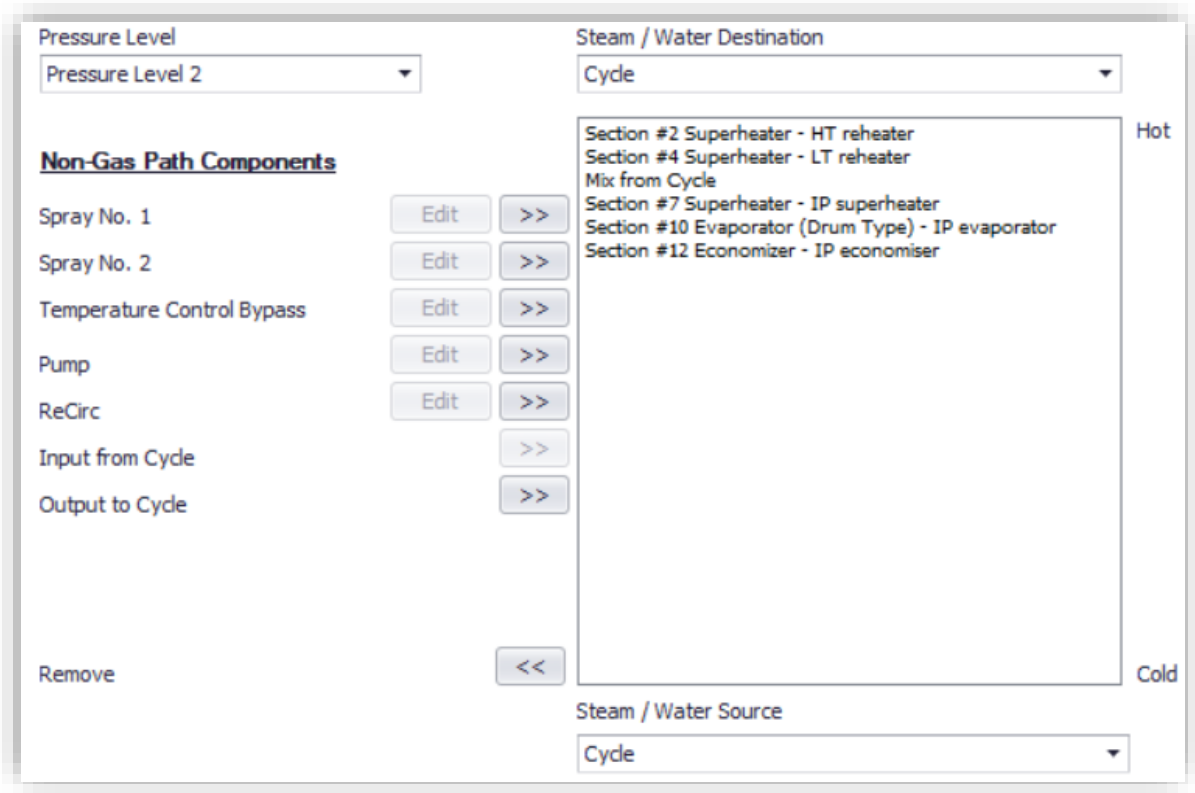

Figure 73: Intermediate-pressure arrangement

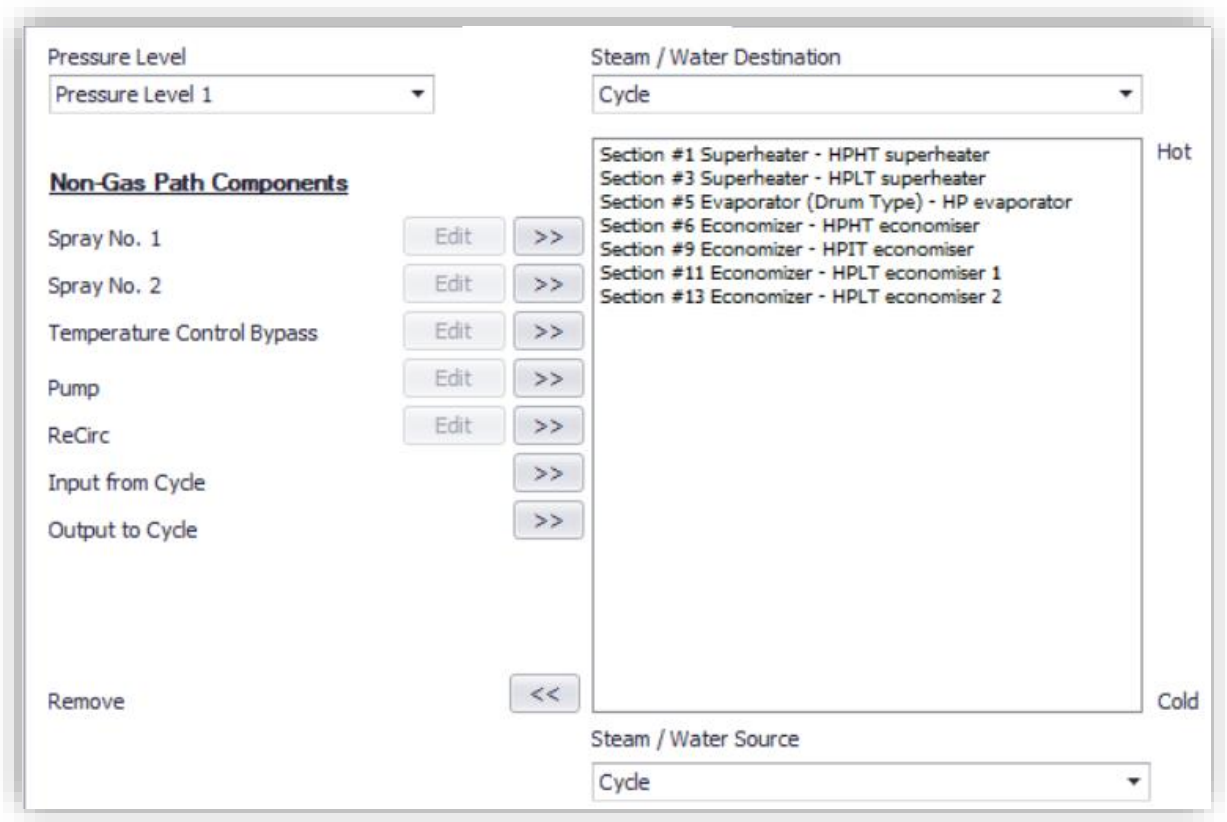

Figure 74: Low-pressure arrangement

Figure 75 shows the design data for the HRSG. The inlet flow and temperature of gas were specified. For each component, pressure (inlet and outlet), enthalpy (inlet and outlet) and mass flow (outlet) were entered, as well as the UA mass flow scaling exponent.

HRSG Gas Inlet Flow	587 kg/s	HRSG Gas Inlet Temperature	624.8 °C

Section Conditions

	Pressure (bara)	Enthalpy (kJ/kg)	Flow (kg/s)				
Section No. 1 - Superheater - HPHT superheater					UA Adjustment Multiplier	1	Scaling
Steam Outlet	97.7	3546.46	78.2	Calc	UA Mass Flow Scaling Exponent	0.65	
Steam Inlet	97.7	3176.18		Calc	Section Heat Loss (%)	0	%
Section No. 2 - Superheater - HT reheater					UA Adjustment Multiplier	1	Scaling
Steam Outlet	21.4	3615.55	83.2	Calc	UA Mass Flow Scaling Exponent	0.65	
Steam Inlet	21.4	3305.51		Calc	Section Heat Loss (%)	0	%
Section No. 3 - Superheater - HPLT superheater					UA Adjustment Multiplier	1	Scaling
Steam Outlet	97.7	3176.18	78.2	Calc	UA Mass Flow Scaling Exponent	0.65	
Steam Inlet	97.7	2729.62		Calc	Section Heat Loss (%)	0	%
Section No. 4 - Superheater - LT reheater					UA Adjustment Multiplier	1	Scaling
Steam Outlet	21.4	3305.51	83.2	Calc	UA Mass Flow Scaling Exponent	0.65	
Steam Inlet	21.4	3131.67		Calc	Section Heat Loss (%)	0	%
Section Number 5 - Evaporator - HP evaporator					UA Adjustment Multiplier	1	Scaling
Steam Outlet	97.7	2729.62	78.2	Calc	UA Mass Flow Scaling Exponent	0.65	
Water Inlet		1385.85		Calc	Section Heat Loss (%)	0	%
Section No. 6 - Economizer - HPHT economiser					UA Adjustment Multiplier	1	Scaling
Water Outlet	97.7	1385.85	78.2	Calc	UA Mass Flow Scaling Exponent	0.65	
Water Inlet	97.7	1137.77		Calc	Section Heat Loss (%)	0	%
Section No. 7 - Superheater - IP superheater					UA Adjustment Multiplier	1	Scaling
Steam Outlet	21.4	2940.17	5	Calc	UA Mass Flow Scaling Exponent	0.65	
Steam Inlet	21.4	2799.71		Calc	Section Heat Loss (%)	0	%
Section No. 8 - Superheater - LP superheater					UA Adjustment Multiplier	1	Scaling
Steam Outlet	4.1	3025.82	9.8	Calc	UA Mass Flow Scaling Exponent	0.65	
Steam Inlet	4.1	2739.18		Calc	Section Heat Loss (%)	0	%
Section No. 9 - Economizer - HPIT economiser					UA Adjustment Multiplier	1	Scaling
Water Outlet	97.7	1137.77	78.2	Calc	UA Mass Flow Scaling Exponent	0.65	
Water Inlet	97.7	938.95		Calc	Section Heat Loss (%)	0	%
Section Number 10 - Evaporator - IP evaporator					UA Adjustment Multiplier	1	Scaling
Steam Outlet	21.4	2799.71	5	Calc	UA Mass Flow Scaling Exponent	0.65	
Water Inlet		915.28		Calc	Section Heat Loss (%)	0	%
Section No. 11 - Economizer - HPLT economiser 1					UA Adjustment Multiplier	1	Scaling
Water Outlet	97.7	938.95	78.2	Calc	UA Mass Flow Scaling Exponent	0.65	
Water Inlet	97.7	632.83		Calc	Section Heat Loss (%)	0	%
Section No. 12 - Economizer - IP economiser					UA Adjustment Multiplier	1	Scaling
Water Outlet	21.4	915.28	5	Calc	UA Mass Flow Scaling Exponent	0.65	
Water Inlet	21.4	609.66		Calc	Section Heat Loss (%)	0	%

Figure 75: Virtual Plant inputs for HRSG design data